THE EFFECTS OF POST PROCESSING ON
L-PBF PRODUCED Ti6Al4V
Master's Thesis

Aslınur ATAKLI

Eskişehir 2025

THE EFFECTS OF POST PROCESSING ON L-PBF PRODUCED Ti6Al4V

Aslınur ATAKLI

MASTER'S THESIS

Department of Material Science and Engineering
Supervisor: Assoc. Prof. Dr. Erhan AYAS

Eskişehir
Eskişehir Technical University
Institue of Graduate Programs
January 2025

FINAL APPROVAL FOR THESIS

This thesis titled “THE EFFECTS OF POST PROCESSING ON L-PBF PRODUCED Ti6Al4V” has been prepared and submitted by Aslınur ATAKLI in partial fullfillment of the requirements in “Eskişehir Technical University Directive on Graduate Education and Examination” for the Degree of Master's in Material Science and Engineering Department has been examined and approved on 16/01/2025.

Committee Members	**Title, Name and Surname**	**Signature**
Member	: Assoc. Prof. Dr. Erhan AYAS	
Member	: Prof. Dr. Hakan GAŞAN	
Member	: Assoc. Prof. Dr. Ali ÇELİK	

Prof. Dr. Semra KURAMA
Director of the Institute of Graduate Programs

16/01/2025

SUPERVISOR APPROVAL

Master's student Aslınur ATAKLI, whom I supervise, has completed this thesis titled “THE EFFECTS OF POST PROCESSING ON L-PBF PRODUCED Ti6Al4V”. According to my inspections, the work is scientifically and ethically appropriate for the student to the thesis defense exam.

Supervisor

Assoc. Prof. Dr. Erhan AYAS

ABSTRACT

THE EFFECTS OF POST PROCESSING ON L-PBF PRODUCED Ti6Al4V

Aslınur ATAKLI

Department of Materials Science and Engineering
Eskişehir Technical University, Institute of Graduate Programs, January 2025

Supervisor: Assoc. Prof. Dr. Erhan AYAS

This study investigate the effects of various post-processes on materials produced by selective laser melting using Ti6Al4V ELI alloy. The aim of the study is to determine the appropriate production flow for design by extracting the effects of different production processes for aerospace applications and to evaluate the outputs. The process in this study adresses the relationship between microstructure characterization and mechanical test results after annealing heat treatment, hot isostatic pressing (HIP), sand blasting and pickling processes applied after additive manufacturing. The fracture mechanism of the alpha layer determined as the original value of the study and the extraction of mechanical test results have been obtained, which will guide the design evaluation of Ti6Al4V additive production parts. In the experimental process, microstructure characterization, fracture surface examination, hardness measurements, porosity measurement, tensile tests and high cycle fatigue (HCF) tests were performed. The material microstructures, fracture surface defect types, hardness values and tensile tests results of the final processes gave results compatible with literature. At the end of the study, it was concluded that the HIP process is neccesary for parts with critical fatigue strength and that approximately 2 times improvement is observed in material life. While no effect of the alpha layer was observed in the tensile test results, it was revealed that the fatigue strength decreased by %15 compared to the annealed material. As a result of the thesis study, a material database serving various conditions for titanium additive parts was also created.

Keywords: Ti6Al4V ELI, Additive, Characterization, Post processes, Aerospace.

ÖZET

L-PBF İLE ÜRETİLEN Ti6Al4V ÜZERİNDE İKİNCİL PROSESLERİN ETKİLERİ

Aslınur ATAKLI

Malzeme Bilimi ve Mühendisliği Anabilim Dalı

Eskişehir Teknik Üniversitesi, Lisansüstü Eğitim Enstitüsü, Ocak 2025

Danışman: Doç. Dr. Erhan AYAS

Bu çalışma Ti6Al4V ELI alaşımı kullanılarak seçici lazer ergitme yöntemi ile üretilen malzemelerde çeşitli üretim sonrası proseslerin etkilerini araştırmaktadır. Çalışmanın amacı havacılık ve uzay uygulamaları için farklı üretim süreçlerinin etkilerini çıkararak tasarım için uygun üretim akışını belirlemek ve çıktılarını değerlendirmektir. Bu çalışmadaki süreç katmanlı üretim sonrası uygulanan tavlama ısıl işlemi, sıcak izostatik presleme (HIP), kumlama ve asit ile aşındırma proseslerinden sonra mikroyapı karakterizasyonu ile mekanik test sonuçları arasındaki ilişkiyi ele almaktadır. Çalışmanın özgün değeri olarak belirlenen alfa katmanın kırılma mekanizması ve mekanik test sonuçlarının çıkarılması ile Ti6Al4V katmanlı üretim parçalardaki tasarım değerlendirmesine yol gösterecek sonuçlar elde edilmiştir. Deneysel süreçte mikroyapı karakterizasyonu, kırılma yüzeyi inceleme, sertlik ölçümü, porozite ölçümü, çekme testleri ve yüksek frekanslı yorulma (HCF) testleri gerçekleştirilmiştir. İkincil proseslerin malzeme mikroyapıları, kırılma yüzeyindeki hata tipleri, sertlik değerleri ve çekme testi sonuçları literatür ile uyumlu sonuçlar vermiştir. Çalışma sonunda yorulma dayanımı kritik olan parçalarda HIP prosesinin gerekli olduğu, malzeme ömründe yaklaşık olarak 2 kat iyileşme görüldüğü sonucu elde edilmiştir. Alfa katmanın çekme testi sonucunda etkisi görülmezken, tavlanmış malzeme durumuna kıyasla yorulma dayanımında %15 düşüş gösterdiği sonucu ortaya konmuştur. Tez çalışmasının sonucunda titanyum katmanlı parçalar için çeşitli koşullara hizmet edecek bir malzeme veri tabanı oluşturulmuştur.

Anahtar Sözcükler: Ti6Al4V ELI, Katmanlı, Karakterizasyon, İkincil işlemler, Havacılık.

ACKNOWLEDGEMENTS

I would like to express deep appreciation to my thesis supervisor Assoc. Prof. Dr. Erhan AYAS for his technical assistance and direction in guiding the thesis.

I would like express my deepest gratitude to my family for their moral support during my thesis and for helping me complete the work with great motivation.

I would like to express my endless gratitude to my friend Buket PARLAK for important ideas and great contributions to the directions of the thesis structure.

I'm extremely grateful to TEI Engineer Numan Berat YONDU for him great contributions to the performance of fatigue tests and the evaluation of material testing outputs.

I would like to thank to TEI Engineers Çağlar ÜNVER, Hatice KARADİL and Oğuz ACAR for their helpfulness in SEM investigations and production of additive test specimens.

I am also thankful to TEI technician Ramazan ALTAŞ for his support in the metallographic sample preparation processes.

16/01/2025

STATEMENT OF COMPLIANCE WITH ETHICAL PRINCIPLES AND RULES

I hereby truthfully declare that this thesis is an original work prepared by me; that I have behaved in accordance with the scientific ethical principles and rules throughout the stages of preparation, data collection, analysis and presentation of my work; that I have cited the sources of all the data and information that could be obtained within the scope of this study, and included these sources in the references section; and that this study has been scanned for plagiarism with "scientific plagiarism detection program" used by Eskişehir Technical University, and that "it does not have any plagiarism" whatsoever. I also declare that, if a case contrary to my declaration is detected in my work at any time, I hereby express my consent to all the ethical and legal consequences that are involved.

Aslınur ATAKLI

CONTENTS

Page

LIST OF TABLES

Page

LIST OF FIGURES

Page

GLOSSARY OF SYMBOLS AND ABBREVIATIONS

α	: Alpha
AM	: Additive Manufacturing
AMS	: Aerospace Material Society
ASTM	: American Society for Testing And Materials
β	: Beta
BCC	: Body Centered Cubic
DMLS	: Direct Metal Laser Sintering
EBM	: Electron Beam Melting
EDM	: Electro Discharge Machining
ELI	: Extra Low Intersititial
HCF	: High Cycle Fatigue
HF	: Hydrofluoric Acid
HIP	: Hot Isostatic Pressing
HNO_3	: Nitric Acid
LPBF	: Laser Powder Bed Fusion
NASA	: National Aeronautics and Space Administration
OM	: Optic Microscope
Ra	: Roughness Average
SEM	: Scanning Electron Microscope
SLS	: Selective Laser Sintering
TEI	: Tusaş Engine Industries
UTS	: Ultimate Tensile Strength
XRD	: X-ray Diffraction

1. INTRODUCTION

The use and potential of the additive manufacturing process is increasing day by day. Considering important parameters such as production volume, customization and complexity, compared to conventional methods such as casting and forging; complex designs, machining and production costs, and production durations are the main advantages stated in the literature as the reasons for preferring additive manufacturing methods. (Attaran, 2017; Frazier, 2014; Pereira et al., 2019)

Additive manufacturing (AM) technologies included methods of classification powder bed fusion, directed energy deposition, extrusion, binder jetting etc. Among the these techniques, powder bed fusion methods are the most preferred primary additive manufacturing methods. High material density, high material strength, a variety of material options, and high precision details are the reasons it is favored over other techniques.(Song et al., 2015)

The aerospace industry is one of the sectors where additive manufacturing methods gain importance. Because AM can solve a number of important issues and well-known advantages, it has revolutionized the aerospace industry. Due to the many advantages it provides, it is used by the world's leading aerospace companies such as NASA, Boeing, SpaceX, Airbus and General Electric. It has been projected that AM contribution to the aerospace sector will continue to grow as they develop further, allowing for advancements in aircraft operations, production and design. (Alami et al., 2023)

Ti6Al4V material provides advantages in the aerospace industry due to its features such as high strength, specific strength, low cost, good machinability and good corrosion behavior under operating conditions. Therefore, it is one of the best candidate materials for use in additive techniques. Also, it is a widely preferred material, especially in aerospace jet engine parts and fan and compressor module parts such as vanes, blade disk etc. (June et al., 2023)

The literature has concentrated on studies regarding the use of Ti64 materials, which are widely utilized in the aerospace industry, through using AM manufacturing considering the benefits of AM parts in this particular field. The issues that determine the subject of the study and create a gap in the literature can be stated as the lack of data on mechanical properties, the effect of post processes on microstructure and mechanical properties, and the difference between coupon geometries. For this reason, in order to benefit from the advantages of AM techniques in the production of critical parts used in the aerospace industry, the mechanical behavior of AM metals must be thoroughly examined. The fatigue property of the material is one of the major drawback in AM parts and restricts its use in critical parts. Therefore, there is a need to improve the strength and fatigue properties of AM Ti64 materials according to the applied process flow and to determine their relationship with the microstructure. As a result, studies were carried out within the scope of the thesis to complete the deficiency in this literature and to obtain outputs that will guide the design of AM parts.

1.1 Introduction to Titanium Alloys

Titanium (Ti) exists in two allotropic phases: the body-centered cubic (BCC) β phase at high temperatures and the hexagonal close-packed (HCP) α phase at low temperatures. Changes in material properties are achieved by creating different variations of these two phases at room temperature with the addition of elements; α alloys, near α alloys, α + β alloys, β alloys and Ti based intermetallic compunds. The α ↔ β phase transition temperature for unalloyed Ti is 882 °C. (Williams & Boyer, 2020)

Since two distinct crystal structures and associated allotropic transformation temperature constitute the foundation for the wide range of qualities that titanium alloys can acquire, their existence is significant. The related crystal structure has a relationship with both plastic deformation and diffusion rate. Furthermore, the titanium exhibits a unique anisotropy in its mechanical behavior due to the hexagonal crystal lattice. As given in Figure 1.1., crystal structures are shared for the low temperature phase HCP (α), and high temperature phase BCC (β). (Leyens & Peters, 2003) For the hcp crystal structure, there are only three slip systems, whereas the bcc lattice has twelve. This also explains why hcp titanium has less plastically deformable than bcc titanium.

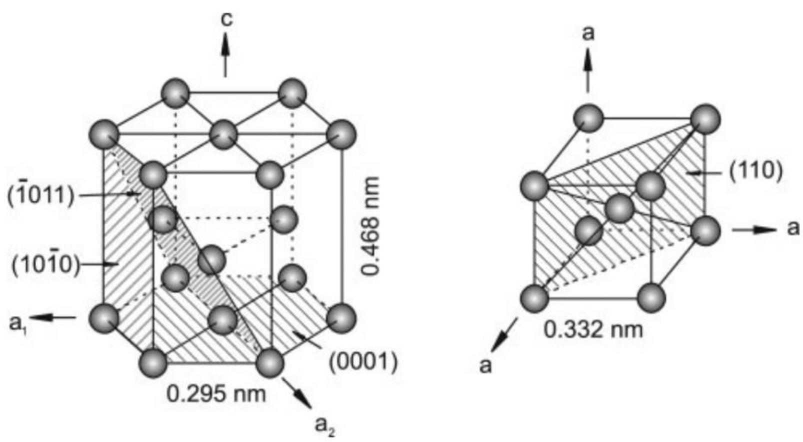

Figure 1.1. *HCP (a) and BCC (β) phase unit cells (Leyens & Peters, 2003)*

According to their impact on the beta transus temperature, the titanium alloying elements are separated into three categories: neutral, alpha stabilizers and beta stabilizers. The elements belonging to these categories, their transition temperature and their effects on the titanium matrix are given in Table 1.1.

Table 1.1 *Stabilizer elements of Ti alloys and how they affect the Ti matrix and transition temperature (Cordeiro & Barão, 2017)*

	Element	Influence on the transition temperature	Main effect on Ti matrix
α-stabilizer	Al, O, N, C	Increase	Hardening
β- stabilizer	Mo, V, Fe, Cr, Ni, Co, Nb	Decrease	Grain Refiners
Neutral	Zr, Sn	No significant effect	Hardenening

Titanium and its alloys are materials with outstanding properties, like high specific strength and good corrosion behavior, that are preferred in various engineering disciplines, including aerospace, automotive, and biomedical. Because of the high specific strength behavior that titanium alloys exhibit at high service temperatures, it is one of the most important materials used in aerospace. (Williams & Boyer, 2020) Titanium's specific strenght value is significantly higher than that of other metallic material classes, as seen in Figure 1.2. (Leyens & Peters, 2003).

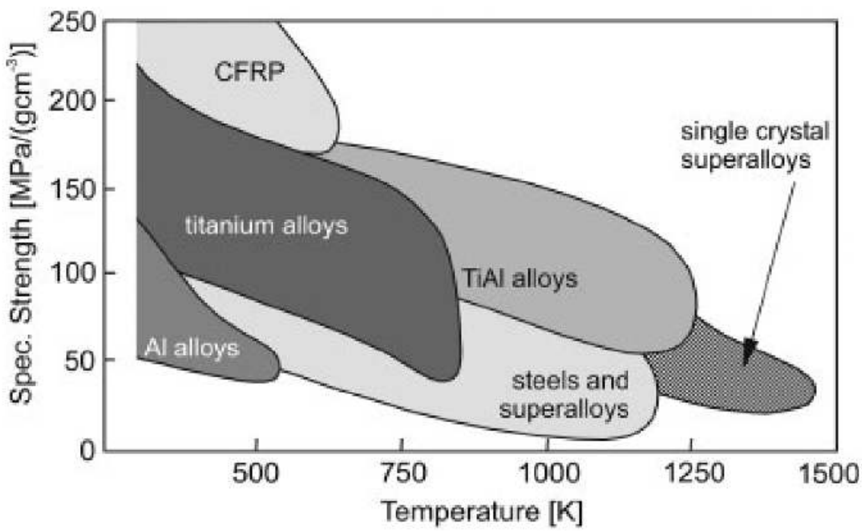

Figure 1.2. *Specific strength versus use temperature of selected structural materials (Leyens &Peters,2003)*

Comparison of the properties of titanium alloys compared to aluminum, nickel and iron materials is given in Table 1.2. (Veiga et al., 2012). When this comparison is examined, it is seen that aluminum alloys are the alternatives to titanium alloys for aerospace parts where the weight gain is very important and the service temperatue is relatively lower from the material density values. Just because the density value is low is not enough for every application, the strength value of the material also gains importance. In this case, when compare the elastic modulus, titanium alloy become a more suitable option.

Table 1.2. *Comparison of properties of titanium alloy with other metallic materials (Veiga et al., 2012)*

	Ti	**Al**	**Fe**	**Ni**
Density (g/cm3)	4.5	2.7	7.9	8.9
Elastic modulus (GPa)	115	72	215	200
Reactivity with oxygen	High	High	Low	Low
Corrosion resistance	High	High	Low	Medium

The corrosion behavior of aircraft engine parts, which is especially determined as the focal point within the scope of the thesis, is an important factor in material selection. Titanium alloys are noted for having better corrosion resistance than materials such as stainless steel or cobalt-chromium alloys when exposed to harsher environments such as hot, oxidizing salts or acids etc. The development of a titanium oxide (TiO_2) passive layer on the surface of titanium, which is chemically stable in environments and self-repairs accounts for the metal's resistance to corrosion (Schenk, n.d.).

The oxide scale is protective in the early phases of oxidation, however it loses this protective characteristic and promotes high oxygen penetration through the oxide after extended oxidation. When oxygen diffuses inward to material, an oxygen riched layer called the alpha case forms below the scale (Mohite et al., 2017). Since it significantly affect the material's fatigue properties, numerous methods are being researched to remove this layer, which has a hard and brittle feature. The chemical abrasion procedures known as pickling and chemical milling are considered to be most widely used (Deshmukh et al., 2017). The result showing the change in the hardness profile of Ti64 according to the alpha layer thickness are given in Figure 1.3.

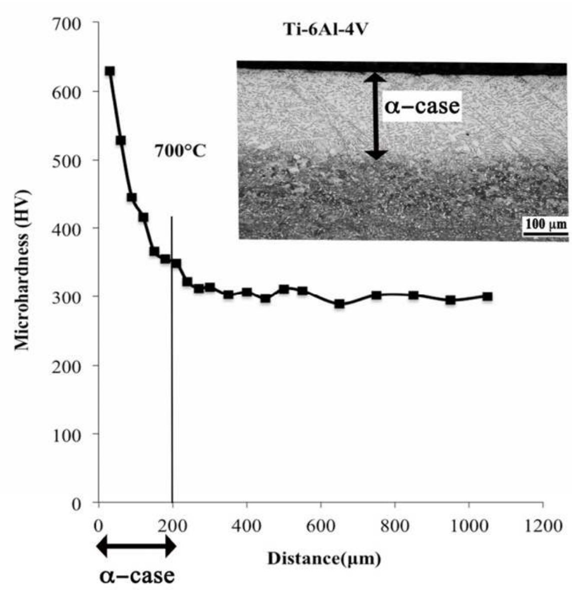

Figure 1.3. *Difference in hardness between the Ti64 sample's surface after 500 hours at 700°C (Gaddam et al., 2013)*

Due to the mentioned advantages, titanium alloys are preferred in aviation engine parts, especially in parts in the fan and compressor module, in accordance with the operating temperature. One of the best examples of using titanium AM parts is the 48 inlet guide vane in the front bearing assembly of Rolls Royce's Trent series XWB-97 engine (Meier et al., 2020). The image of this part, produced with the laser powder bed fusion method (LPBF), was shared in Figure 1.4.

Figure 1.4. *Titanium additive part application examples of Rolls Royce Trent XWB engine front bearing bed (Özsoy et al., n.d.)*

Other examples of titanium additive aerospace applications can be given in Table 1.3.

Table 1.3. *Titanium LPBF aerospace part applications (Blakey-Milner et al., 2021)*

Part	OEM
A350 cabin bracket connector	Airbus
Hydaulic spoiler manifold	Airbus and EOS
NACA inlet	General Electric (GE)
Satellite fuel tank	Lockheed Martin
HP hydraulic manifold	Siemens

1.2 Ti6Al4V ELI Alloys

Ti6Al4V, an α+β alloy, is widely used in implant, energy and other sectors, especially in the aerospace field due to its superior mechanical properties, corrosion resistance, biocompability and high temperature stability. Ti6Al4V is an improved variant of Ti6Al4V ELI (Extra low intersititial) with some modifications to its chemical composition. A comparison reveals that the Fe element has been added to the composition content to Ti6Al4V, along with minor additions of H and O (Mishra et al., 2020).

In order to observe the changes in the material characteristic the chemical composition of Ti6Al4V and Ti6Al4V ELI is given in the Table 1.4.

Table 1.4. *Chemical compositions of Ti6Al4V ELI and Ti6Al4V alloys.*

	(Specification for Additive Manufacturing Titanium-6 Aluminum-4 Vanadium ELI (Extra Low Interstitial) with Powder Bed Fusion, 2014)		*(Specification for Additive Manufacturing Titanium-6 Aluminum-4 Vanadium with Powder Bed Fusion, 2014)*	
Element	**Ti6Al4V ELI Min. and Max.**		**Ti6Al4V Min. and Max.**	
Aluminum	5.50	6.50	5.50	6.75
Vanadium	3.50	4.50	3.50	4.50
Oxygen		0.13		0.20
Carbon		0.08		0.08
Hydrogen		0.012		0.015
Iron		0.25		0.30
Nitrogen		0.05		0.05
Yttrium		0.005		0.005
Other elements, each		0.10		0.10
Other elements total		0.40		0.40
Titanium	reminder		reminder	

It is claimed that the alloy's ductility, fracture toughness, and general performance at cyrogenic service temperatures are enhanced by the reduction of intersitital components that cause variations in chemical composition. Ti6Al4V ELI is also utilized when critical uses call for a higher quality material than standard grade (Ti6Al4V). Aside from applications in the space and defence industries, Ti64 ELI is highlighted as being preferred in medical implants because of its enhanced qualites, particularly in orthopedics and dental implants where biocompability are crucial. Additionally, it is widely used for high-performance parts in aircraft where precise control over material qualities is essential (Cerri et al., 2022).

If the effect on mechanical properties resulting from the compositional differences of intersitial elements is to be summarized, it can be sait that while the standart grade exhibit better performance in terms of strength, Ti6Al4V ELI (grade 23) is better in terms of optimization of toughness and fatigue behavior required for critical application in hardness and elongation values. The comparison of mechanical test results is shared in Figure 1.5. (Mashigo et al., 2021).

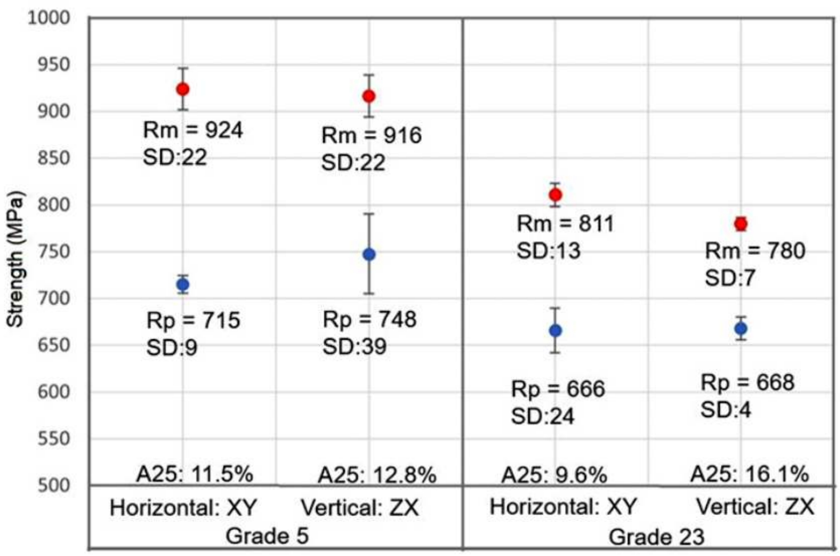

Figure 1.5. *Comparison of grade 5 and grade 23 titanium tensile test results (Mashigo et al., 2021)*

1.3 Selective Laser Sintering Method

The literature emphasise that the additive manufacturing methods become more advantageous in aviation sector, their potential will progressively grow. Compared to traditional production methods, it is stated that it stands out due to the benefits of being able to manufacture complex shapes, life-cycle environmental savings and low buy-to-fly ratio (Huang et al., 2016).

With AM techniques, the principle of layer by layer material laying can be used to produce complicated shape components in near net shape. One production technique that is classified as laser powder bed fusion (L-PBF) is the SLM process. This is because of the manufacturing basis is based on the idea of using a laser beam to melt the powder material after it has been spread out on the build platform for use in the machine. The classification of additive manufacturing methods is shared in Figure 1.6 (Joshi & Sheikh, 2015).

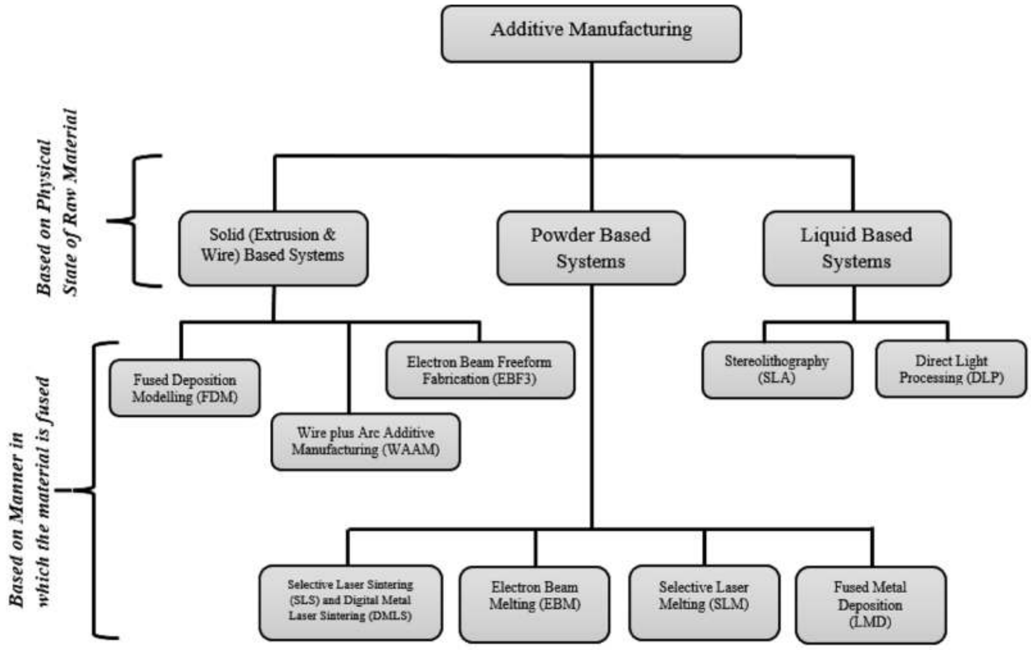

Figure 1.6. *Classification of additive manufacturing methods.(Joshi & Sheikh, 2015)*

When compared with electron beam melting, it can be stated that the SLM method, which has the working principle as indicated in Figure 1.7., provides a better quality production capability with the laser source having good focal point to melt the fine powder material.

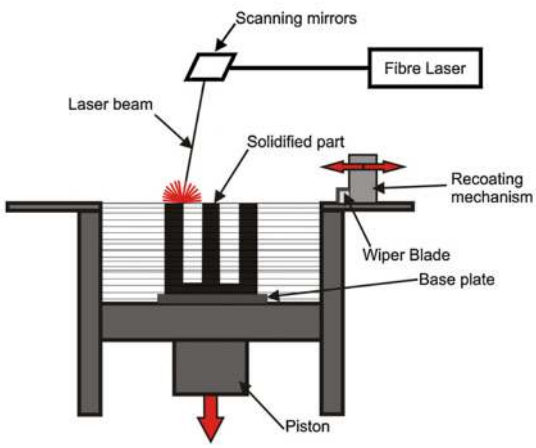

Figure 1.7. *Mechanism of SLM process (Louvis et al., 2011)*

Comparing the SLM process with the EBM process, one of most widely used techniques in the aerospace industry, it is has been reported that the Z layer resolution is better in SLM, the mechanical properties can be better in SLM because of a more uniform microstructure, and the surface roughness is higher in material produced with EBM beacause of powder spreading (Yihong et al., 2014). For this reason, according to the application, metod selection can made depending expected requirements.

In contrast to other additive manufacturing techniques, the SLM process offers design flexibility for complex geometries, and it can be said that it performs as predicted in aerospace application areas where these design criteria are essential (Gao et al., 2023).

1.4 Conditions Limiting Additive Manufacturing Ti64 Parts in Aerospace Engine Components

Aerospace application areas of additive manufacturing production parts, which have an indispensable place recently due to their benefits in the field of aviation, are shared through the examples given in the Table 1.5 in the literature (Tepylo et al., 2019).

Table 1.5. *AM equipment and process abilities (Tepylo et al., 2019)*

AM manufacturer and machine	Process
EOS, EOSINT M270	DMLS
Concept laser Gmbh-, XLine 2000R	SLM
3D Systems -DMP Flex 350	SLM/SLS
SLM solutions, SLM 500	SLM
Arcam, Q20 plus	EBM

One of the main factors limiting the use of additive manufacturing production methods in aerospace parts is the mechanical properties obtained at the end of production, which are important for ensuring the structural integrity and performance of the components. In addition to its advantages, one of the main reasons limiting the use of additive manufacturing methods in aerospace applications is that they exhibit anisotropic properties. For this reason, different studies are being carried out on the properties in the XY and Z build directions. The relationship between the distribution of direction-dependent properties and process parameter is being tried to be clarified. According to literature outputs, it can be said that lower mechanical strength is provided in the Z direction due to the change in material microstructure and the nature of production (Funch et al., 2020).

As a result of the nonconformities obtained in the microstructure due to various process related factors such as porosity, micro voids, insufficient melting and insufficient cooling rates, the decrease in material data and lower mechanical properties compared to conventional material froms (forging, bar and sheet) are major limiting factors. The use of additive manufacturing parts cannot be considered as an alternative, espacially in components operating under cyclic loads and where fatigue properties are important in part design (Shunmugavel et al., 2015).

Another factor is the surface roughness value and quality obtained after production, although it is variable depending on the additive manufacturing method used compared to traditional methods. Surface roughness is important factor that limits the use of additive parts, especially in aerospace engine parts, as it changes the aerodynamic performance due to the effect of air flow. It has been stated in the literature as a point to be taken into consideration for parts with non-machined surface profiles with an example from compressor blade parts and presented as an output where its effects are revealed (Lim et al., 2024).

If the part to be produced has thin wall locations, obtaining sufficient layer resolution with additive manufacturing can be one of the challenging stages. Although it depends on the production capacity of the additive device used, the production volume is another limiting factor. It may reveal the need to select the appropriate machine and method for the production of very large volume parts. The support structures needed for production are a limiting factor in the part design and the at the same time, the damage and delamination defects that may occur during the removal of the support structures after production are another notable restricted aspect (Dangal & Jung, 2023).

In traditional methods of production, blade parts usually obtain a single crystal or equaxed grain structure from production by casting method. The effect of the columnar grain structure generally obtained as a result of additive production on the creep resistance of the material compared to conventional methods is an open issue and creates an uncertainty in terms of design processes (Xu et al., 2019). The image of the additive turbine blade design was shared in Figure 1.8 (Magerramova et al., 2016).

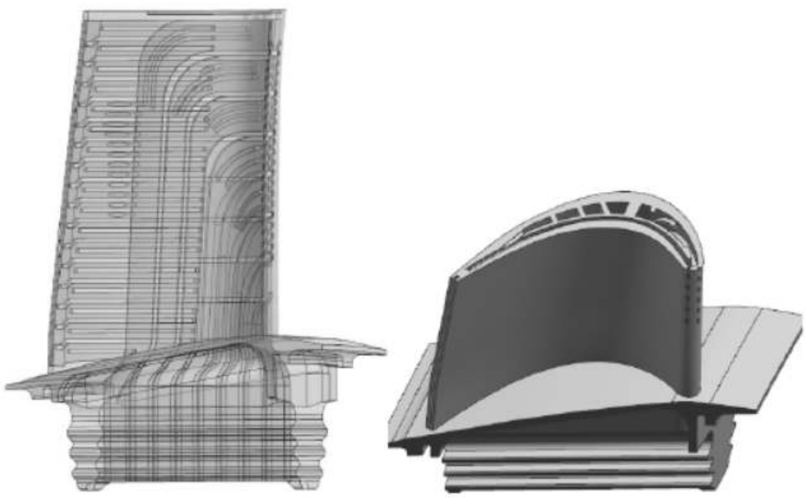

Figure 1.8. *Additive turbine blade example (Magerramova et al., 2016)*

1.5 Post Processes and Their Impacts on Ti64 SLM Parts Mechanical Behavior

The fatigue and tensile properties of materials used in all sectors, especially in the aerospace industry, are very important to ensure part life and to prevent failure in critical applications. Therefore, in order to increase the usage potential of additive parts, the material properties and microstructure relationships obtained as a result of various post-processes need to be examined in detail. The main topics that can affect material properties and whose studies are found in the literature are various heat treatment applications, HIP and surface improvement methods.

1.5.1 Sand blasting process

Sand blasting or abrasive blasting process is a mechanically applied surface treatment. The sandblasting mechanism is used to remove the oxide layer or other particles on the surface of a material by pushing abrasive grains through the used media at high speed or pressure. The cutting and cleaning effect of the abrasive sand completely cleans the part surface. With the effect of the process, surface roughness and mechanical properties can be improved (Isa et al., 2018).

Studies have been carried out in the literature on the mechanical and microstructural effects of different processes on Ti64 additive parts. One of the post processes whose effects have been studied is sandblasting. For this reason, some studies have been carried out on the mechanical effects of this process, which is generally used for surface preparation before coating process or material removal. In a study conducted that the sandblasting process applied with glass bead had no effect on the tensile test. However, in these studies, the effects of the sandblasting process on fatigue were not examined. (Cerri et al., 2022)

In another study, the effects of surface finishing processes such as turning, polishing, grinding and sandblasting on fatigue were studied and it was evaluated that increased compressive residual stresses by sandblasting could extend fatigue life. At the same time, it was emphasized in the study that surface defects resulting from processes and therefore crack initiation behaviors may be different (H. Yu et al., 2019).

In an investigation that was on inconel 718 material, the effects of sand blasting, sand-blasting and HIP processes on fatigue were observed. It was concluded that the fatigue test results obtained in the samples where both processes were applied did not have a major effect when compared to the results of the sample where only sand blast was applied. Considering the relationship between microstructure and properties, this effect is associated with the increase in the ability to undergo plastic deformation due to grain growth after the HIP process. Measurement results have shown that the sand blast process also reduces the internal stresses occurring in as-built samples due to the inherently rapid cooling rates of the SLM process (C. Yu et al., 2022).

Another study on Ti64 SLM lattice structures found that applying three post processes; chemical etching, HIP and sand blasting significantly improved the material's fatigue behaviour. The essential role of sandblasting in post-processing was demonstrated by the study (Karami et al., 2020).

In addition to the importance of sand blasting as a post process, studies have also shown that the effects of the process are different samples produced in different build direction due to the nature of additive manufacturing. Literature demonstrated that important factors impacting effciency include the consequences of build direction on mechanical properties of materials produced by additive manufacturing, the resulting variation in surface roughness and the surface quality that can be enhanced through post-processing. (Kónya et al., 2024)

In summary, although there is not much study outputs on mechanical effects, assumptions are made that is has a healing effecty, and it is observed that it is difficult to make a clear assessment due to the lack of sufficient data.

1.5.2 Pickling/chemical etching

The surface of titanium alloys generates a layer known as the "alpha case" when the materials are exposed to an atmosphere of oxygen and nitrogen at high temperatures (Seth et al., 2022). This layer, which exhibits a hard and brittle behavior, needs to be removed because it affects the mechanical strength of the material, especially the fatigue properties of the material. It is important to consider the impact of alpha layer on fatigue in aerospace parts operating under the cyclic loads to prevent the critical failures.

The pickling process, a surface treatment, is the process of immersion in an aqueous acid solution to chemically remove the surface oxide. For this process, nitric and hydrofluoric acid generally used in titanium alloys. One could argue that proper solutions ratios are critical to the material etching process and have a significant impact on its efficiency.(Say & Tsai, 2004)

According to ASTM B600, the titanium pickling processing solution in this specification utilize a nitric acid/ hydrofluoric acid ratio of least 10:1. But using this ratio, hydrogen pick up from nitric acid/ hydrofluoric acid pickling in titanium alloys will be minimized. At the same time, the requirement for process solution and chemical ratio is specified in the same way in the NASA PRC-5010D standard.(Gonzalez, 2020)

The effect of the alpha layer removal from the material surface in the experiments carried out various rates for the purpose of material abrasion from the material surface is shared in Figure 1.9.(Say & Tsai, 2004). Based on this, it is important to apply the ideal solution concentrations for this process. In order to avoid any negative effects on the material, such as hydrogen emibrittlement on the material in mechanical sense and to carry out effective process, the solution concentration must be used and controlled appropriately.

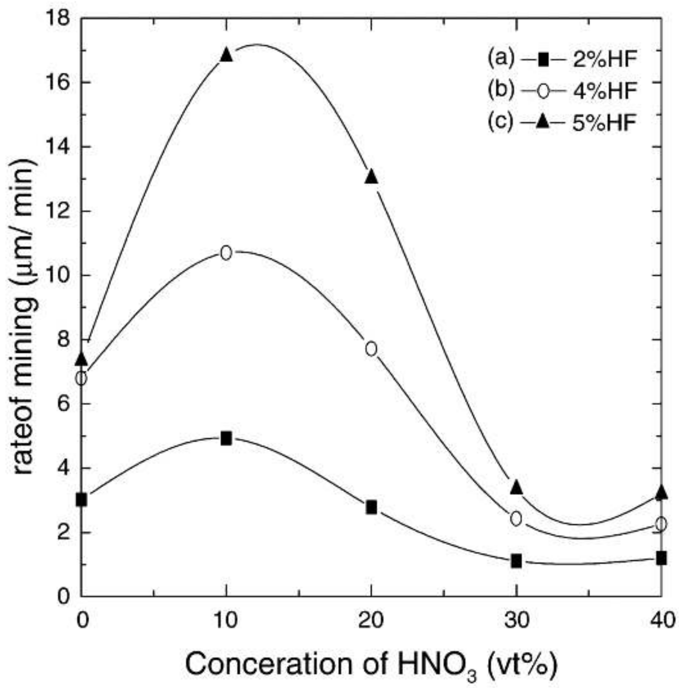

Figure 1.9. *Material removal rate depending on HNO_3-HF concentration (Say & Tsai, 2004)*

Due to the limited number of publications and research in the literature on the pickling process, not much information has been found on its mechanical effects. In general, it is stated that it can have a positive effect as it can reduce the risk of crack initiation on sharp lines by obtaining a smooth and clean surface and surface defects associated with oxide layers. In a study conducted on forged and rolled Ti64 material, the effect of surface treatments such as pickling and anodized coating on the endurance limit was examined. It has been stated that the endurance limit of the material may decrease after the pickling operation by associating the amount of residual stress measured from the material as the study output. It was emphasized that further study outputs were required to clarify this minor change (Vermesse et al., 2013).

According to the results of a comparative study conducted on aluminum alloy, it is reported that the pickling process has lower success on the fatigue life of the material compared to machining methods such as electroplish, which can achieve excellent surface profiles (Spear & Ingraffea, 2013).

As in the pickling process, there are not many studies with mechanical test results fort he sandblasting post process. Since the purpose ofe use in existing studies is for different applications or material forms, SLM stands out as a subject that needs to be studies in the literature for Ti64 materials.

1.5.3 Hot isostatic pressing (HIP)

The HIP process is a thermo-mechanical process that is widely used, especially on cast materials, to eliminate internal defects and porosities that cannot be eliminated by standard heat treatment applications. Figure 1.10. indicated that schematically present working mechanism of the HIP process (Sahoo et al., 2021).

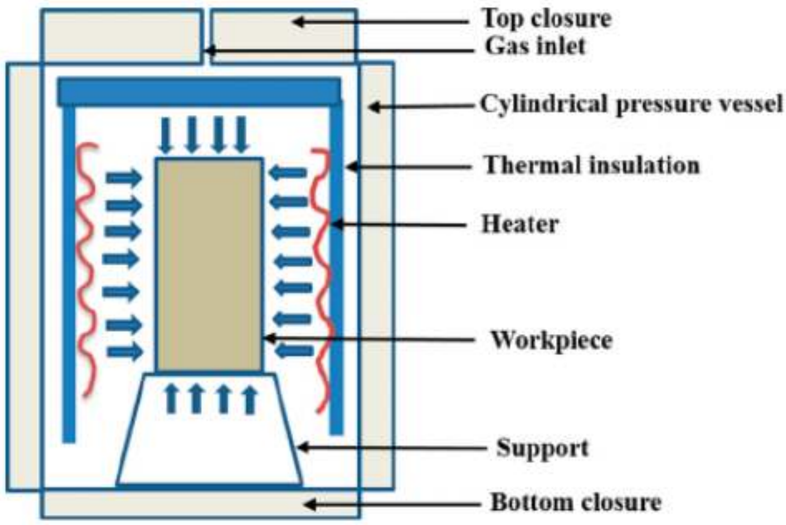

Figure 1.10. *HIP process mechanism (Sahoo et al., 2021)*

There are two major parameters in the HIP process, temperature and pressure, which change the final properties and affect the improvement obtained with the process. It is stated that the efficiency of the process outputs changes depending on the process parameters and the amount of improvement on the mechanical properties changes (Popovich et al., 2016).

As a result of the additive manufacturing method, which is based on the principle of building the material layer by layer with the laser power, irregularities such as porosity, micro void and pockets that affect the material strength formation in the microstructure due to the nature of the process. For this reason, attention was drawn to the effect of the amount of porosity, distribution and shape on the mechanical properties in the microstructure obtained as a result of SLM production (Petrousek et al., 2017).

Pressure is generally more dominating for the densification and porosity elimination of Ti6Al4V components processed by SLM and HIP, according to the results of various process parameters. Therefore, pressure can be regarded as the most important component in increasing the part's density and mechanical strength when compared to the temperature parameter. Although temperature plays a significant role in improving the microstructure through phase change and achieving the desired material properties, comparative studies have shown that components cannot achieve the sufficient density or structural integrity without adequate pressure. (Cegan et al., 2020)

It has been reported that the HIP process, especially on the Ti64 additive materials evaluated within the scope of the thesis showed an improvement in the fatigue limit and a decrease in tensile properties compared to the as-build and stress relief conditions. (Dolev et al., 2022)

Another noteworthy issue is the effectiveness of porosity elimination in optimizing HIP process parameters as well as the blister effect it reveals. It is reported that this blister formation is detected after the process due to the rapid expansion of gas or vapor trapped within the pores or internal cavities of the part under the high pressure and temperature conditions applied during the HIP process. It is observed that extreme blistering may result in weak or concentrated stress areas which could have a major impact on the part's mechanical performance. According to reports, blistering is a disadvantages of the HIP process that can lead to cracking or structural problems in under extreme conditions. In summary, this leads to the conclusion that it is critical to research process parameter optimization and identify the proper process parameters (du Plessis & Macdonald, 2020).

In the literature, comparison of as-build and HIP applied material cases has been carried out in many studies. It is seen that HIP has a data reducing effect on UTS and yield strength properties. The results reported in the literature are shared in Figure 1.11. According to these results, a correct relationship can be established between the microstructure result and the change in mechanical properties, which are discussed in detail in the section of the thesis where the literature microstructure results are discussed.

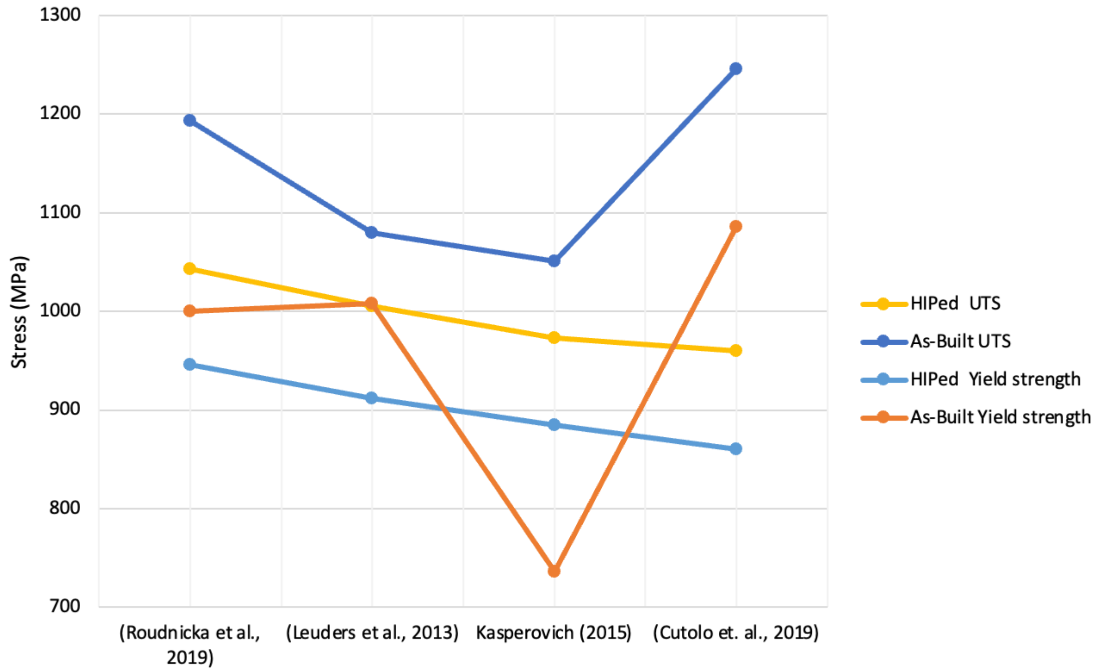

Figure 1.11. *As-built and HIPed conditions tensile properties (Cutolo et al., 2019; Kasperovich & Hausmann, 2015; Leuders et al., 2013; Roudnicka et al., 2019)*

As a result of the HIP process, although the material tensile properties are low, it is noticable that the ductility behavior of the material is improved. In the test results, it can be said that the ductility is increased compared to the as-built and heat-treated conditions (Cutolo et al., 2019; Kasperovich & Hausmann, 2015; Leuders et al., 2013; Roudnicka et al., 2019).

1.5.4 Heat treatment

The mechanical properties of titanium alloys can be altered by through modifiying the phase balance and microstructure, which is based on the princible of optimizing the alpha and beta ratios in the material. Heat treatment is another post process to optimize the mechanical properties of the material, which exhibits high strength but low ductility due to the alpha material phase obtained as a result of the SLM process, and to be used especially aerospace parts.

In the literature, two different heat treatments applied to Ti64 SLM parts are emphasized; stress relief heat treatment and annealing heat treatment. The annealing heat treatment which is used to improve grain structure and reduce stresses, is specified in aerospace standards and various research results as heating Ti6Al4V material to 700-800 °C and holding for a certain period of time to obtain a homogeneous microstructure. Another heat treatment, stress relief heat treatment, is generally distinguished by heating the material to 600-700 °C to reduce residual stresses without significantly changing the microstructure, compared to the annealing heat treatment. The reason why the optimum temperature of the stress relief heat treatment is determined as approximately 593 °C is explained as depending on the duration and temperature of the stress relief heat treatment, as in NASA Figure 1.12. *(Schmidt & Wood, n.d.).*

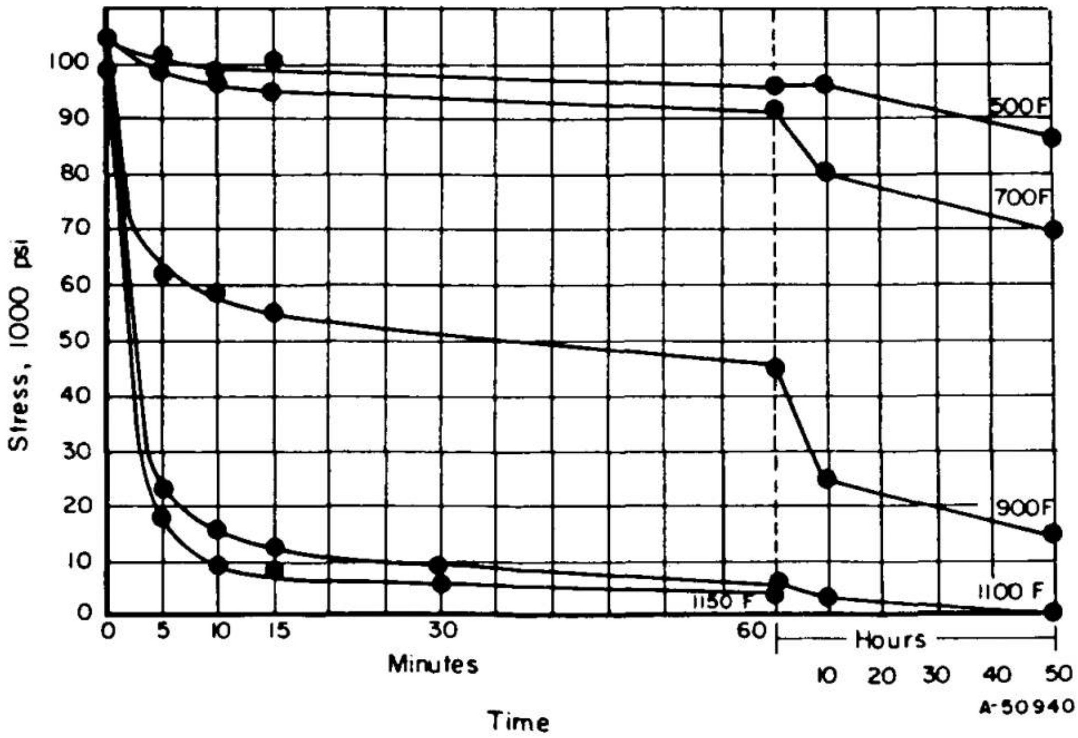

Figure 1.12. *Heat treatment duration and temperature's impact on residual stress relief in Ti64 (Schmidt & Wood, n.d.)*

Since stress relief heat treatment is a factor affecting the alpha layer thickness, which is a drawback of titanium material, it should be optimized at the minimum temperature and time possible. It can also be stated that the appropriate heat treatment procedure for the annealing heat treatment is determined as the temperature at which is ductile and stable α+β structure can be obtained. It is stated that the ideal mechanical property balance targeted to be achieved as a result of the oxiadtion effect and annealing heat treatment is obtained at around 704 °C temperature.

The XRD results showed that the intensity of the β phase reflections increased as the annealing temperature increased when the annealing heat treatment was applied above 800-830 °C. The mechanical properties have been reported to start showing declining effect as a result of this mechanism. The reduction in the hcp phase's reflections upon annealing, the transition from needles phase to lamallae α phase (Gaiani et al., 2023).

1.6 Ti64 SLM Post Processes Response on Material Microstucture

In order to establish a relationship between the microstructure obtained as a result of the post processes applied within the scope of the thesis and the test results performed, a detailed research was carried out on the effects of the processes in the literature.

1.6.1. As-build and heat-treated microstructure

Examining the relationship between as-built microstructure and fatigue property is gaining importance, especially due to the problems encountered in removing the alpha layer that will occur as a result of heat treatment in aviation engine parts and the failure to ensure part tolerances after the alpha layer removal process. It is necessary to evaluate whether the microstructure of the part obtained without heat treatment and whether the mechanical properties to be obtained due to this microstructure meet the mechanical requirements. Comprehensive studies on the characterization of the microstructure acquired after production and mechanical test results have been conducted in the literature in order to make assessments.

The as-build microstructures are defined by columnar β grains and fine martensite alpha structure. The literature results demonstrated that the as-build materials attributes include high strength, poor ductility and noticeable anisotropy (Tao et al., 2018). As a result of the high cooling rate occurring in the SLM process, the as-built microstructure of the produced Ti64 material, which generally consist of acicular a′ martensite phase rather than equlibrium α and β phases, is as shown in Figure 1.13. (Eshawish et al., 2021; Rafi et al., 2013).

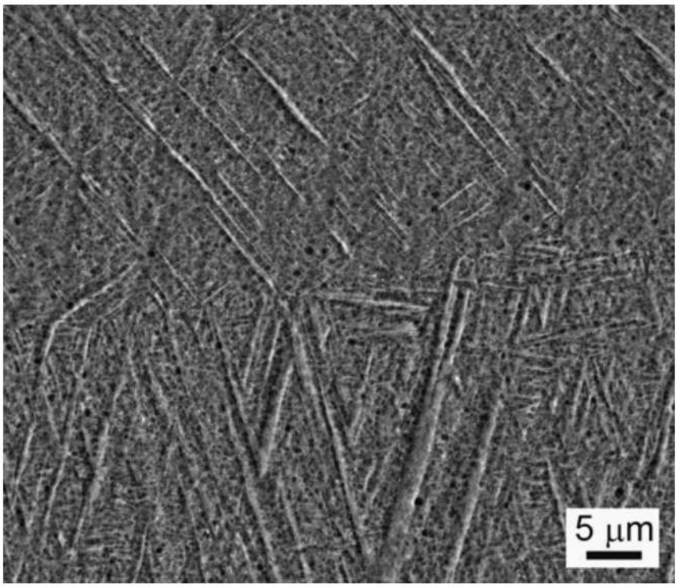

Figure 1.13. *SEM-SE Ti64 as-built microstructure (Rafi et al., 2013)*

Metastable hcp a′ martensite phase is formed by decomposition of high temperature β phase during SLM production cycle. It is stated that the a′ martensite phase, which provides strength and reduces ductility by resticting dislocation motions in the microstructure, has different classifications in the literature. This classification is made according to the phase size (major and minor axis size) and the formation order of the phase depending on the thermal history. Accordingly, a′ martensite phase can be mainly classified as primary, secondary, ternary and quartic phases. The appearance of primary, secondary and quartic a′ martensitic phases is given in Figure 1.14. the SEM microstructure (Cerri et al., 2022; Yang et al., 2016).

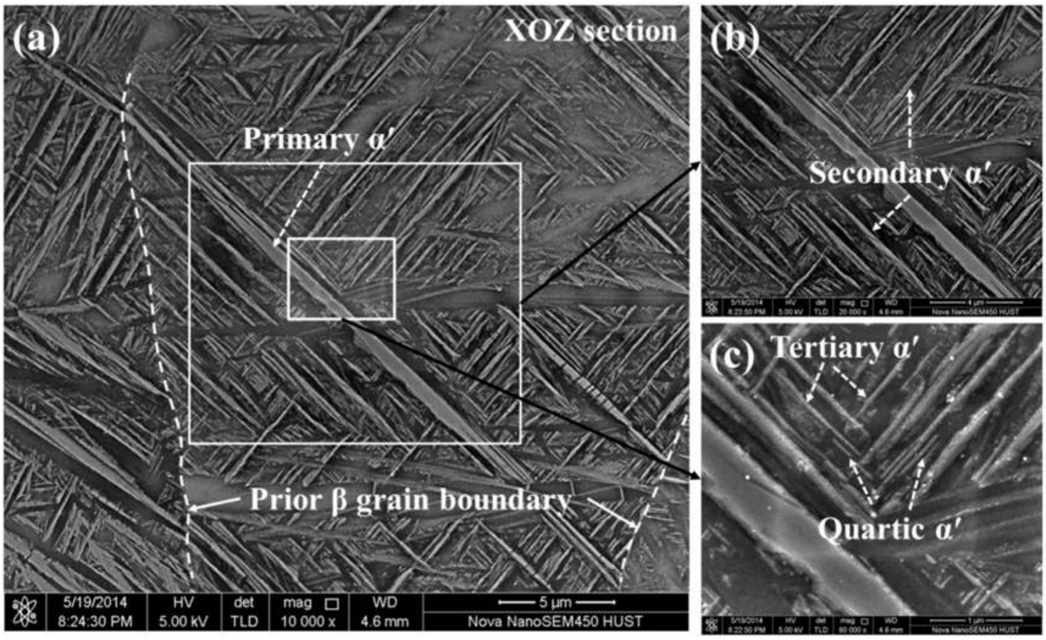

Figure 1.14. *SEM microstucture of martensite phases in Ti64 SLMed material (Yang et al., 2016)*

Researches indicates that strain localization within the primary α' martensite phase creates both macroscopic brittle fractures and ductile microvoids (Moridi et al., 2019). At the same time, it is demonstrated that β grains elongated in the build direction in the as-build microstructure reduce fatigue strength and cause intergranular failure due to the mechanical anisotropy (Kouprianoff & du Preez, 2023).

Although its varies depending on application area, heat treatment is typically given to the materials along with the build substrate because to the brittle and poor elongation value of the as-build microstructure due to its martensitic structure. In order to achieve proper equlibrium strength and ductility, the microstructure altered using post production heat treatment, which also homogenizes microstructure and reduced anisotropy.

Apart from the microstructure and mechanical properties, stress relief heat treatment shall be applied to the produced part due to the high residual stress that occurs as a result of SLM manufacturing process. Many studies have been conducted in the literature on the internal stresses observed in parts as a result of part production. The effects of residual stress on mechanical properties are demonstrated by mechanical test and simulation results (Chen et al., 2021; Nagesha et al., 2020).

As a result of the transformation of the α′ martensitic structure formed as a result of SLM production into α+β, ductility increases and internal stresses decrease. It has been stated in studies that this transformation occurs at approximately 570 °C (Jaber et al., 2022).

Microstucture and mechanical properties were examined by conducting heat treatment trials for temperature ranges determined in literature between 700 °C and β transus temperature 980 °C for annealing (Liu & Shin, 2019; M. Wang et al., 2024). Studies with varying heat treatment temperatures found that the coarsening effect and annealing temperature increased, leading to rise in alpha lath thickness. The effect of this change in microstructure on tensile strength and elongation is given Figure 1.15 (D. Wang et al., 2022).

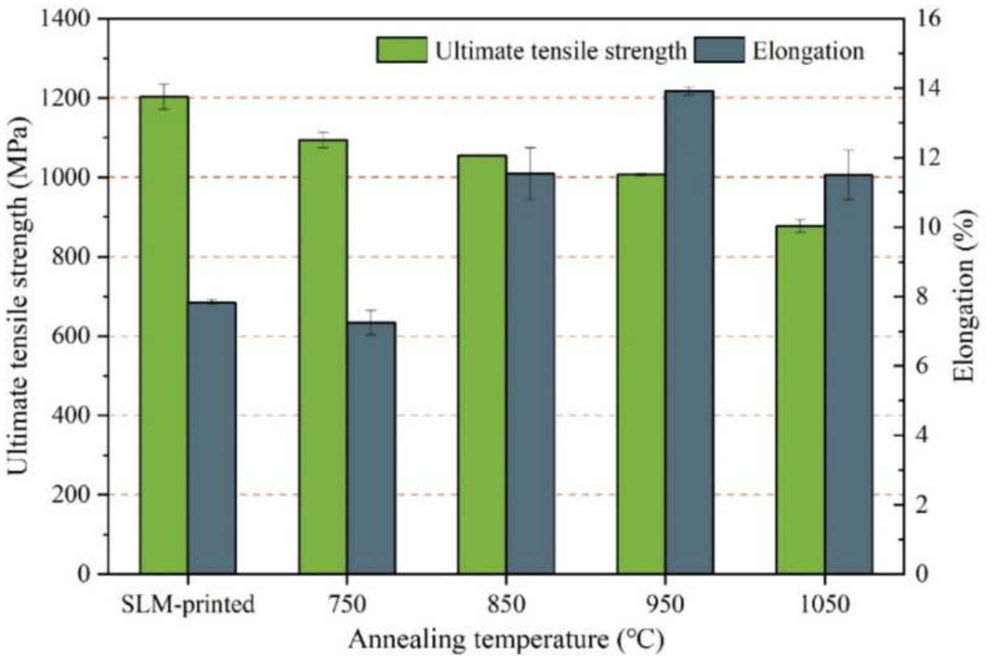

Figure 1.15. *Change in tensile strength and elongation data according to different anneal heat treatment temperatures (D. Wang et al., 2022)*

Within the studies found in the literature, according to the mechanical test results performed by increasing the heat treatment temperature, it is seen that the strength value decreases while the elongation value is improved. Therefore, achieving optimum ductility also requires improving the fatigue behavior of the material by reducing its internal stresses. In the studies, the relationship between material microstructure and mechanical properties was examined by conducting low temperature and high temperature stress relief/annealing heat treatment trials.

As a result of the annealing heat treatment experiments carried out between 427-610 °C temperature range for 5 to 30 minutes, it was concluded that the minimum temperature at which internal stresses decreased by 90% was 560 °C and the best ductility value was obtained at 650 °C (Ter Haar & Becker, 2021).

In another study, the difference in microstructure obtained as a result of heat treatment procedures at different annealing temperatures and different cooling rates and the changing mechanical properties as a result of this microstructure were examined (Bartolomeu et al., 2022).

Although many different heat treatment procedures have been studied in the literature, many of them are not suitable in terms of both cost and efficiency. For this reason, different aviation standards use a heat treatment procedure that provides optimum mechanical properties for Ti64. In a study, the microstructure and mechanical properties of lower and higher annealing temperatures (300 °C, 550 °C, 900 °C, 1000 °C) than the 704 °C anneal temperature specified in aerospace standards were compared. As explained in Figure 1.16 (b), the α phase dissociates at 973 K due to the sudden decrease of the lattice strain to the lowest value. As a result of this phase change, it is stated that optimum mechanical properties are obtained by heat treatment applied at 704 °C (P. Wang et al., 2021).

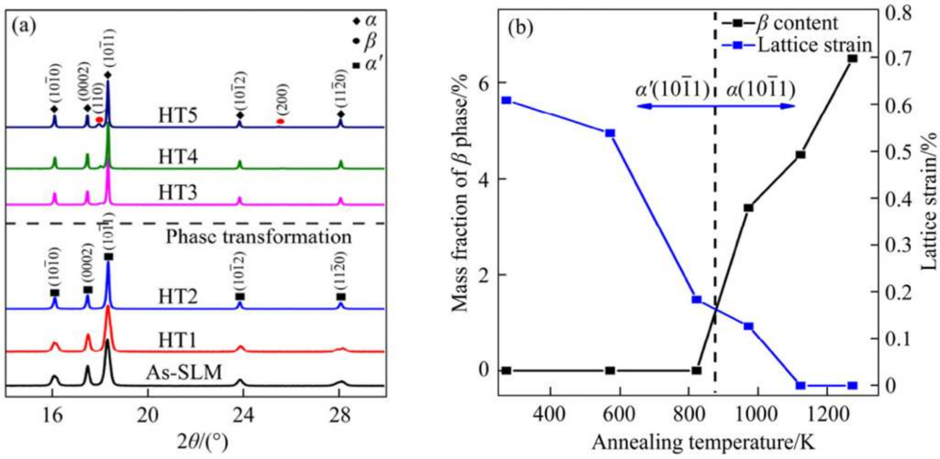

Figure 1.16. *XRD results of Ti64 samples under different heat treatments a), (HT1-300℃, HT2-550℃, HT3-704℃, HT4-900 ℃, HT5-1000 ℃), mass fraction of β phase and lattice strain of hcp phases (b) (P. Wang et al., 2021)*

Recommended stress relief and annealing heat treatment procedures for titanium materials in aviation standards and references are given in Table 1.6.

Table 1.6. *Titanium heat treatment procedures according to aerospace standards*

Specification	Heat Treatment	Procedure	Reference
ASTM F3001	Stress Relief	593 °C for 2 hours	*(Designation: F3001 − 14 Standard Specification for Additive Manufacturing Titanium-6 Aluminum-4 Vanadium ELI (Extra Low Interstitial) with Powder Bed Fusion 1, n.d.)*
ASTM F3001	Annealing	704 °C for 2 hours	
ASTM F2924	Stress Relief	593 °C for 2 hours	*(Designation: F2924 Standard Specification for Additive Manufacturing Titanium-6 Aluminum-4 Vanadium with Powder Bed Fusion, 2014)*
ASTM F2924	Annealing	704 °C for 2 hours	
SAE AMS 2801/H81200	Stress Relief	593 °C for 2 hours	*(Designation: AMS2801C Specification for Heat Treatment of Titanium Alloy Parts, 2022*
SAE AMS 2801/H81200	Annealing	704 °C for 2 hours	*Designation: AMSH81200 Standard Specification Heat Treatment of Titanium and Titanium Alloys, 2001)*
NASA-HDBK-6025	Stress Relief	593 °C for 2 hours	*(Superseding Nasa-Hdbk-6025 Guıdelınes For The Specıfıcatıon And Certıfıcatıon Of Tıtanıum Alloys For Nasa Flıght Applıcatıons, 2014)*
NASA-HDBK-6025	Annealing	704 °C for 2 hours	

In NASA-HDBK-6025 and ASTM F3001–F2924 additive manufacturing standards, it is stated that stress relief and annealing heat treatment procedures specified in AMS 2801 and AMS-H-81200 standards can be applied to materials after L-PBF production. In aviation applications, heat treatment procedures specified in the standards are applied according to the part mechanical requirements. For SLM Ti64 materials, guidance is given to the heat treatment procedures recommended for wrought alloys, as in the aviation standards and other literature studies referenced. Therefore, it is important to gain awareness of the differences between microstructure and material properties in two different material forms.

Titanium alloys can have equaxed, lameller or bimodal microstucture depending on the termomechanical process applied. Bimodal microstuctures are known for their high yield, tensile, ductility and fatigue stresses; fully lamaller microstucture, on the other hand, are thought to have high fracture toughness and fatigue crack propagation resistance (Shunmugavel et al., 2015). Annealing aproaches used in forged materials do not influence SLM Ti64 materials in the same manner. Therefore, the difference between heat treatment and microstructure relationship should be taken into consideration. While a bi-model microstructure consisting of large equiaxed/spherical α grains in a matrix consisting of long α + β layered grains is obtained in wrought Ti64 materials; in SLM Ti64 materials, the martensitic structure decomposes into alpha+beta lamellar structure after annealing heat treatment (Ter Haar & Becker, 2018). (Shunmugavel et al., 2015) shared the difference in the optical and SEM microstructures of wrought and SLM Ti64 materials as shown in Figure 1.17.

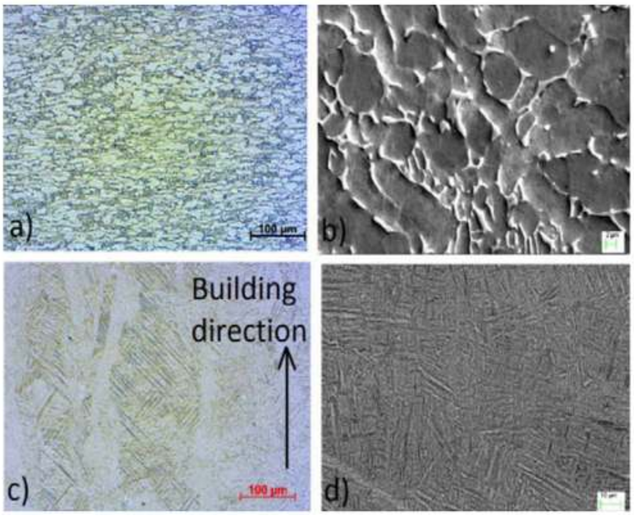

Figure 1.17. *Wrought (a, b) and SLM (c, d) Ti64 optical microscope and SEM microstructures (Schunmugavel et al., 2015)*

The typical Ti64 SLM microstructure obtained after applying the annealing heat treatment procedure specified in aviation standards is given in Figure 1.18 (Eshawish et al., 2021)

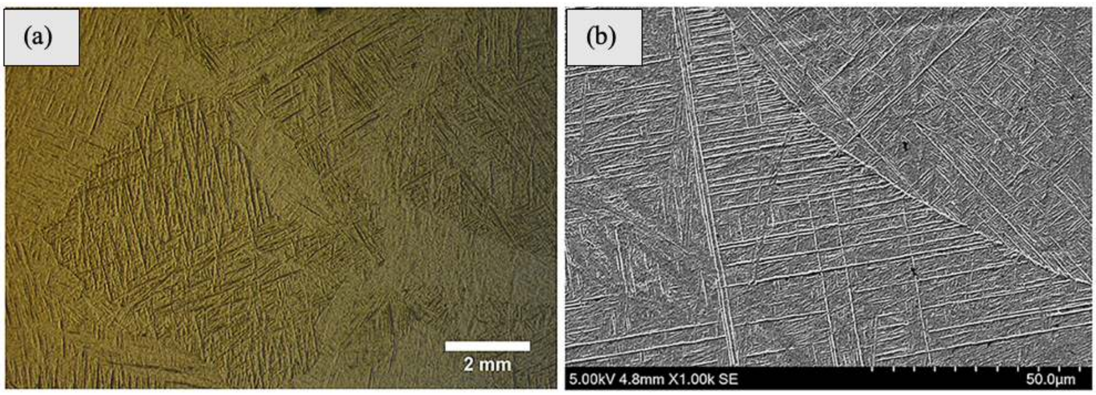

Figure 1.18. *OM (a) and SEM (b) images of the microstructure of Ti-6Al-4V produced by SLM Stress Relief Material at 704 ℃ (Eshawish et al., 2021)*

1.6.2 Effects of HIP on microstructure

The HIP application can be carried out as a post process application following the SLM production, contignent on the mechanical requirements neccesary for the application. As in casting materials, it has a critical place in terms of increasing the density of the material and eliminating porosities in the internal structure and thus improving mechanical properties. Therefore, it has been one of the most studied topics in recent years for additive materials. Numerous investigations of the SLM-produced titanium alloys (Dolev et al., 2022) utilized in the aerospace industry, as well as nickel based (Moussaoui et al., 2018), aluminum-based (Hirata et al., 2020), and cobalt-based (AlMangour et al., 2020), have been published in the literature. Although there are many different HIP process parameter experiments studied for titanium alloys, the process parameters recommended for the process in aerospace standards are given in Table 1.7.

Table 1.7. *HIP process parameters recommended by aerospace standards*

Specification	Temperature (°C)	Pressure (MPa)	Duration (min)	Atmosphere	Reference
ASTM F2924	895-955 °C	≥ 100 MPa	180 ± 60	Argon atmosphere below under to 425 °C	*(Designation: F2924 Standard Specification for Additive Manufacturing Titanium-6 Aluminum-4 Vanadium with Powder Bed Fusion, 2014)*
ASTM F3001	895-955 °C	≥ 100 MPa	180 ± 60	Argon atmosphere below under to 425 °C	*(Designation: F3001 − 14 Standard Specification for Additive Manufacturing Titanium-6 Aluminum-4 Vanadium ELI (Extra Low Interstitial) with Powder Bed Fusion 1, n.d.)*

Although it depends on the applied HIP process parameters, the differences between as-built, annealed and HIPed microstructures and mechanical properties are among the main studies emphasized in the literature. The microstructure variations in different conditions are indicated as shared in the Figure 1.19.(Roudnicka et al., 2019)

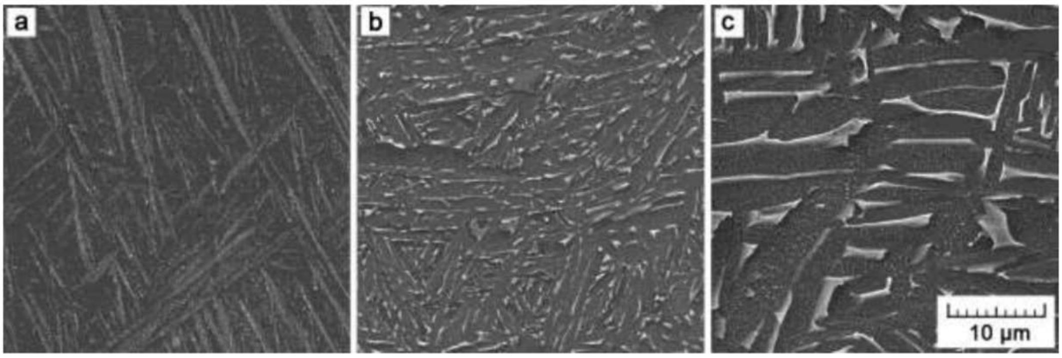

Figure 1.19. *SLM manufactured Ti64 as-built (a), annealed heat treated (b), and HIPed (c) microstructures (Roudnicka et al., 2019)*

If it is required to relative the variation in microstructure with the change in phase transformation; the martensitic microstructure formed by the α ' martensite phase growing between β grains in the as-built state can be explained by obtaining a stable microstructure consisting of α + β by increasing the temperature above Ms (800 °C) with the HIP process. Figure 1.19 (a), explains that the martensitic structure obtained after as-built begins to transform into α + β after annealing (b), and a stable microstructure consisting of lamellar α + β phases is obtained after the HIP temperature (c). Figure 1.20 shows the recommended HIP process temperature in the phase diagram (Alegre et al., 2022).

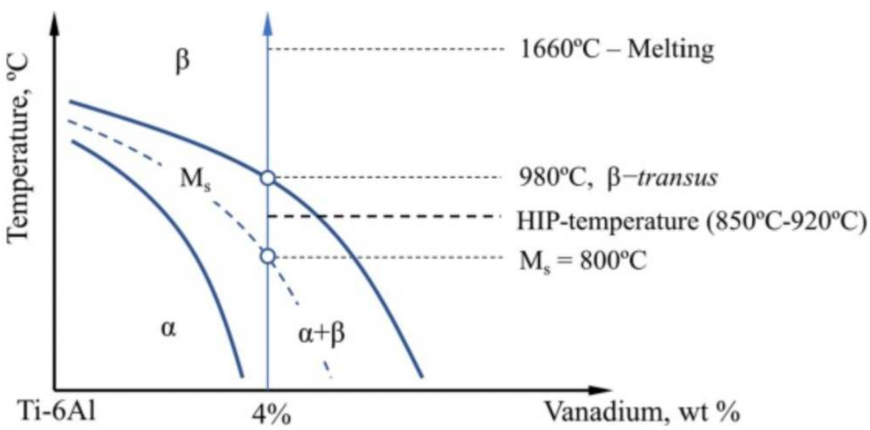

Figure 1.20 *Ti64 binary phase diagram (Alegre et al., 2022)*

Since there is a wide temperature range that can be applied in the process recommended by the standards, the effects of temperature change on microstructure and mechanical properties are one of the issues that are frequently emphasized in studies. Considering the studies on HIP temperature independent of the pressure parameter, it is stated that 920 °C is the ideal process temperature because it can eliminate internal porosities and reduce lack of fusion defects to a lower resolution level (Qian et al., 2016).

In the study where the variability of both process parameters was investigated, it was emphasized that as the temperature increased, the α lath thickness in the microstructure increased and the amount of β phase increased, as a result of the trial matrix in which the HIP temperature varied between 910-950 °C and the process pressure value varied between 110-150 MPa. This change in the microstructure is clearly illustrated in the SEM microstructure images given in Figure 1.21. (Lv et al., 2023).

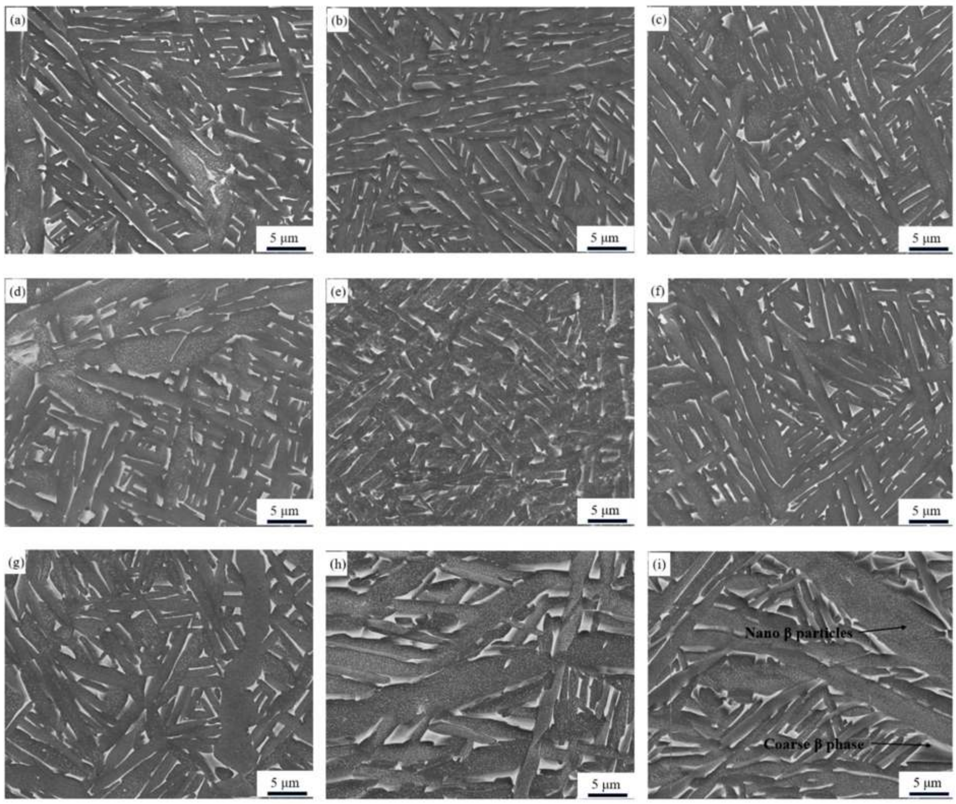

Figure 1.21. *Ti64 SEM microstructures of different HIP process parameters; (a) 910 ºC + 110MPa, (b) 930 ºC + 110MPa, (c) 950 ºC + 110MPa, (d) 910 ºC + 130MPa, (e) 930 ºC +130MPa, (f) 950 ºC + 130MPa, (g) 910 ºC + 150MPa, (h) 930 ºC + 150MPa, (i) 950 ºC + 150MPa (Lv et al., 2023)*

Apart from inducing phase and structural alterations in the material microstructure, the HIP process also contributes to the elimination of various forms of porosity within the microstructure. After additive manufacturing, there are porosities in the material microstructure that differ depending on their morphology, size and structure, which are seen in different locations.

Depending on the variability of porosites, their domains are schematized in the Figure 1.22.(Al-Maharma et al., 2020).

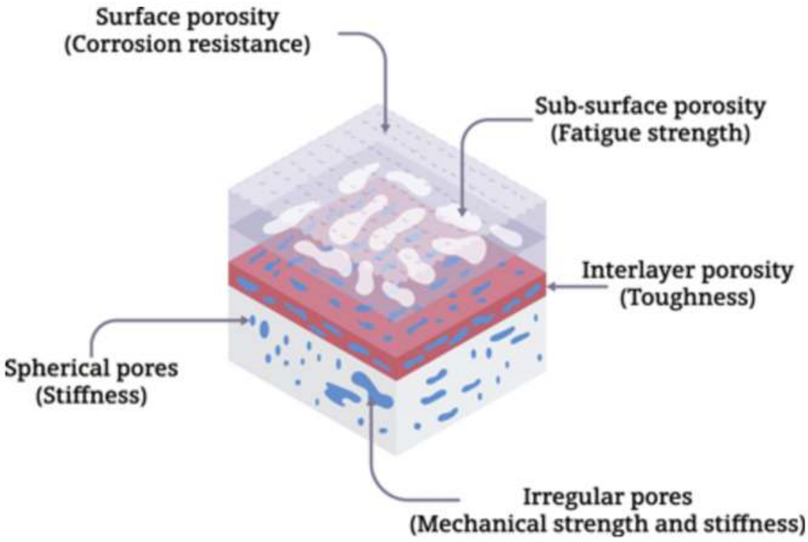

Figure 1.22. *The impact of pore types and positions on additive material's mechanical properties (Al-Maharma et al., 2020)*

Since it has been stated in different studies that sub-surface porosities affect the fatigue properties of the material, it is of great importance to predict the effects of these porosities in aviation layered parts that will work under cyclic loads and to eliminate them from the structure. It is reported that the amount of porosity coming from production after SLM is 0.49±0.17% and with HIP the porosity rate can be minimized to 0.01±0.01% (Roudnicka et al., 2019).

1.6.3 Effects of sand blasting on microstructure

Since there is a surface dominated by the distribution of adherent particles, unlike wrought alloys, which are clearly visible in the microstructure on the material surface after SLM production, studies have been carried out in the literature on the effect of the process on the surface quality after different surface improvement processes. One of the most common of these processes in the aerospace sector is sand blasting (Bernevig-Sava et al., 2019). Comparisons of the effects of different surface modification processes can be seen in the microstructures given in Figure 1.23.(Kuntoğlu et al., 2023).

Investigations concentrate on how surface roughness is affected by after sandblasting process. When the surface roughness measurement results on the material surfaces without sand blasting, single-stage and double-stage sand blasting applied after SLM production with Co-Cr alloy powder material are evaluated. It was concluded that surface roughness was reduced by sand blasting, but there were deviations in surface profile measurements due to particles adhered to the surface observed in the SEM microstructure after layered AM (Bernevig-Sava et al., 2019).

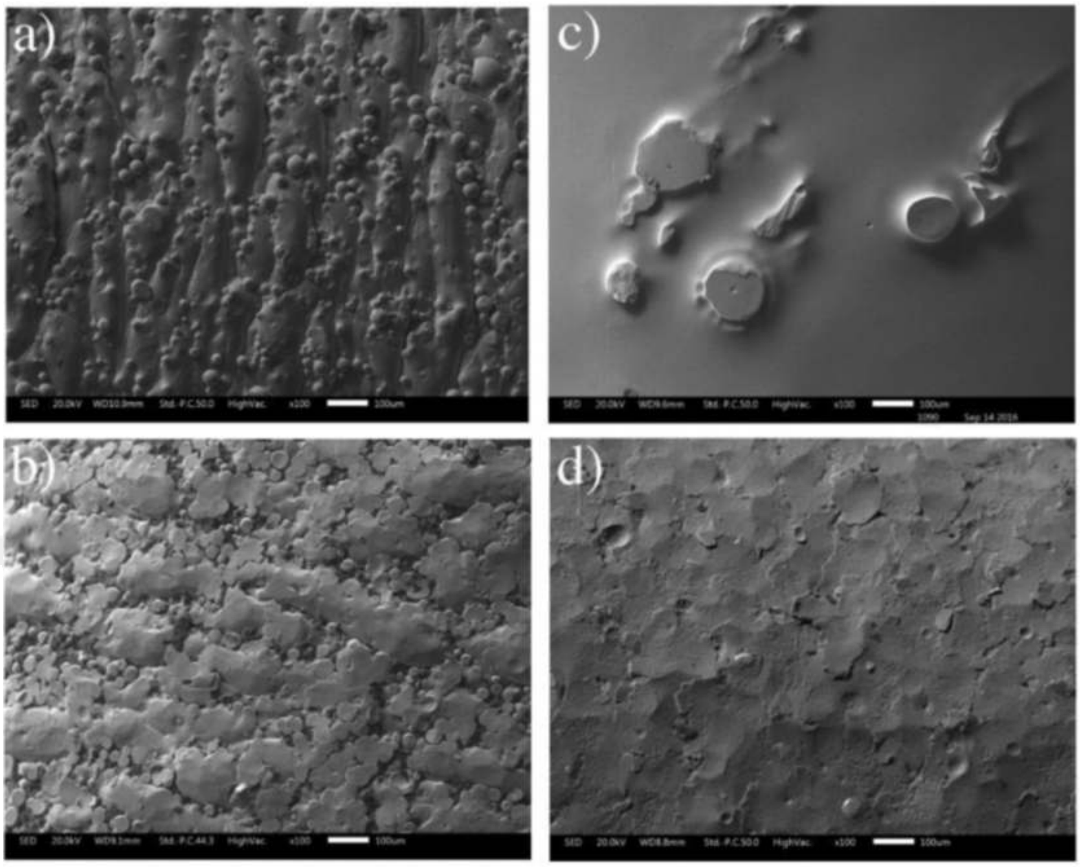

Figure 1.23. *Different proses effects on AM material (a)as-built, (b) tribofinished, (c)electropolish, (d) shot- peened.(Kuntoğlu et al., 2023)*

After AM, the inspection and quality control stages of the part must be carried out successfully, especially in the aerospace industry. However, part control becomes a challenging step due to the dust particles that create high surface roughness obtained after production. For this reason, surface modification methods also have an important place at this stage. On the other hand, due to the necessity of the produced parts to comply with design specifications and standards including mechanical/thermal/chemical properties, size and surface requirements, it reveals the need to work on new strategies in the surface texture measurement and control stages (Townsend et al., 2016).

When the surface roughness, weight loss and removal of adhered particles from the surface of various surface improvement methods such as sand blasting, chemical polishing, electrolytic polishing and abrasive flow polishing were compared, it was established that the sand blasting process achieved the best effect in terms of reducing surface roughness and mass loss.

The microstructure results of various methods obtained in the research are given in the Figure 1.24.(Lu et al., 2023).

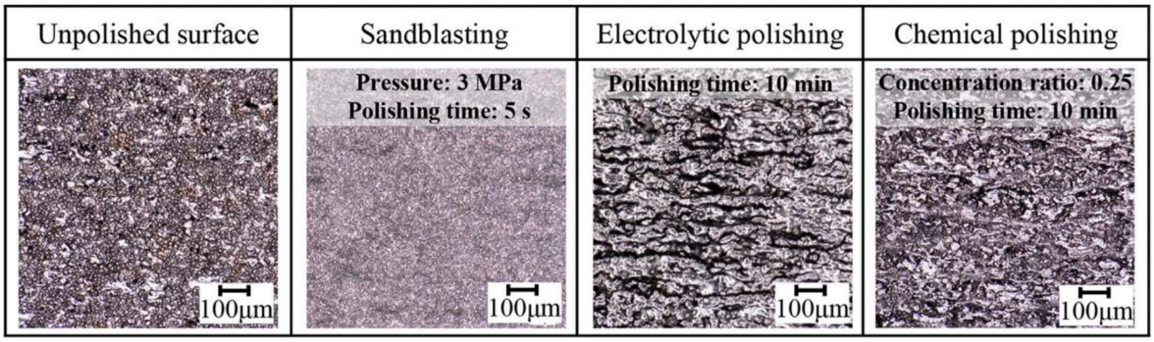

Figure 1.24. *Ti64 microstructures processed with different surface modification methods (Lu et al., 2023)*

There is a dearth of research on the combinations of mechanical and chemical surface processes in the literature, despite the fact that various processes and their effects on the material microstructure have been extensively researched. In one of the limited studies, it was observed that lower surface roughness and a homogeneous surface distribution were obtained as a result of the combined application of sand blasting, a mechanical process, and chemical etching, a chemical process. The change in microstructure for the case where three methods are applied, such as as-built, sand blasted, chemical etching, electro polishing, sand blasted and chemical etching combination, is explained as in Figure 1.25. (Longhitanoa et al., 2015)

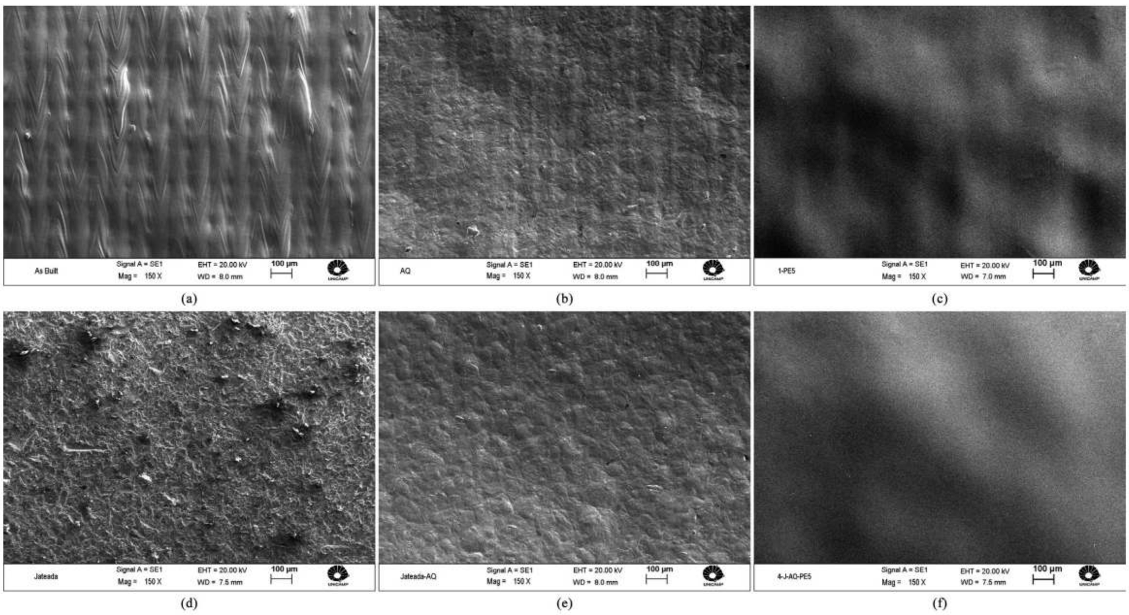

Figure 1.25. *SEM microstructures obtained as a result of the processes: As-built (a), chemical etching (b), electropolishing (c), sand blasting (d), sand blasting and chemical etching (e) and after combining the three surface process (f) (Longhitanoa et al., 2015)*

It has been stated that the same fatigue value can be achieved if the surface conditions of SLM Ti64 material are the same as conventional material forms.(Nicoletto et al., 2017) In this respect, the quality of the surface profile obitaned is important.

1.6.4 Effects of pickling on microstructure

Machinability in different materials is one of the open issues in the development of additive Ti64 parts. The outputs of variable parameters such as cutting force and cutting length depending on the different conditions of the material are finalized in the literature (Al-Rubaie et al., 2020). Although the effects of the machining process on fatigue have been studied in the literature, it is important to study the effects of different processes such as pickling (chemical milling) for surface improvement and alpha case removal operations, as the geometry of some aerospace parts is not suitable for machining. For parts with channels, complex and closed geometry parts, machining is no longer an option and is replaced by the pickling process. For this reason, literature outputs on the effects of pickling, one of the post processes studied within the scope of the thesis, on the microstructure were investigated in detail. However, there aren't many research in the literature on how the pickling (chemical milling or chemical etching) procedure affect the material microstucture of SLM Ti64 materials. Thus, it is possible to exhibit limited output results.

After SLM production, the Ti64 material exhibit a non-uniform microstructure compared to wrought/casting forms, including regions with variable grain sizes formed on the surface or unmelted powder particles shared the result section. Pickling, especially when compared with other surface treatments, is used in the aerospace industry as a method that can help correct some of these irregularities at the surface level. However, it is stated in the study results that pickling generally does not significantly affect the main material microstructure that remains far below the surface of the material. The effect of the pickling process on the material microstucture can be generally summarized as grain boundary and surface textured refinement. In the Figure 1.26., electron microscope results of the pickling process using only HF acid and HF+HNO_3 are shared. It is evident that the surface profile obtained is influenced by the type of acid used in the process as well as the relative amounts od the acid solution (Fraczek-Szczypta et al., 2017).

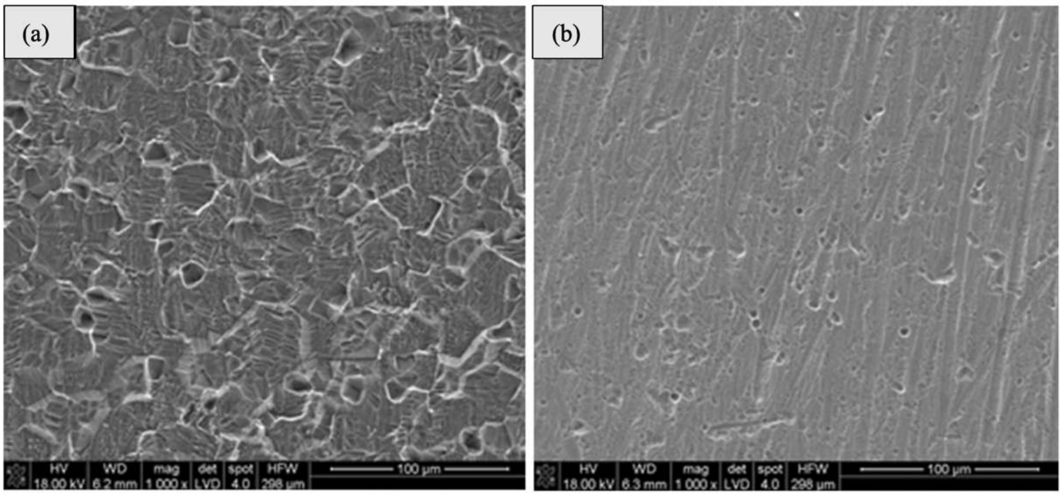

Figure 1.26. *Titanium substrate following pickling: only 5% HF pickling etchant (a), combination of HNO3+HF etchants (Fraczek-Szczypta et al., 2017)*

1.7 Fractography Analysis and Post Process Effects on Fatigue

Tensile and fatigue sample fracture analysis using fragmentography enables to identification of the microstucture based influencing factors, common fracture features and temperature related variations. For this reason, after the mechanical testing of Ti64 SLM materials subjected to various post processes, the fracture surfaces of the the test samples are examined and the research results are tried to be correlated.

Following the tensile tests on the as-built samples, the fracture surfaces exhibit a dimple rapture linked to pore coalescence and a ductile mode, as well as a cup and cone shaped necking zone (Gorsse et al., 2017). The fracture surface microstructure of as-build Ti64 SLM material given in Figure 1.27. (Krakhmalev et al., 2016).

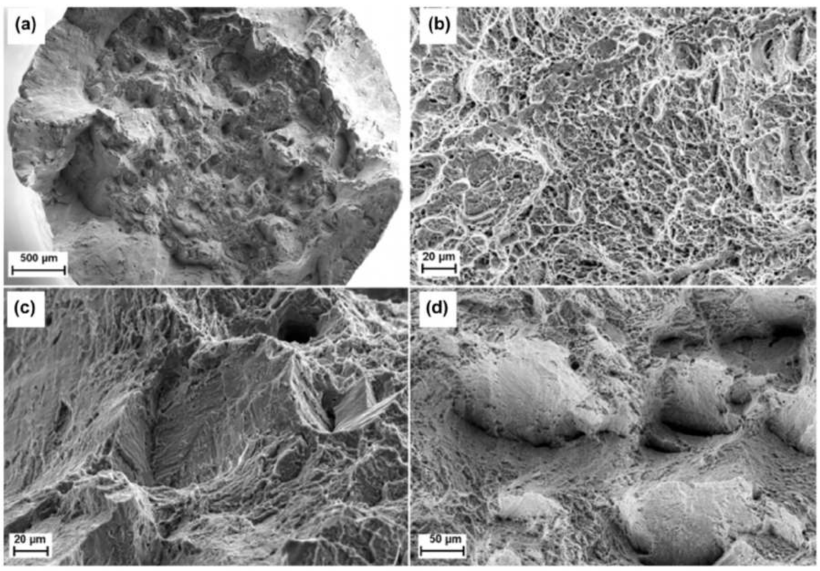

Figure 1.27. *Ti64 SLM tensile test coupon fracture surface SEM microstructure (a)cup and cone, (b) dimples, (c)-(d) quasi-cleavage facets.(Krakhmalev et al., 2016)*

When the as-built microstructure fracture surfaces are examined, it is stated that the striations and deep dimples formations in the microstructure exhibit lower ductility and therefore a poor fatigue crack growth behavior compared to heat treated and HIP conditions (ZHANG et al., 2019). A comparison between as-built fracture surfaces and stress relief samples reveals that the stress relief material has very fine grained structure, highlighting the impact of heat treatment. The Hall-Petch equation states that a lower grain size strengthens material by creating more graing boundaries and limiting the dislocation movement. However, after heat treatment, high dislocation density vanished, the number of twins drastically dropped and the sample's strength reduced concurrently with a portion of the unstable α' phase changing into an $\alpha + \beta$ phase (He et al., 2019).

It is reported that upon comparison of the as-built and HIP fracture surfaces, the samples applied with HIP+PL exhibit a fracture surface that significantly thinner, more consistent and ductile dimpled fracture morphology than the as-built condition. Additionally, the influence of HIP has greatly decreased amount of voids in the samples, with dimples mainly controlling on the fracture surface. This difference in fracture surfaces is illustrated in Figure 1.28. (Jamshidi et al., 2020)

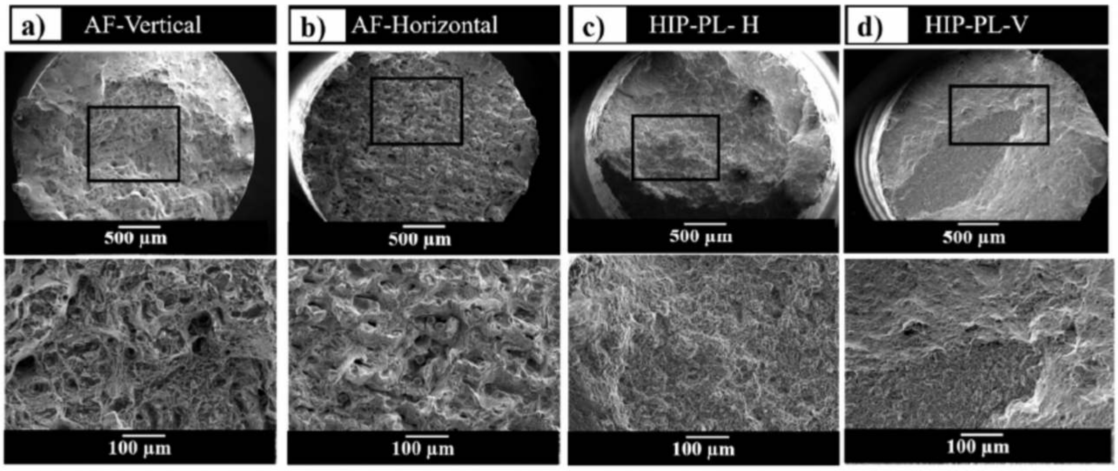

Figure 1.28. *Tensile fracture surface of Ti64 SLM (a-b) as-built condition vertical and horizontal sections (c-d) HIP + polished veritical and horizontal sections (Jamshidi et al., 2020)*

In the research conducted on fatigue coupons, the internal defects and surface conditions of the samples were evaluated and the fracture surfaces obtained as a result of post-processing were compared. As a post process, when the effects of two different machining parameters, HIP and chemical etched (pickling) processes, on surface roughness and sub-surface porosities are evaluated, the fatigue performance is concluded that HIP + deep machining method> deep precision machining without HIP> HIP + chemical etching > chemical etching > HIP +shallow machining > shallow machining >

as-built condition. The variability of fatigue behavior resulting from the microstructure formed by machining, etching and HIP is given in Figure 1.29.(Sun et al., 2020). When the different post process effects are evaluated, the positive effect of deep machining and HIP processes on fatigue is evident.

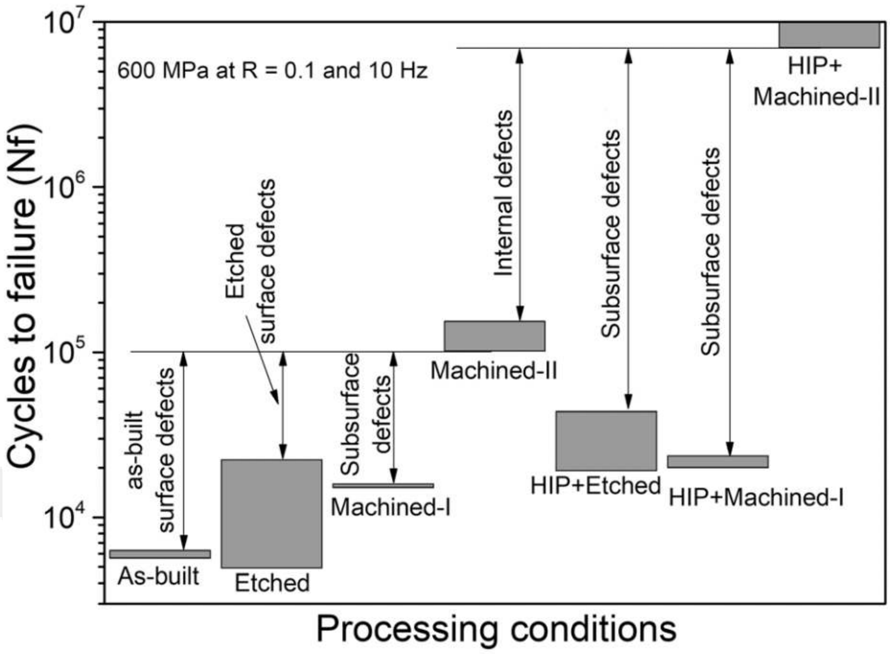

Figure 1.29. *Variability in Ti64 fatigue performance under 600 MPa, 0.1 R ratio as a function of surface or subsurface defects (Sun et al., 2020)*

The effects on different HF-HNO_3 concentrations on surface roughness and fatigue have been studied in the literature. It was emphasized that it effectively removed sintered dust particles at all solution concentrations. In the experiments carried out at different HF concentrations, it was observed that the samples with polished surfaces had higher fatigue strength and less surface crack inititation points than the samples with the as-built surfaces. While an increase was observed between the fatigue strength up to certain limit depending on the HF concentration, no statistical significance was detected after a certain limit. The fractographs have arrows indicating the locations of crack initiation sites. The fracture surface of as-built specimen show many starting sites around the specimen edges represented Figure 1.30. (a-b). On the pickling specimens represented Figure 1.30. (c-h), the visible initiation site were decreased three or less compare to the as-built specimen. At the same time, the fracture surfaces of the mechanically polishes specimen shows that Figure 1.30. (i-j). The results demonstrated the specimens have different failure mechanism in which the dominated by the internal defects (Bezuidenhout et al., 2020).

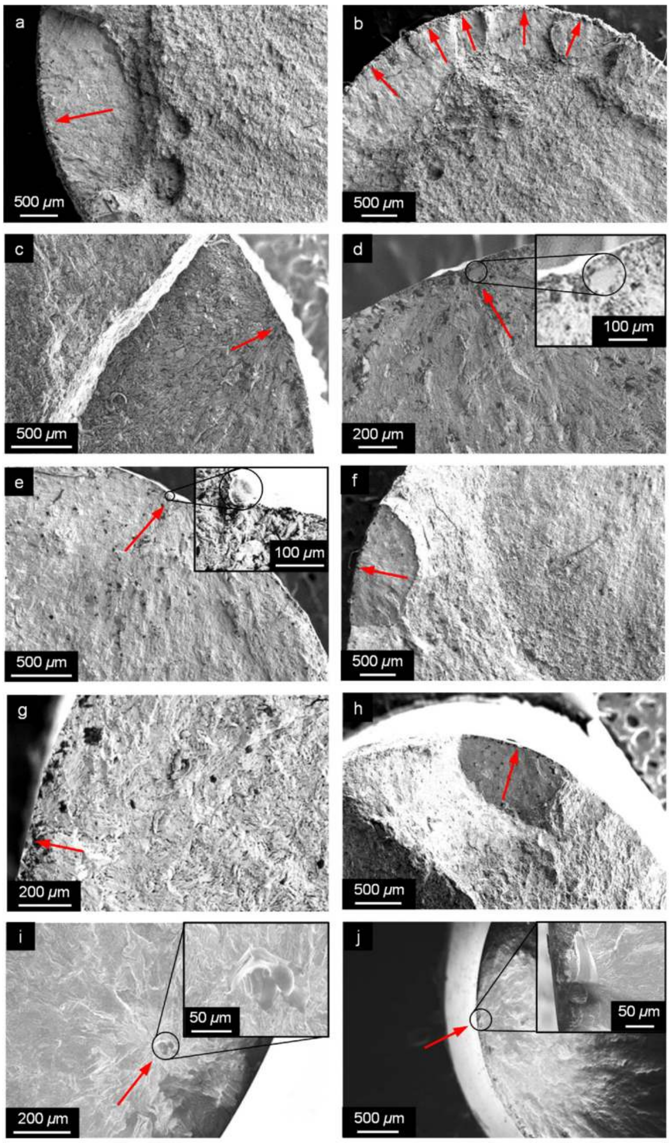

Figure 1.30. *The SEM images of the tensile fatigue specimens of (a-b) as-built, (c-h) pickling, (i-j) mechanically polishes specimens (Bezuidenhout et al., 2020)*

2. THE AIM OF THE STUDY

The studies carried out within the scope of thesis primarily aimed to optimize the processes of part produced with the SLM Ti64 process, which is one of additive manufacturing methods that has been trending in recent years for the aerospace parts. The process parameters of the processes studied in the test and characterization matrice determined for the experimental phase of the thesis were determined in accordance with aerospace standards and company process experiences. It was aimed to achive standardization in terms of parameters for the company practices.

The unique part of the thesis study when compared with the literature research, is the determination of the process flow for removing the alpha case layer thickness formed on additive manufactured parts in aerospace engine parts and and the study of the impact of alpha layer, which is critical in terms of mechanical properties. In the aerospace sector, the advantages of the additive manufacturing method in production of complex geometries and preference of titanium material for its weight advantage gaining great importance. However, in titanium parts with complex geometries, it brings major drawbacks such as alpha layer together with the heat treatment applied in order to obtain the ideal material properties specified in the thesis. The chemical etching process and other machining processses do not work completely in complex geometry. Therefore, there is a great uncertanity about the additive manufacturing parts with alpha layer and its mechanical effects. In this case, it was included in the thesis because it was determined as a study that limits the potential of the additive part in the engine and needs to be clarified.

The process flows determined as a result of the thesis study and the effects of the post processes to be applied are aimed to shed light on the evaluation of the part in the production and additive manufacturing part design stages. The intention of the thesis process flow determinations and the impact of the post process techniques to be used is to provide insight into the part assessment during the production and additive part design stages.

3. EXPERIMENTAL PROCEDURE

The specimens designated for post process treatment were manufactured under an argon atmosphere. In addition to having dual yttrium fibre laser system, the machine can capable of heating the build plate up to 200°C. The parts were manufactured utilizing 33 J/mm3 volumetric energy density. The scan direction of the parts was not aligned with the direction of gas flow within the process chamber. The process was performed below an oxygen content of 1000 ppm.

Ti6Al4V ELI powder with particle size distributions from 15 to 63 microns was used for completing the fabrication process. The produced samples comply ASTM F3001-14 requirements. The tensile specimens fabricated in the XY and Z build direction and the fatigue specimens were manufactured in the Z build direction. HIP and alpha case specimens fabricated in Z direction. The build orientations of the fabricated specimens are listed in Table 3.1. All specimens are shown in Figure 3.1.

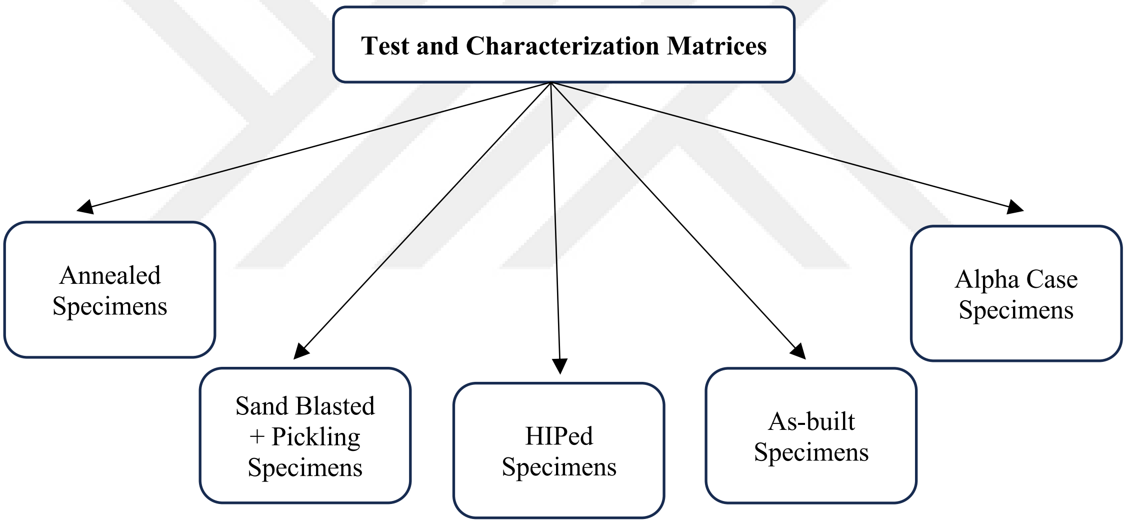

Figure 3.1. *Test and characterization matrices of the thesis*

Table 3.1. *Mechanical test and characterization specimens build orientations*

Specimen	Build Orientation
Annealed Specimens	XY and Z
Sand Blasted + Pickling Specimens	Z
HIPed Specimens	Z
As-build Specimen	Z
Alpha Case Specimens	Z

Some of mechanical test specimens produced for the thesis study are represented in Figure 3.2. In order to investigate the effect of the test geometry for mechanical tests in the thesis study, tests were carried out on both flat and round specimens. At the same time, some of coupons were extracted from a additive part selected as a candidate and included in test matrice. Flat and round specimens used in tensile testing, and images representing round specimens used in fatigue tests are also shared in Figure 3.3. The aim here was establish a correlation of the mechanical properties of the test specimen positioned on the build substrate and the produced part.

Figure 3.2. *Some of mechanical test coupons produces for the thesis study*

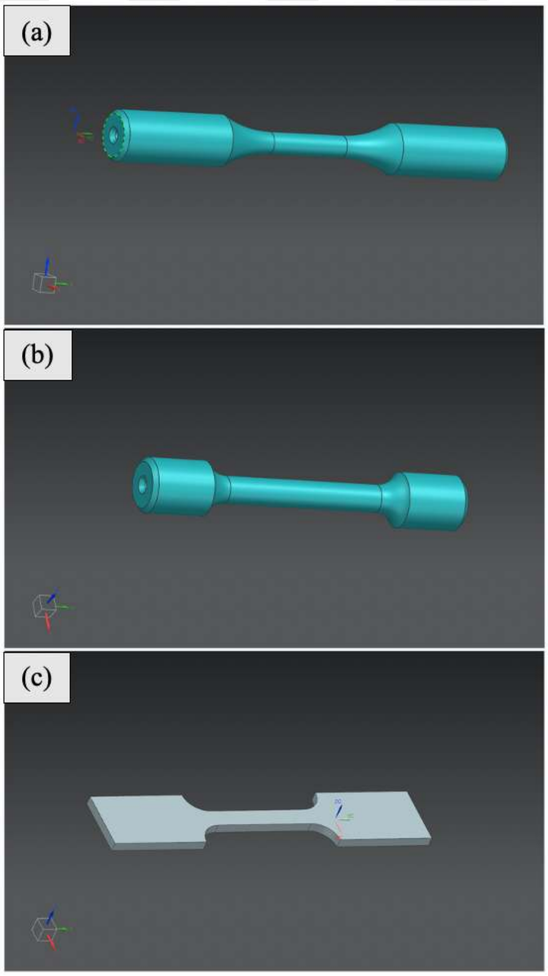

Figure 3.3. *Round test specimen geometry used in fatigue tests (a), round and flat test specimen geometries for the tensile tests (b) and (c)*

Zwick Roell Z100 was used for tensile tests and Zwick Vibrophore 100 was used for fatigue tests. In the thesis study, in addition to tensile and high cycle fatigue mechanical test, microstructural examination (optic microscope and SEM), XRD analysis, microhardness measurement, porosity measurement and examination of fracture surfaces of the fatigue test specimens (Stereo microscope and SEM) were carried out for characterization. Hardness measurements were performed using an Falcon 500 device, optical microscope examinations were performed using a Nikon Eclipse MA200 and SEM characterizations were performed using a HITACHI SU5000 scanning electron microscope.

The process flow in the experimental matrix determined within the scope of the study was starts SLM production. Afterwards, the coupons and mechanical test samples (except for as-built microstructure coupons) were applied to the 2 hours annealing heat treatment at 704 °C together with the build substrate in accordance with the Heat Treatment of Titanium Alloys Parts AMS 2801C and Heat Treatment of Titanium and Titanium Alloys AMSH81200 standarts. The proses flow chart of the mechanical test, microstructure coupons and witness coupons, exclusing the post processes, are given Figure 3.4.Within the research, fatigue test performed to meet ASTM E466 and tensile tests were performed to meet ASTM E8 standards. Figure 3.5. illustrate a view of round fatigue test specimens that were produced for the thesis.

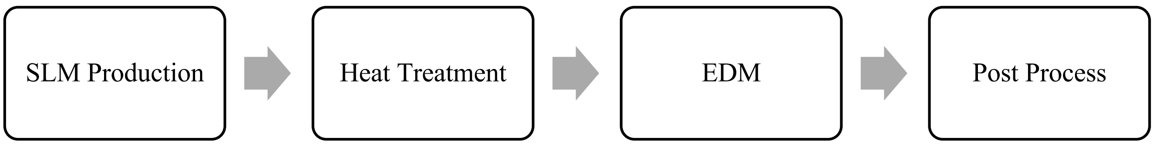

Figure 3.4. *Process flow chart*

Figure 3.5. *The some of fatigue test specimens produced for the thesis after SLM production.*

Specimens representing the machined specimens of final dimensions in accordance with the test standards to be applied by machining from round specimen geometry are shared in Figure 3.6.

Figure 3.6. *Machined specimens for fatigue and tensile tests*

After the annealing heat treatment of the samples specified as pickling specimens in the test matrix, were separated from the build substrate. Then, sand blasting process was applied to the test samples and microstructure coupons. Three different sand blasting parameters were tested on microstructure coupons. A sand blasting parameter determined according to the surface roughness and etch rate levels symbolizing the activity of the pickling process was used in the thesis study. The sand blasting process was carried out in accordance with MIL-STD-1504 specification.

Sand blasting machine was used for parameter studies. The sand blasting parameters are shared in Table 3.2.

Table 3.2. *Sand blasted process parameters*

Media Type	Pressure (Bar)	Automatic or Manual Process
Alumina	4 Bar	Automatic process

The samples referred to as HIPed specimens were subjected in the experiment matrix, similarly the other samples, to an annealing heat treatment together with the build substrate. Following that using the process parameters listed in Table 3.3., the HIP process was carried out. The HIP process parameters are in accordance with the parameters specified in the ASTM F3001 specification and were determined as a result of many parameter studies highlighted in the literature section of the study.

Table 3.3. *HIP process parameters*

Temperature	Pressure	Duration
920 ºC ± 10 ºC	Min. 100 MPa	180 min ±10 min

After the HIP process, the coupon images were shared in Figure 3.7. The specimens were then machined to remove the alpha layer on the coupons and bring them to the final test geometry.

Figure 3.7. *HIPed specimens after HIP process and before the machining*

The pickling process was carried out in titanium pickling tanks of TEI Chemical Operations Directorate. The ASTM B600 Descaling and Cleaning Titanium ans Titanium Alloy Surfaces specification was utilized for the pickling process. Nitric acid (HNO_3) and hydrofluoric acid (HF) solutions were used in the etching tank as specified in the specification. While the mechanical test specimen and microstructure coupons were being processed, the process was carried by measuring the bath etch rate using witness Ti64 sheet coupons. Optical microscope was used on the coupons and test specimens for material microstructure and alpha case layer examination. Figure 3.8.

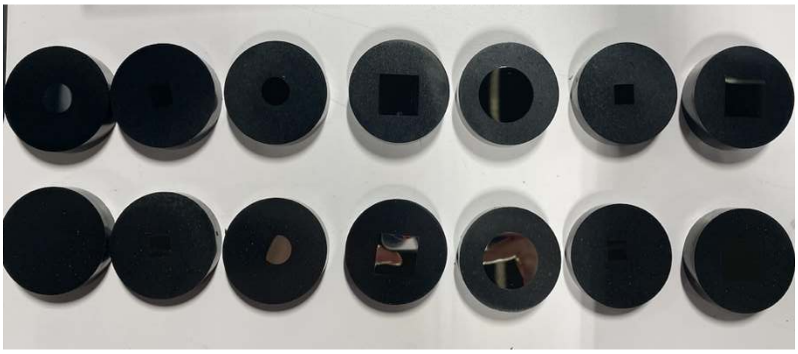

Figure 3.8. *Microstrcuture coupons for optical microscope and SEM examinations*

The fracture surfaces of the samples from the fatigue test have been examined employing the a stereo microscope in order to comprehend the post process impacts. The gauge regions was examined at 20x and the radius regions on the fracture specimens were observed at 10x magnification. The fracture surfaces of all samples in the test matrice were investigated and a image representing some of coupons examined is shared in Figure 3.9.

Figure 3.9. *Some of fatigue coupons whose fracture surfaces were examined*

Selected fatigue test samples were examined on scanning electron microscopy at TEI. For the SEM characterization, beam potentials of 3kv and 15kv were utilized for secondary electron detection. Before imaging the fracture surfaces the specimen cleaned by ethanol.

4. RESULTS AND DISCUSSION

4.1 Microstructure Examinations

SEM and optical microscope analyses of each instances were carried out in order to comprehend and connect to impact of the post treatments examined for the thesis in the material. As-built microstructure is exhibit a propensity to develop in the direction of production and is characterized by columnar β grains. The rapid cooling process unique to SLM enables the β phase, which is mainly responsible for the martensitic transformation in Ti64, to transform into alpha prime martensite (α') phase. The subsequently created microstructure in as-built condition which is typically thin and needle-like, is given Figure 4.1. In optical microscope microstructure, the α phase typically appears as light gray or white color. Although, it varies depending on the metallographic preparation and etching techniques, the α phase generally stands out against the darker background of β phase. Alpha phase becomes more identifiable by increasing the contrast between phases.

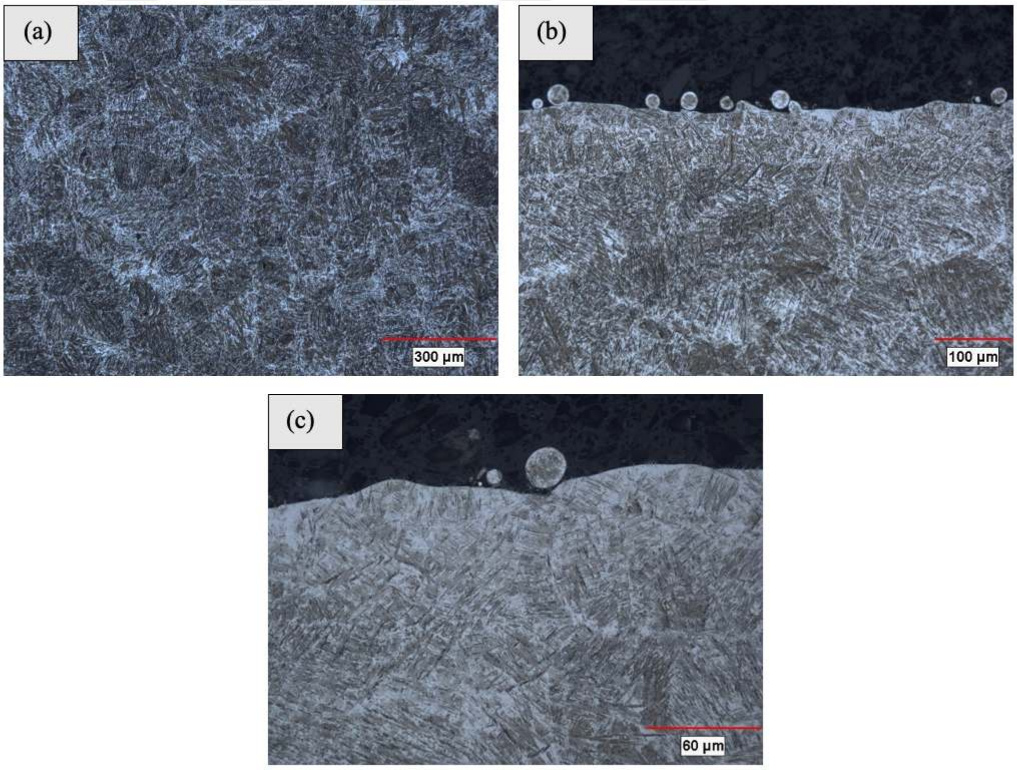

Figure 4.1. *As-built SLM Ti64 microstructure a) 100x, b) 200x and c) 500x*

The Figure 4.2. SEM microstructure taken at 500X magnification effectively illustrates the needle-like phases that have formed. Contrast is due to the electron beam interaction, with α phase appearing brighter in SEM microstructure due to its higher atomic density compared to the β phase. The β phase tends to appear darker than the alpha. Alpha prime martensite and alpha phases, which are formed due to the rapid cooling condition provided in SLM production and whose existence is mentioned in as-built microstrucure, are different from each other even though they share same HCP structure. While the α phase forms with a stable arragement below 882 ºC with slow cooling, the α' martensite is a metastable phase the distrorts the HCP structure obtain under diffusionless rapid cooling conditions. When two are compared, it can be said that they have differences in terms of formation mechanisms, stability and microstructural morphologies. α' needle like phase is clearly observed in SEM microstructure shared below. It forms α phase in areas that lighter in color and have more uniform appearance.

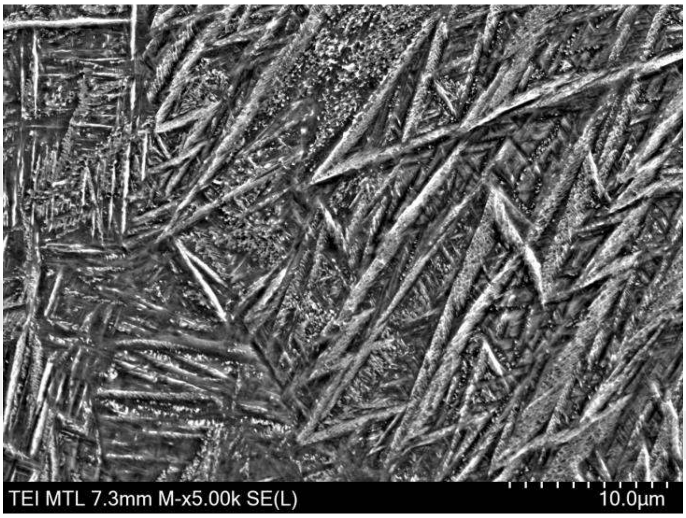

Figure 4.2. *SEM microstructure at as-built condition*

This martensitic transformation contributes to the improved mechanical properties of the material such as increased strength and hardness, which also affecting material ductility, the microstructure results in as-built condition were characterized within the scope of thesis. As stated in literature research findings, no mechanical test study was carried out for the experimental procedure since the material's low ductility behavior in as-built condition is often at an undesirable level in aerospace parts due to its microstructure. When the relationship between literature mechanical properties and thesis microstructure results is established, it shows that the martensite phase, which is a metastable phase observed in as-built condition, should be brought a stable and ideal state by applying the post processes.

The Figure 4.3. indicates the optic microscope result of the material that had annealing heat treatment, one of the processes examined in the thesis study to the achieve the optimal condition of the martensitic formation in the microstructure. For two hours the material was annealed at 704 ºC, it was observed that the martensitic structure obtained at as-built condition began to disintegrate when a some part of martensite phase decomposed into the equilibrium α+β phase by the α phase nucleation. The microstructure still possesses a martensitic phase but the α+β phase balanced is also maintaned.

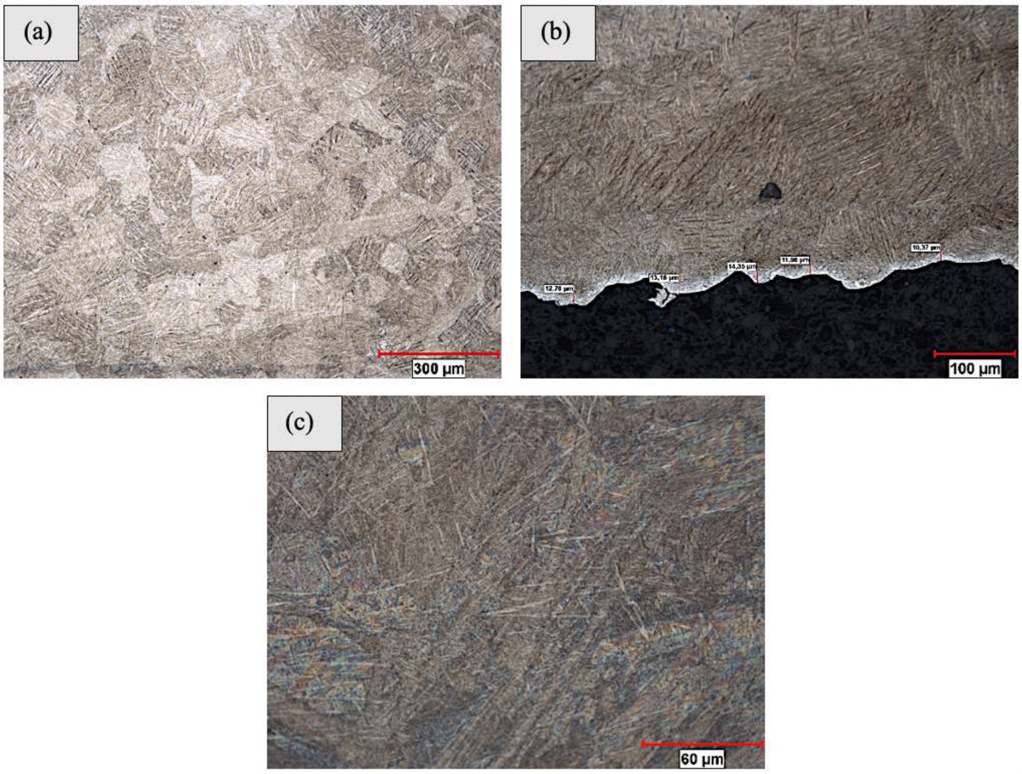

Figure 4.3. *Annealed SLM Ti64 microstructure a) 100x, b) 200x and c) 500x*

Annealed Ti64 SLM SEM microstructure are given in Figure 4.4. It observed that in characterization studies that the β phase become more dominant in microstrucure compare to the as-built microstrucure.

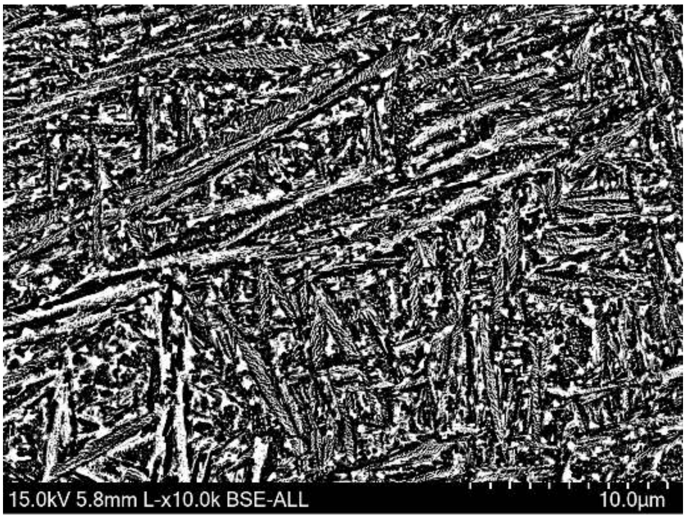

Figure 4.4. *SEM microstructure at annealed condition*

The optic microscope microstructure after HIP is given in Figure 4.5. As the material reached below the β transus temperature during the HIP process following the annealing, some of β phase transform into the α phase. It can be interpreted from the results that a more balanced α/β phase distrubution is exhibited with a decrease in the martensitic microstructure compare the as-built microstucture. The phases become more equiaxed rather than elongated.

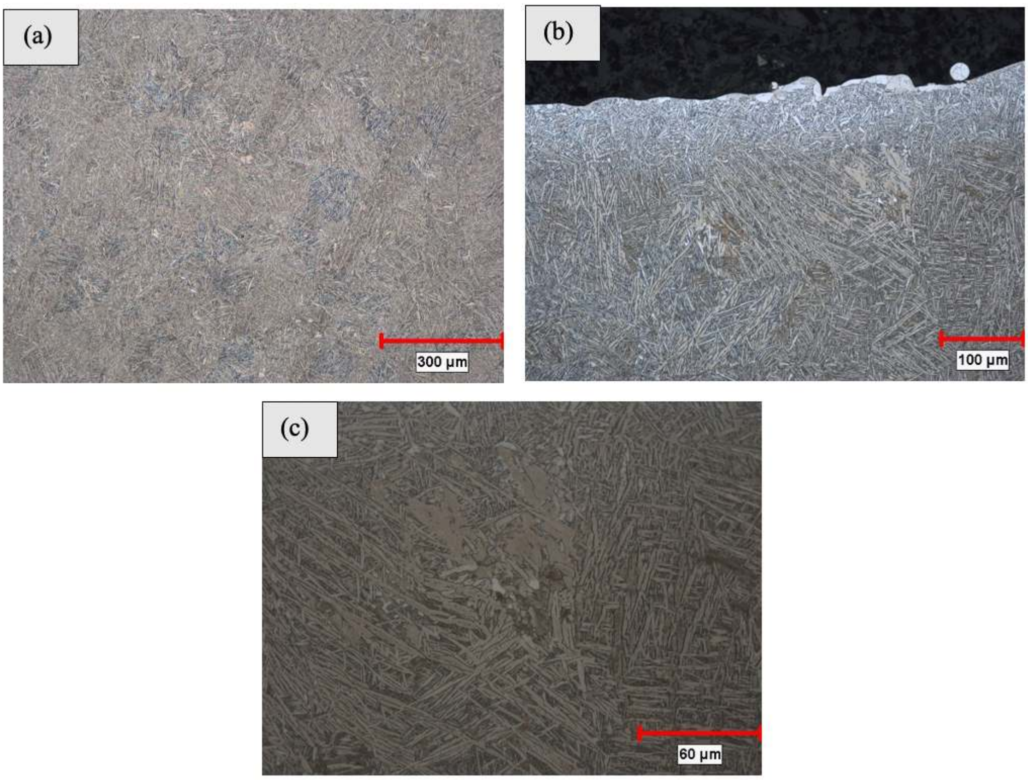

Figure 4.5. *HIPed SLM Ti64 microstructure a) 100x, b) 200x and c) 500x.*

In comparison the annealed condition when the martensitic transition temperature is exceeded for the HIPed material, the SEM microstructure of the case where the martensitic structure has been entirely eliminated is shown Figure 4.6.

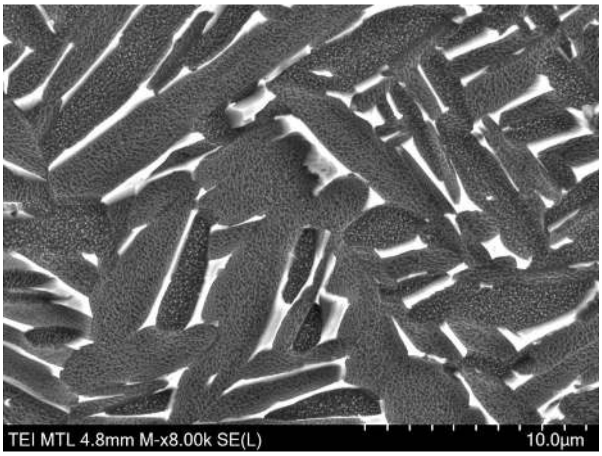

Figure 4.6. SEM microstructure at HIPed condition α/β equiaxed microstructure

The microstructure of the material to which the sand blasting process, one of the post processes studied within the scope of thesis, was applied is given in Figure 4.7. As a result of the microstructure studies, it was concluded that the sand blasting process has an effect on removal of the semi-molten dust particles observed on the surface of the materials as a result of additive manufacturing. The effect of this improvement on the microstructure of the material on mechanical and chemical processes is given under other topics added in the conclusion section.

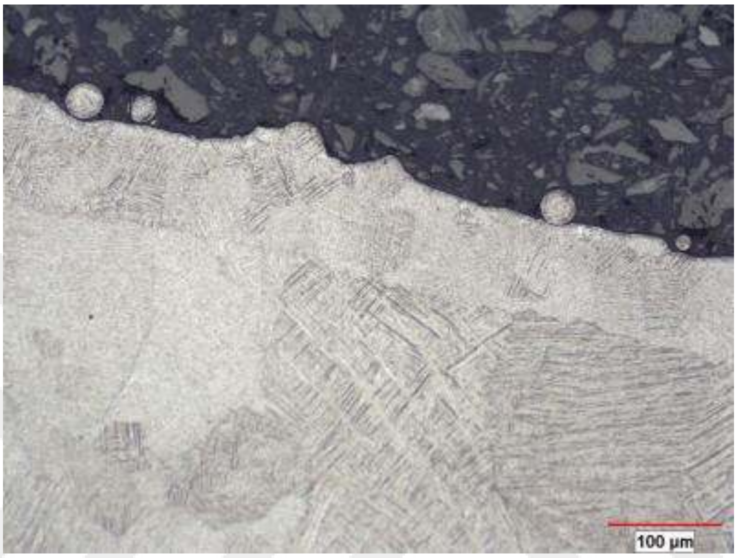

Figure 4.7. *Sand Blasted SLM Ti64 microstructure 200x magnification*

Due to the oxygen affinity of the titanium alloys, the alpha layer formed on the surface of the material. In the thesis study, focusing on a part process to be produced for use in aerospace engine. Considering the determined process flow, the material subjected to a heat treatment together with the build substrate. It is observed that the thickness of the alpha case layer structure formed on semi-molten powder particles and high rougness surface of the additve material is not homogeneous compare to the casting and forging forms. For this reason, coupons on the resulting irregular and non-uniformly thick alpha layer are included in the thesis test matrice.

The optic microscope microstructure of the alpha layer formed on a mechanical test and microstructure coupons are given in Figure 4.8.

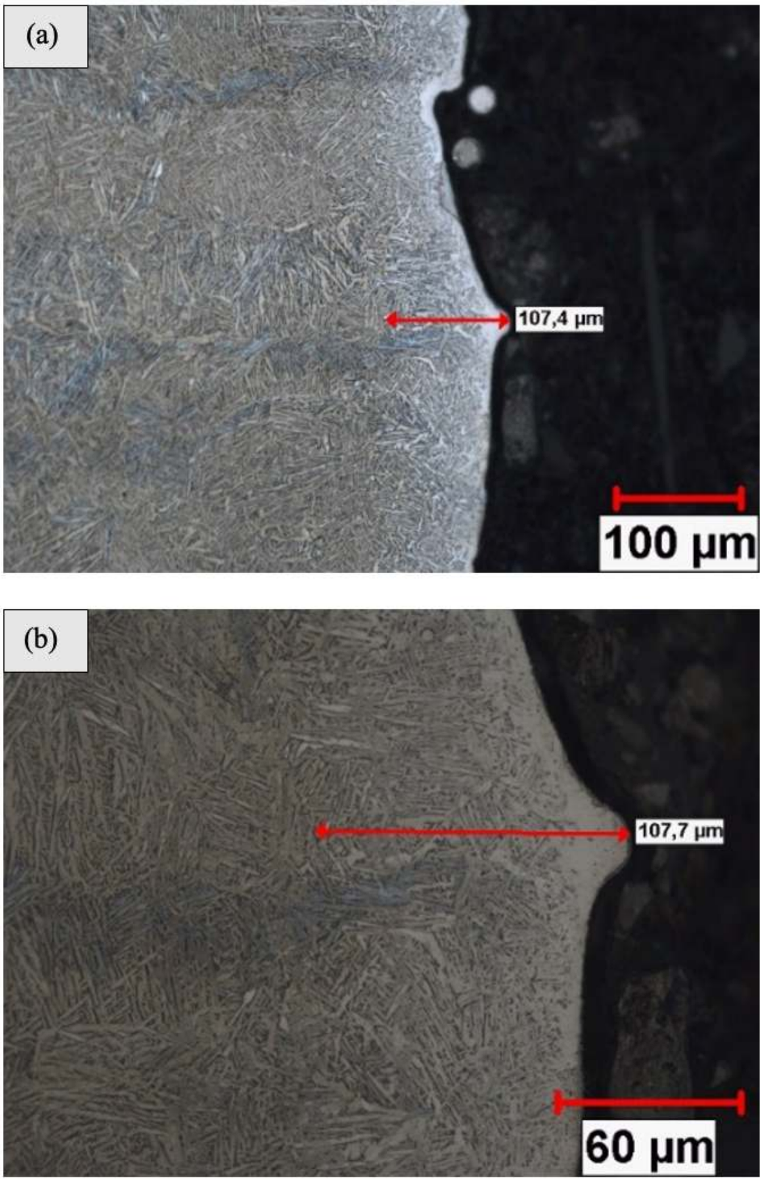

Figure 4.8. *Alpha case layer microstructure after heat treatment 200X (a), 500X (b)*

Due to the high reactivity titanium at high temperatures, the SEM microstructures of alpha case layer that formed during when oxygen easily diffuses to the surface during the annealing heat treatment applied in the process flow. It was detected that a study was needed in order to achieve a clear result in the microstructure studies due to the non-homogeneous of surface and the fact that it varied depending on the part geometry. Since the amount of alpha alyer affects the flow of alpha layer removal processes that will be neccessary after annealing heat treatment, a coupon study was carried out in order to observe the repeatibility of the formed layer.

4.2 Stereo Microscope Fracture Surface Examinations

Since the aim of the study was primarily to investigate the effect of various final procedures applied on mechanical properties, the fracture surfaces of the test specimens were examined for a more comprehensive examination and to identify differences. The selected test specimens for each processes were examined under a stereo microscope for initial evaluation. Fracture analysis studies were carried out on the basis fatigue test coupons. Examinations were completed for each coupon for each fractured surface. SEM analysis was done in further detail, and the outcomes are discussed below.

Fracture was typically observed in gage section, according to the results of fatigue test coupons in the XY and Z directions. These coupons were manufactured in cylindirical form and anneal heat treated with build platform following the production. After the coupons were seperated from the build substrate, the final test test coupon gemetry was machined. Since the was performed with a machined surface profile, surface rougness resulting from SLM manufacturing was eliminated for this test group. The results depending on the direction were compared and evaluated according the result of coupons produced in both directions.

While the fracture zone in XY direction annealed coupons generally occured in gage section. The image of the coupon showing fracture behavior from the gage region is given in the Figure 4.9.

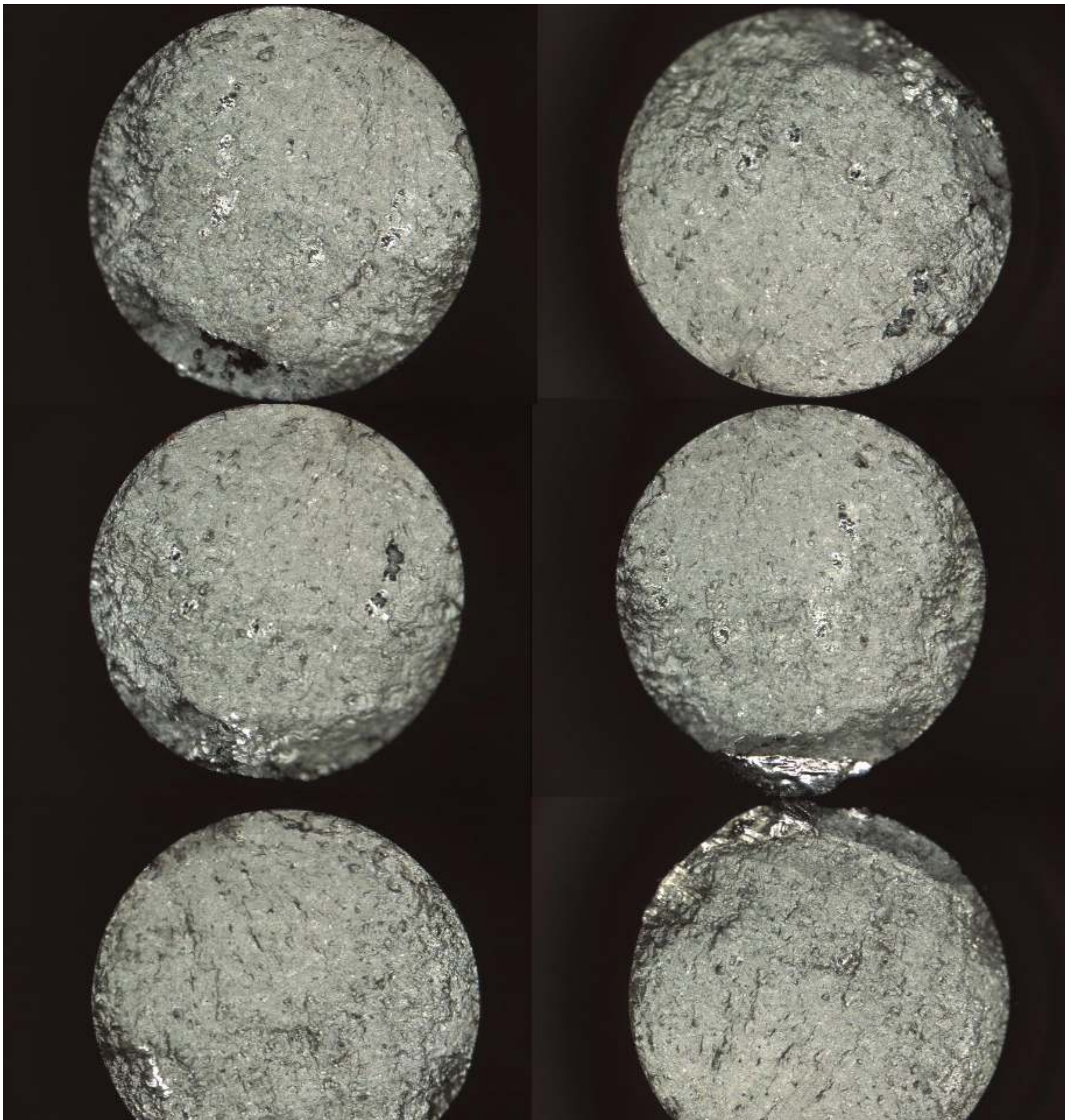

Figure 4.9. *XY direction annealing heat treated fatigue specimens fracture surface*

Fracture observed in a few coupons from radius and thread sections, which is not observed in Z direction coupons. Coupons fractured from the thread and radius reigons are test coupons belonging to the moderate stress level applied in the test matrix. While the situation was not observed coupons tested at higher stress levels, the change in fracture locations in coupons at lower stress levels indicates that the fracture characterization should be examined in more detail and the root cause should be investigated. It is interpreted the different fracture locations indicate in the Figure 4.10. may be due to an inconveience in the material microstructure resulting from the process and machining method.

Figure 4.10. *Z direction annealing heat treated fatigue specimens from radius and thread sections*

When the condition of sandblasted Z direction fatigue coupons after the test was evaluated, the fracture occurred in the gage region in different test parameters. In two coupons, the fracture initiated in the radius section. A detailed examination was made on these coupons in SEM. In this test group, the condition of part after the sand blasting and pickling processes utilized following production was considered and machining was not applied. Therefore, the impact of the sand blasting process on the surface was expected to be seen in gage section compared to the annealed machined test specimens. The radius regions have undergone machining in order to verify the ASTM E466 coupon geometry. Consequently, the impact of notch effect resulting from this machining on the fracture is evident in this area. The fracture surface of the specified coupons are given in Figure 4.11.

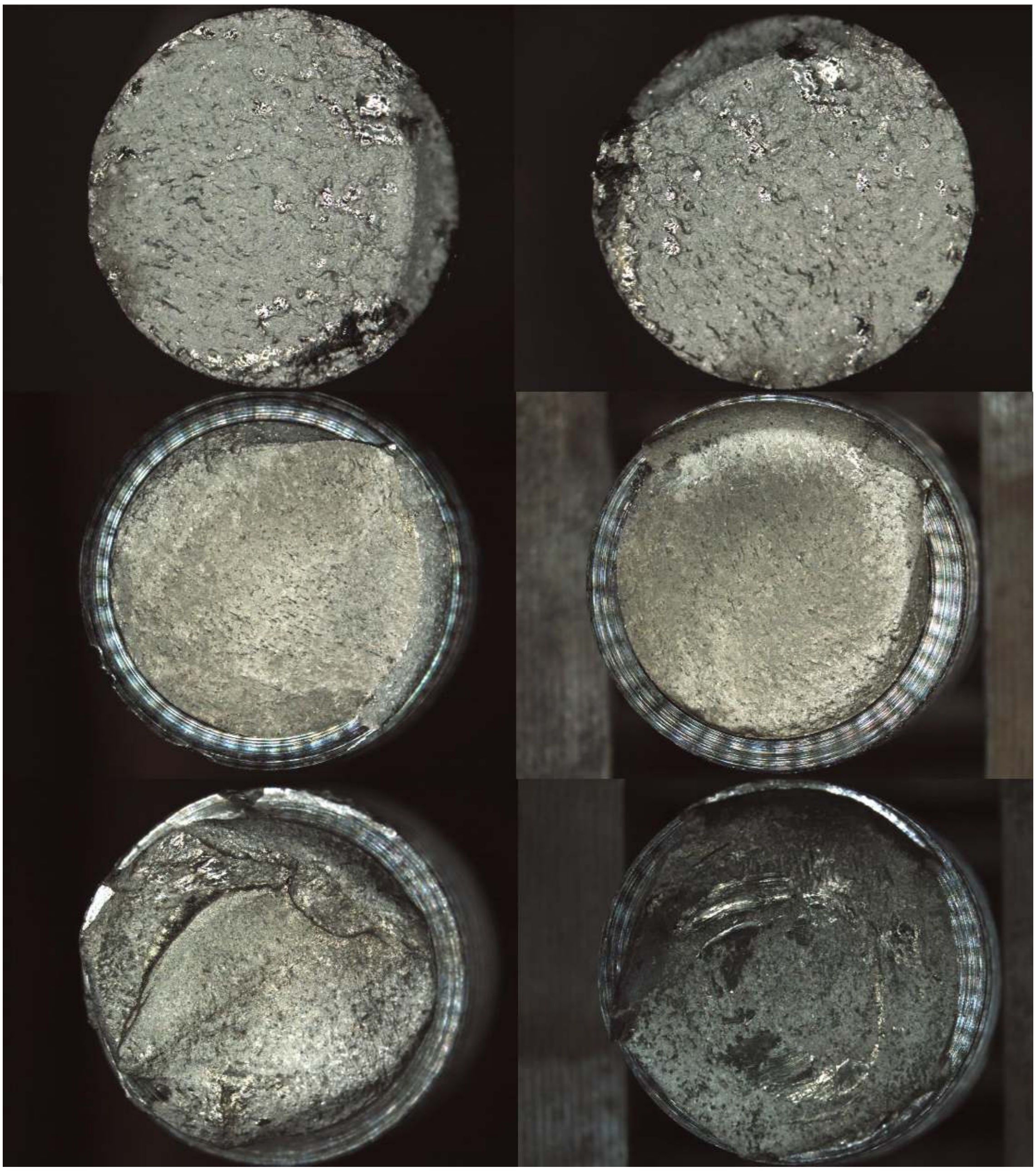

Figure 4.11. *Z direction sanblasted fatigue specimens from radius and gage sections*

In the test group of fatigue coupons to which HIP was applied, it was observed that in a few coupons, except for the coupons that had run out, there was only rapture in the radius region. Coupons that have been HIPed and failed by fractured from the radius region are given in Figure 4.12.

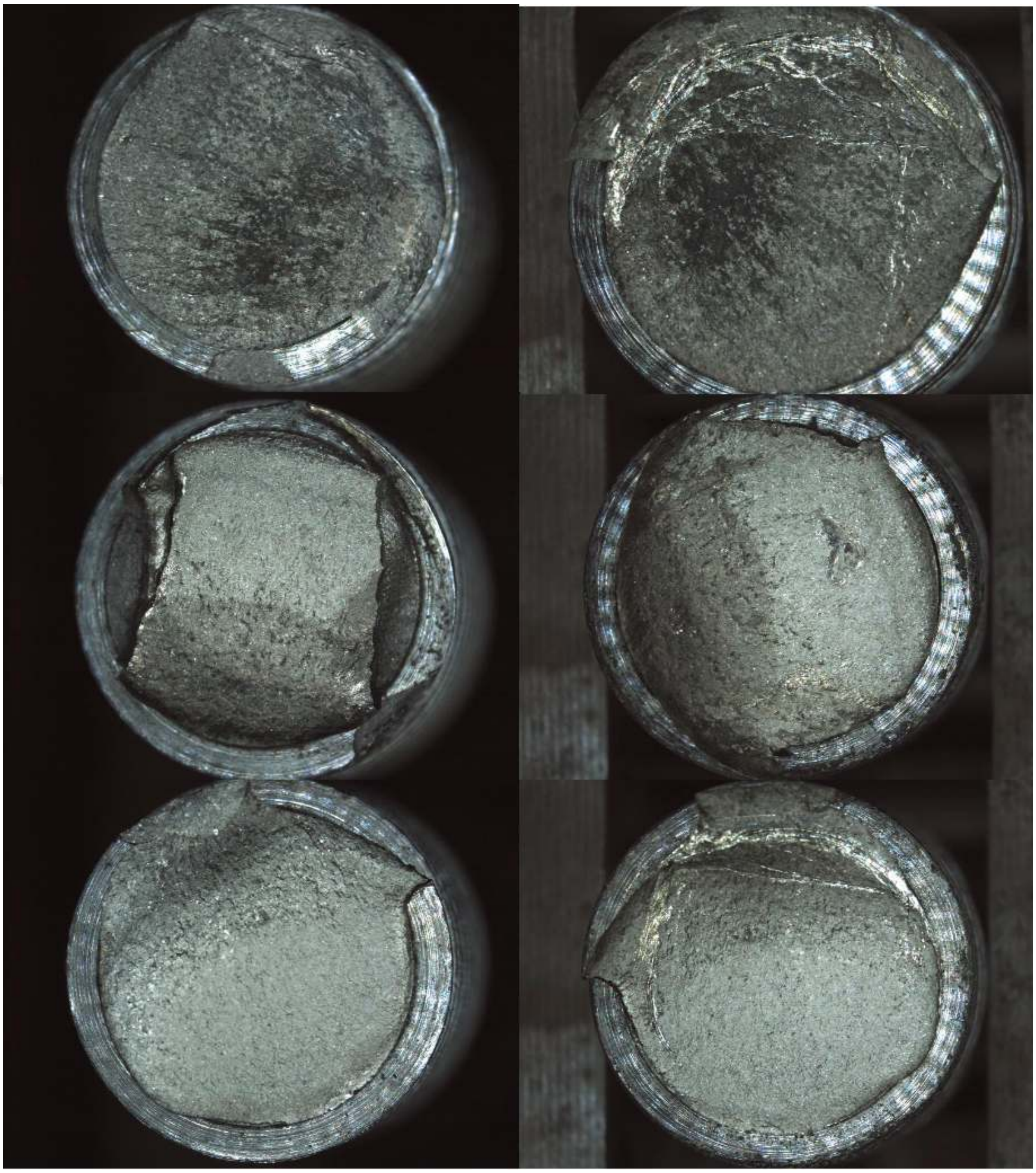

Figure 4.12. *Z direction HIPed fatigue specimens from radius sections*

The propagation of the crack, which initiation from the radius region in the internal structure can be clearly observed in the Figure 4.13. is given below.

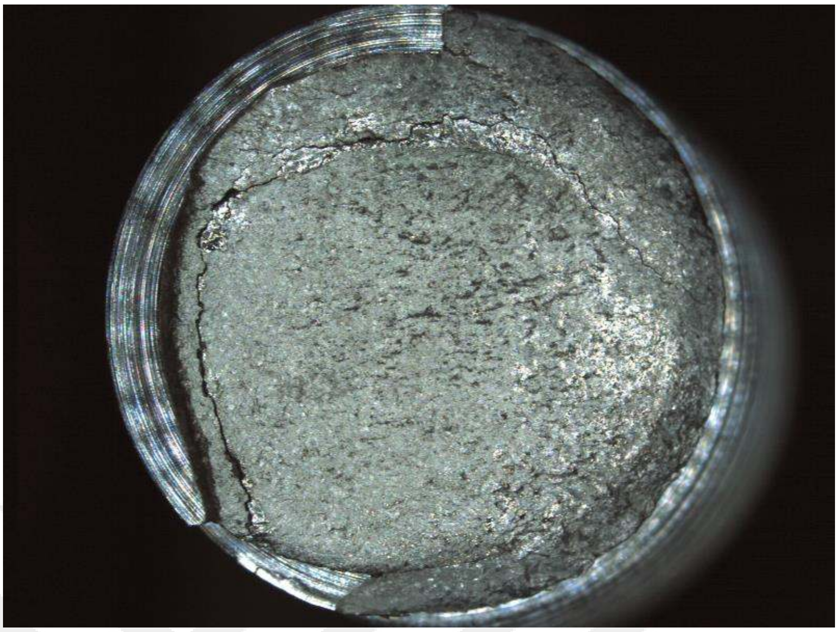

Figure 4.13. *Z direction HIPed fatigue specimen crack intiation and propagation*

As can be clearly observed in the Figure 4.14., the difference in surface roughness of the coupon to which sand blasting + pickling was applied and the test specimens in the machined condition can be observed in shared images.

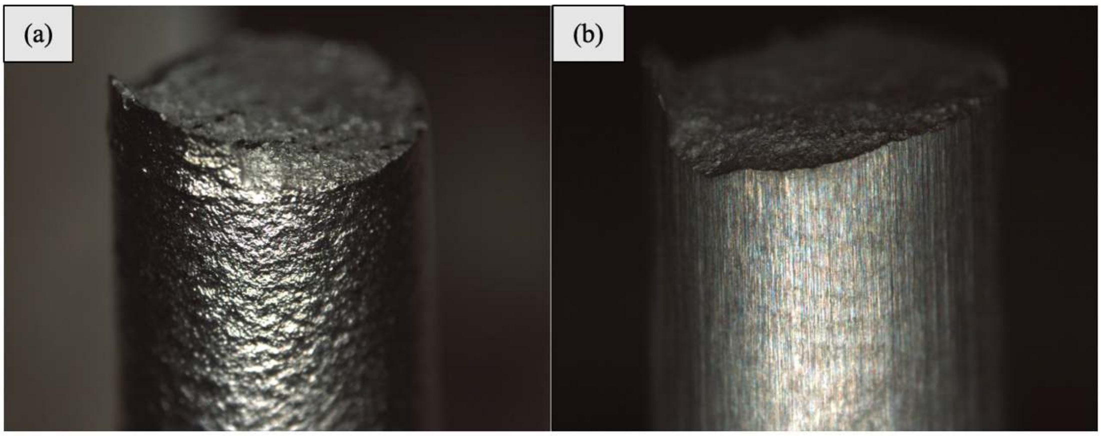

Figure 4.14. *Sand blasted + pickled specimen, (a), and machined post condition specimen (b), fatigue fracture surfaces*

When the post test surfaces and fracture locations of the sample group planned to be examined for the effect of alpha case layer formet after the heat treatment were examined, a few specimen were run out. On the other hand, it was observed that in most coupons, failure occurred from the gage section and the fracture behavior exhibit a more brittle character. Cup and cone structure could not be observed clearly on the fracture surfaces. Since a smooth and flat surface is obtained, it is concluded that no obvious fibrous zone is observed on surface where the fracture is brittle. The fracture surface results outputs as a result of tests performed with the alpha layer are given in Figure 4.15.

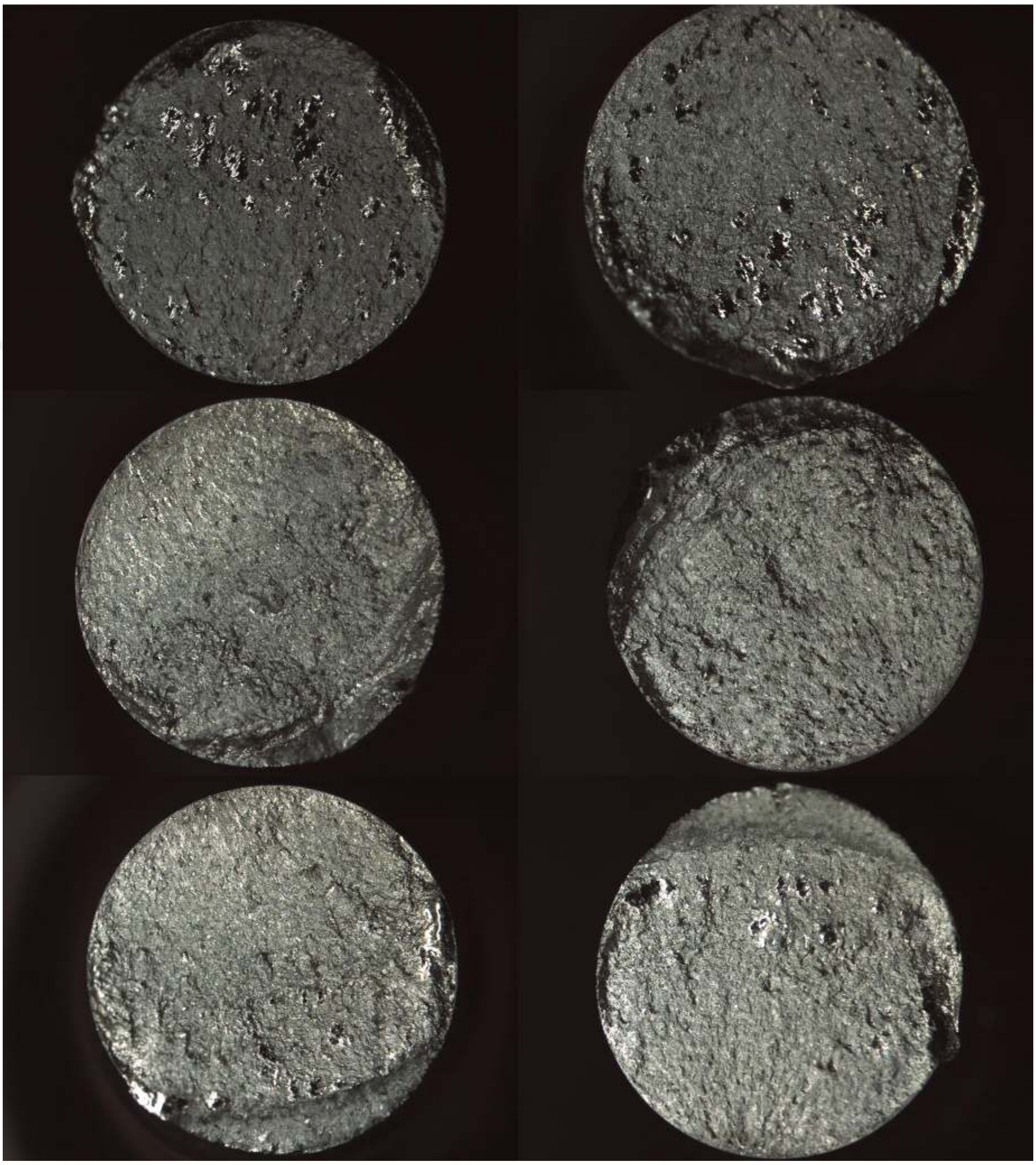

Figure 4.15. *Z direction alfa case fatigue specimens fracture surfaces*

4.3 SEM Fracture Surface Examinations

SEM was used to investigate the impact of the post- processes discussed in the thesis on fracture mechanics through examining at the post-test fracture surfaces on HCF test coupons for each processes. In the examinations, it was aimed to investigate the root cause by examining the surfaces of coupons showing different fracture mechanism, taking into account the fatigue test parameters. After determining the coupons whose fracture would be examined, all coupons were cut to equal length according the fracture areas. In the coupons that were appropriate for examination, crack initiation/propagation points as well as possible nonconformities in the microstructure were examined using a secondary electron detector.

The positive effect of HIP on microstructure and mechanical properties is indisputable and is a subject supported by the literature. For this reason, in the thesis study, the process parameters applied in the literature were examined and the application was made with the determined process parameters. The fracture surfaces of the fatigue coupons from the mechanical test coupons were examined in more detail in SEM after the stereo microscope examination. While most of the fatigue coupons with HIP completed the tests as run out, a few test coupons experienced unexcepted failure at low cycles. A not properly executed HIP process might result in residual porosity or inadequate densification which can create weak zones within the material and raise the risk of the fatigue failure. The objective of HIP process is to eliminate porosity and improve material density. However, when the fracture surfaces of the coupons that failed in unexcepted cycles are examined, it can be commented that subsurface porosities near surface may cause the crack propagation, as shared in Figure 4.16. As seen in the microstucture, the crack initiation due to the porosity near the the specimen edge is given in (a), and a microstructure where the crack propagation in to the internal microsturucture is given in (b), the crack initiation was observed to a defect close to the edge in the radius section (c) and the starting point of the defect that can be called a lack of fusion (d), subsurface porosities in the radius region (e), and crack initiation and propagation from subsurface porosity (f).

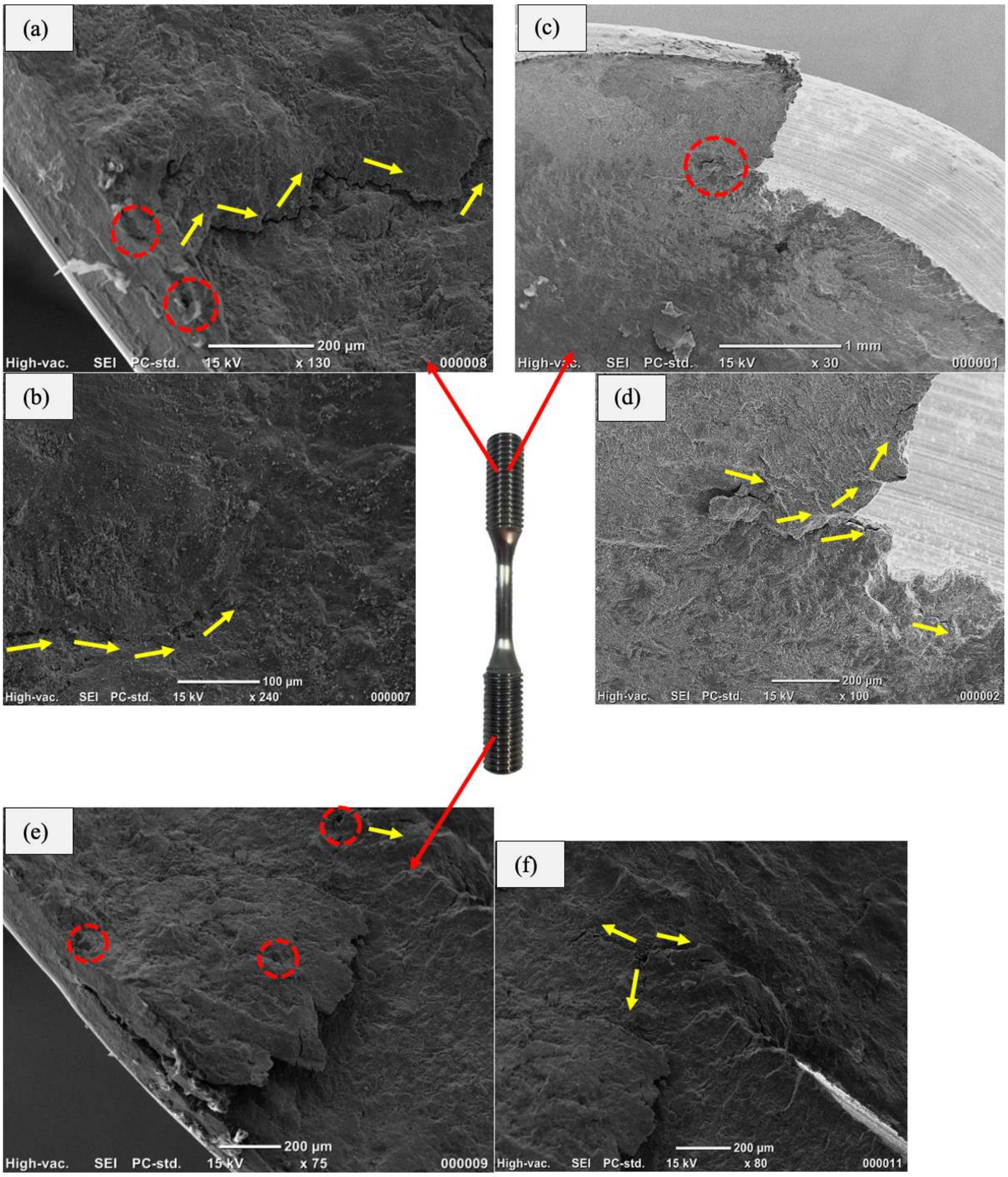

Figure 4.16. *HIP specimen fracture surface, crack initiation site (a), crack propagation into microstructure (b), defect close to the surface in radius section (c), crack propagation site of the defect (d), subsurface porosities in radius region (e), crack initiation and propagation from the sub- surface porosity defect (f)*

According to the SEM examination results, the presence of porosities that can be characterized by electron microscopy at the micron level was detected. This shows that the removal of microporosities close to the surface with HIP process was unsuccessful. It is noted that temperature have a harder time removing smaller pores. Although various temperature and pressures are used in HIP process to eliminate the porosities and minimize their size, very small pores may not collapse completely due to insufficient material flow or diffusion at the micro scale.(Du Plessis et al., 2015) It is also stated that some microporosity was observed when reopened after HIP. (du Plessis & Macdonald, 2020) In light on the findings, some microporosity may still be detected after HIP, especially if distributed within or near the surface. This situation caused the fatigue specimens not to run out and to fail in earlier cycles.

One of the nonconformity examples encountered in coupon with HIP is shared in Figure 4.17. It seen from the microstructure image that there is a unmelted accumulated powder. Such findings can be assumed as a factor that can affect the test results as they can behave like stress concentrators and trigger crack initation.

In these shared examples, fracture surface characterization was performed by detecting various findings. As a result of the HIP process applied to improve material fatigue behavior, in addition to the improvement in mechanical test results, the importance of the porosity size and location of the porosities in the microstructure influencing these results was revealed.

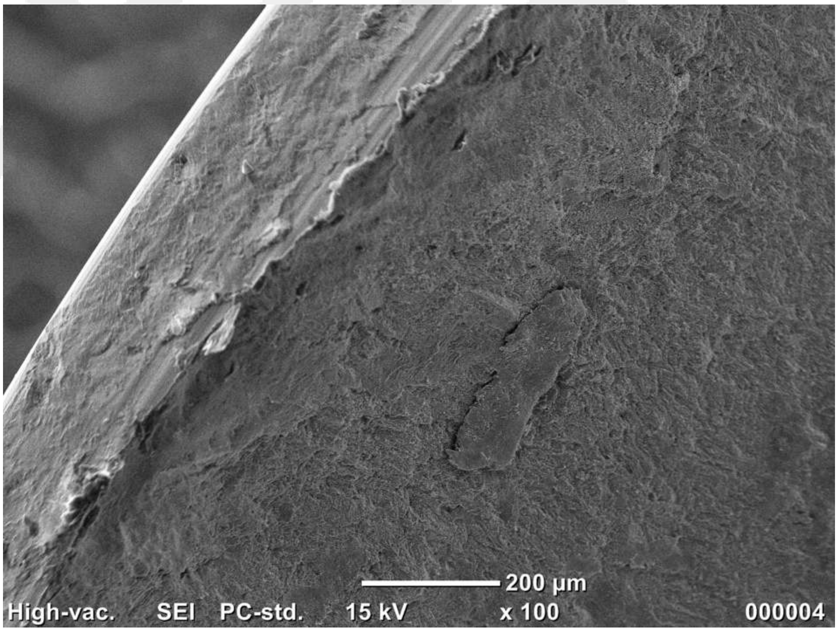

Figure 4.17. *HIPed fatigue specimen microstructure nonconformity example*

The examination results of the heat treated fatigue coupon, which was studied within the scope of thesis and determined as the standard process flow, are shared in Figure 4.18. It has been observed that a crack initiation from the surface is promoted by the coalescence of porosities larger in size than those shared in the HIP coupon findings under the surface, thus advancing the crack propagation mechanisim.

Although annealing heat treatment typically eliminates residual stresses and can enhance the microstructure, it does not apply external pressure to densify the material like the HIP process applied. Since these interconnected pores are the results of partial fusion or lack of bonding between particles, melting or collapsing these voids requires annealing temperatures that are typically between 700-800 °C. After annealing heat treatment, it is found that this condition does not alter based on the shared microstructure results.

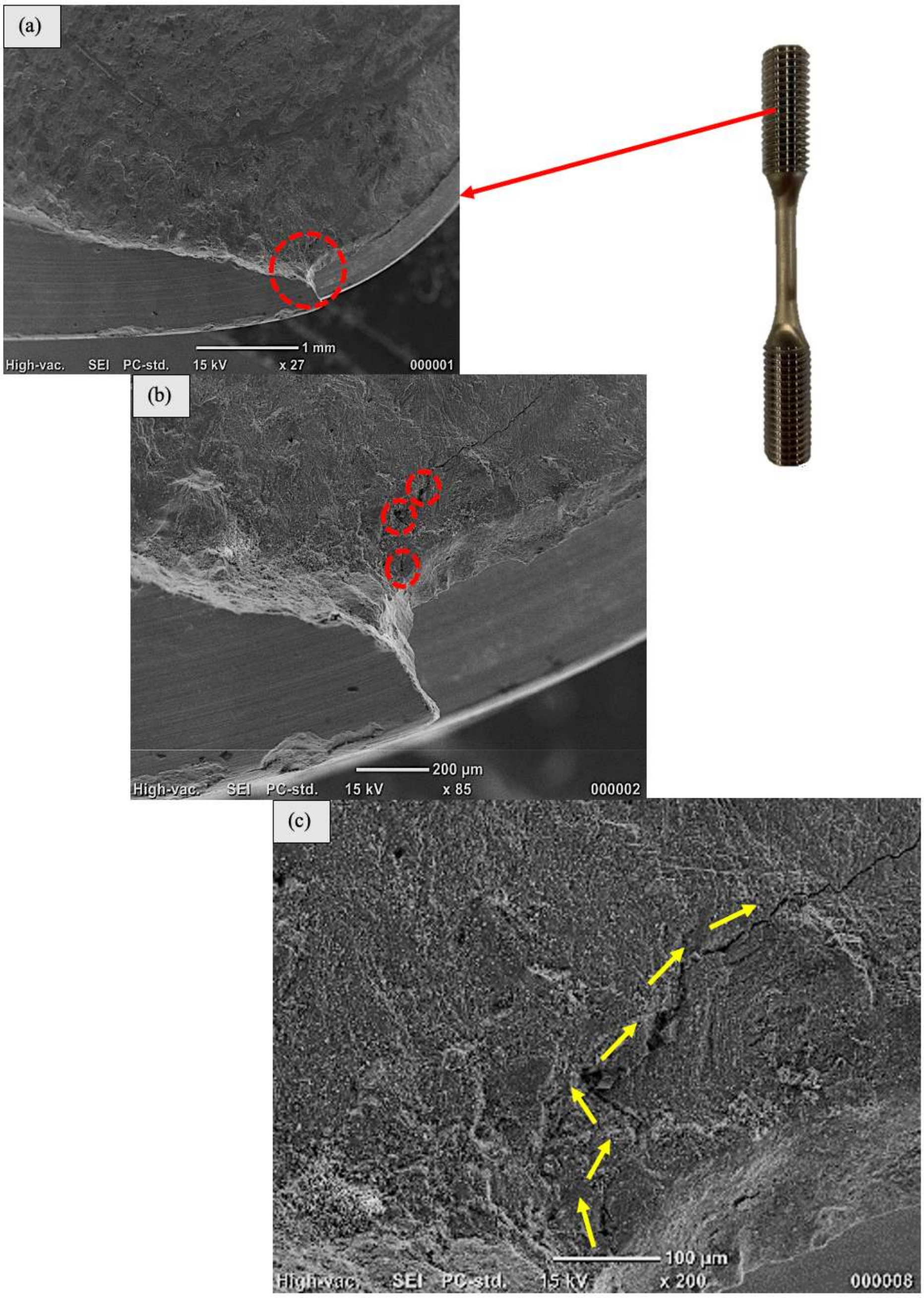

Figure 4.18. *Annealed fatigue specimen fracture surface (a), connected microporosities (b), crack propagation (c)*

The effect of HIP on fracture surface examinations has been revealed with a major difference when compared with annealed microstructure. It has been observed that porosities that cannot be removed in the microstructure with annealing heat treatment and have a major effect on the fracture mechanism and mechanical properties of the material cannot be completely eliminated. In this case, it reveals that the improvement should actually be made in the microstructure obtained after production with SLM process parameters. It is stated that the ideal situation can be achieved with the optimization of SLM process parameters, especiallly the scan speed parameter has a crucial effect on the porosities in the microstructure.(D. Wang et al., 2022)

Another finding observed in annealed fatigue coupons is the presence of unmelted powder particles or incomplete melting on the fracture surface, as shared in Figure 4.19. The annealed Ti64 SLM fracture surface showing incomplete melting of the powder is typically the consequence of issues that arise during the SLM production, which can result in a lack of coalescence between neighboring powder particles.

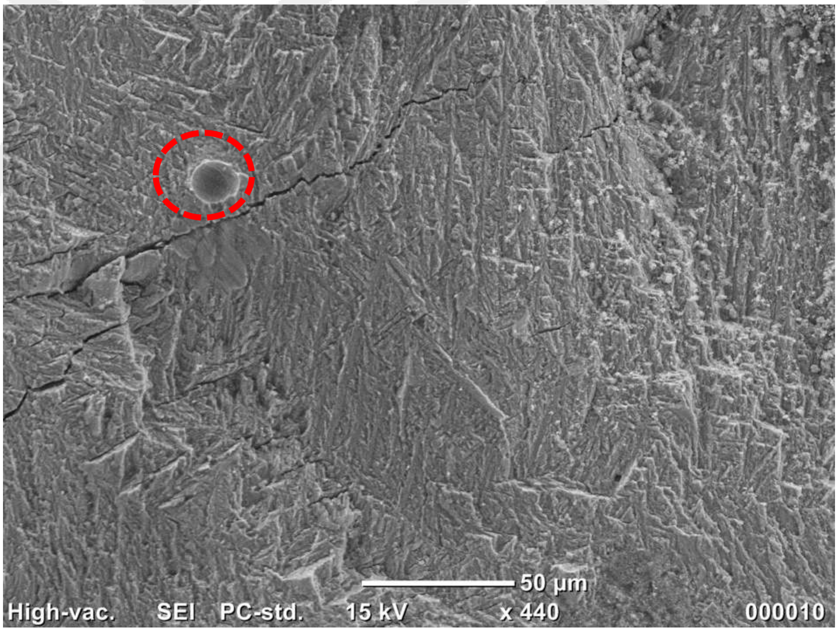

Figure 4.19 Annealed fatigue specimen fracture surface unmelted powder defect example

This situation can be clearly related to the insufficient laser energy, inadequate preheating process of the powder bed, powder quality, powder particle distribution and the dynamics of the melt pool due to thermal gradients formed during SLM production, which are discussed in the literature and stated as the causes of the nonconformance. (Gong et al., 2015)

It can be concluded from the analysis of the fracture surfaces and microstructure that annealing process dissolves the martensitic structure, promotes grain growth, increases ductility and improves microstructure. It can be determined, therfore, that annealing does not resolve the absence of fusion or unmelted powder regions in the microstructure following the SLM process, nor does it densify the material as the HIP process does. Even after the annealing process, these incomplete fusion regions continue to exist as porous areas or connected voids. As a result, the impact of increasing the fatigue strength of annealed coupons is restricted and partially depends on process variables. In a light of theses results, it can be evaluated that additional process applications may be neccessary depending on the expectations from the mechanical requirements in Ti64 SLM materials.

As a result of the SEM fracture surface examinations of the fatigue specimens to which sandblasting + pickling was applied after the annealing heat treatment, it was observed that subsurface unmelted powder defect. This was generally observed in the specimens and could be the crack initiation point was present in the material microsturucture. Since unmelted powder defects create localized stress concentration areas, they create the potential to lead crack initiation. The examination result with this type defect is shared in Figure 4.20. At the same time, it seen in the shared microstructure that the crack initiation and propagation from a region close to the material surface, not from the surface due to a subsurface defect.

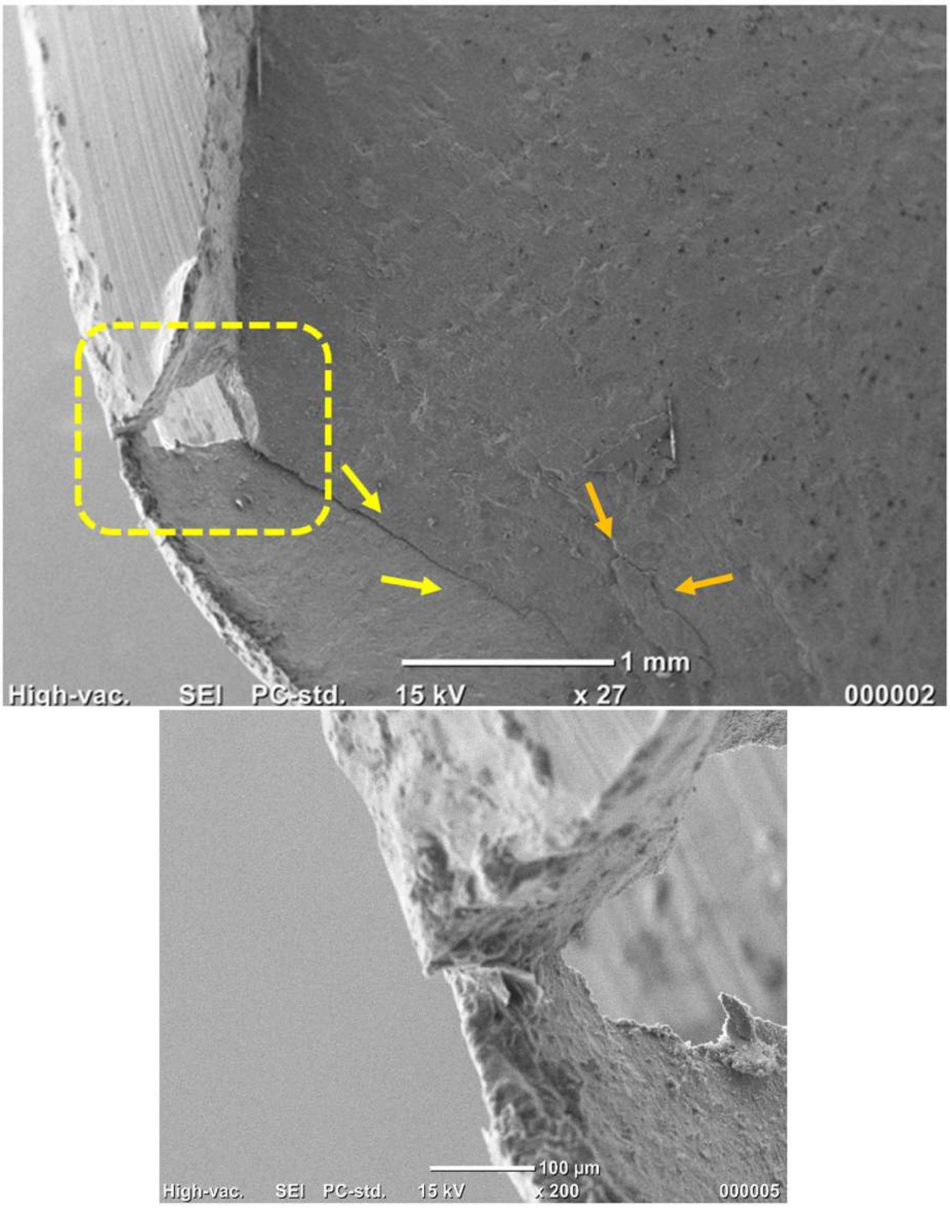

Figure 4.20. *Sand blasted + pickled fatigue specimen crack initiation site*

Examining the specimen fracture surfaces that were subjected to pickling and sand blasting revealed that, with the exception of run-out coupons crack initiation points were caused by subsurface porosity and indications. The fracture surface subsurface porosities of the sample that fractured at earlier cycle than the other test specimens was shown in Figure 4.21.

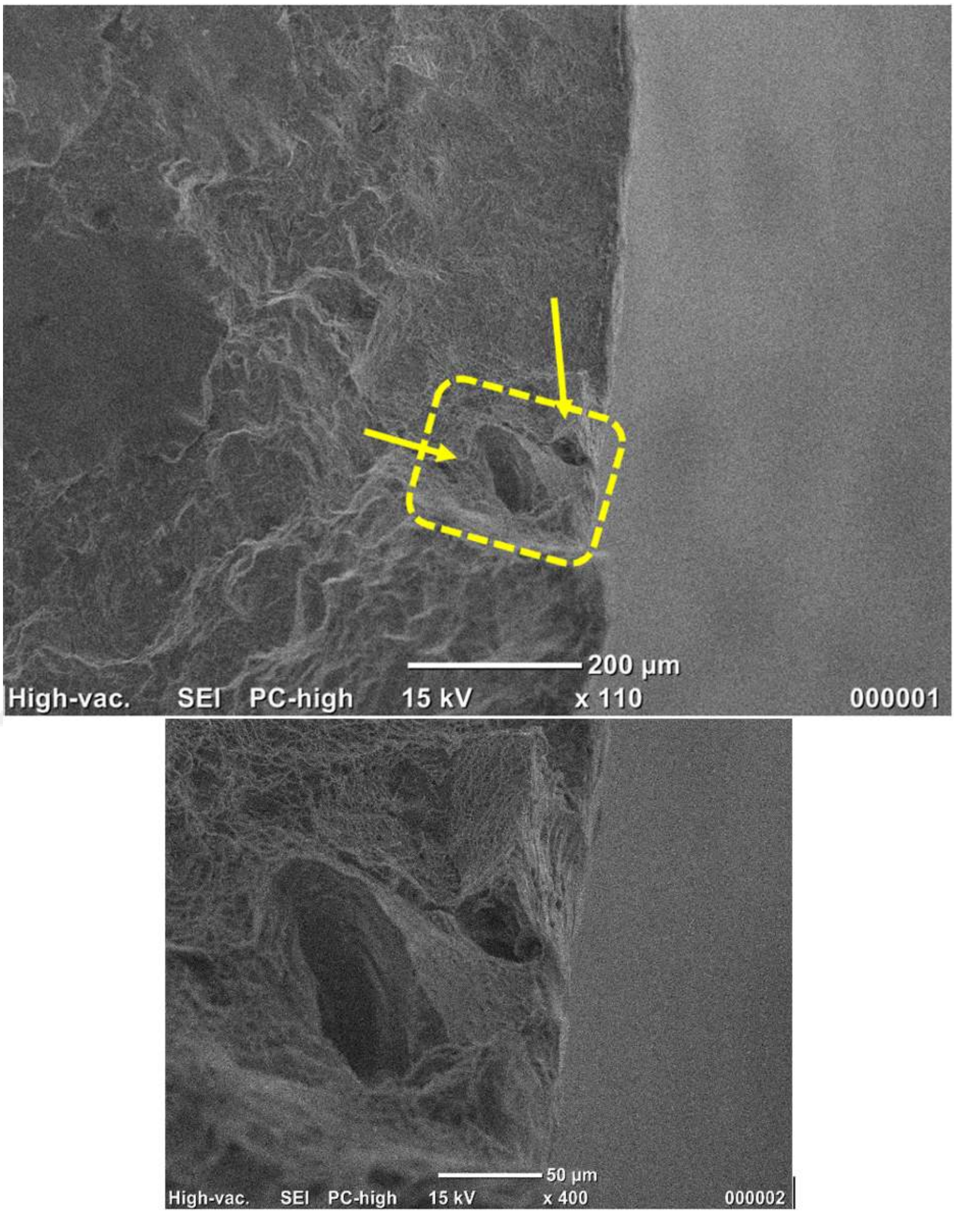

Figure 4.21. *Sand blasted + pickled fatigue specimen microstructure subsurface porosity*

Figure 4.22 shows the numereous cracks that initiate from the alpha layer on the surface during the assessment of alpha layer fatigue coupons, which were examined as part of the thesis and for which there is a lack of material information in the literature. It is observed that the alpha layer which exhibits a hard and brittle behavior at a level approximately 15-20 microns obtained on the test coupons as a result of heat treatment causes many crack initiations on the fracture surface. The decrease in the alpha layer in the mechanical test results conducted for the thesis and the variation in the material's fatigue strength can be linked to this circumstance.

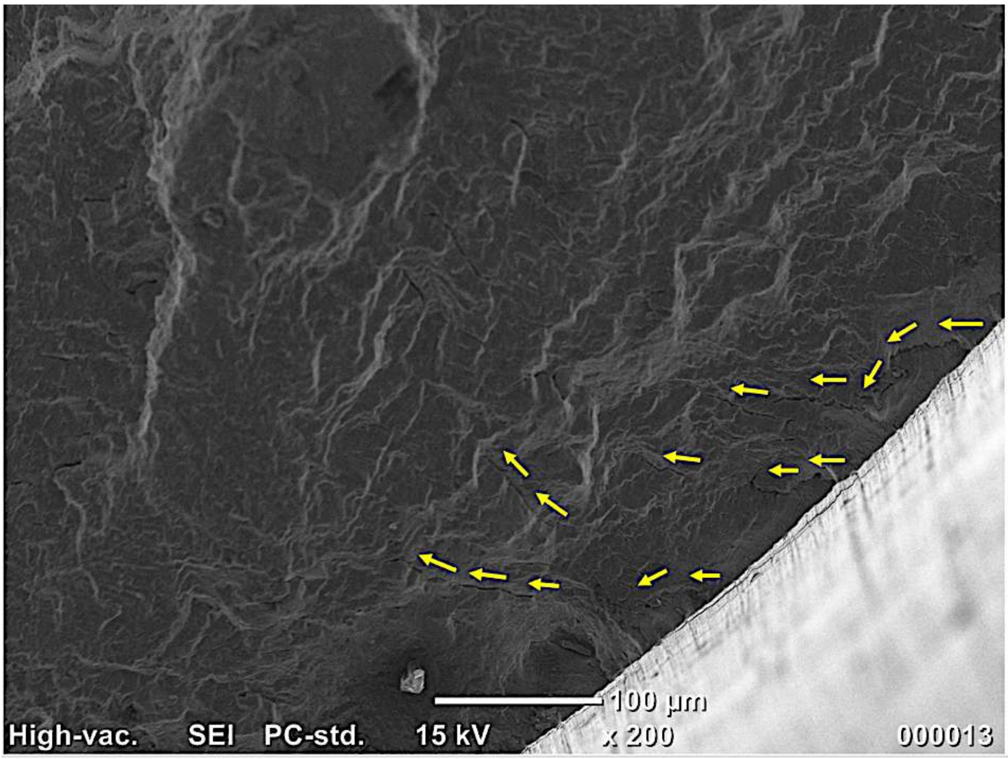

Figure 4.22. *Alpha case layered fatigue specimen fracture surface*

The microstructure results of the fracture surface examinations of the fatigue coupon fractured from the gage region are shared in Figure 4.23. Figure 4.23. (a), shows the result that the fracture surface of the alpha layer in the given microstructure is smooth and exhibits a brittle fracture behavior by showing features such as cleavage planes or intergranular fracture. Figure 4.23. (b), it has been determined that there are lack of fusion defect that can affect the strength and fatigue strength of the material coming from additive production as in the given microstructure. This result can be given as an example to represent this type of additive defect. Figure 4.23. (c), a additive manufacturing defect that can be shared as an example of the presence of unmelted powder in the given microstructure. Figure 4.23. (d), is shared as an example of the microstructure of the alpha layered fatigue coupon where microporosities, which are also seen in other additive samples, are detected in large numbers.

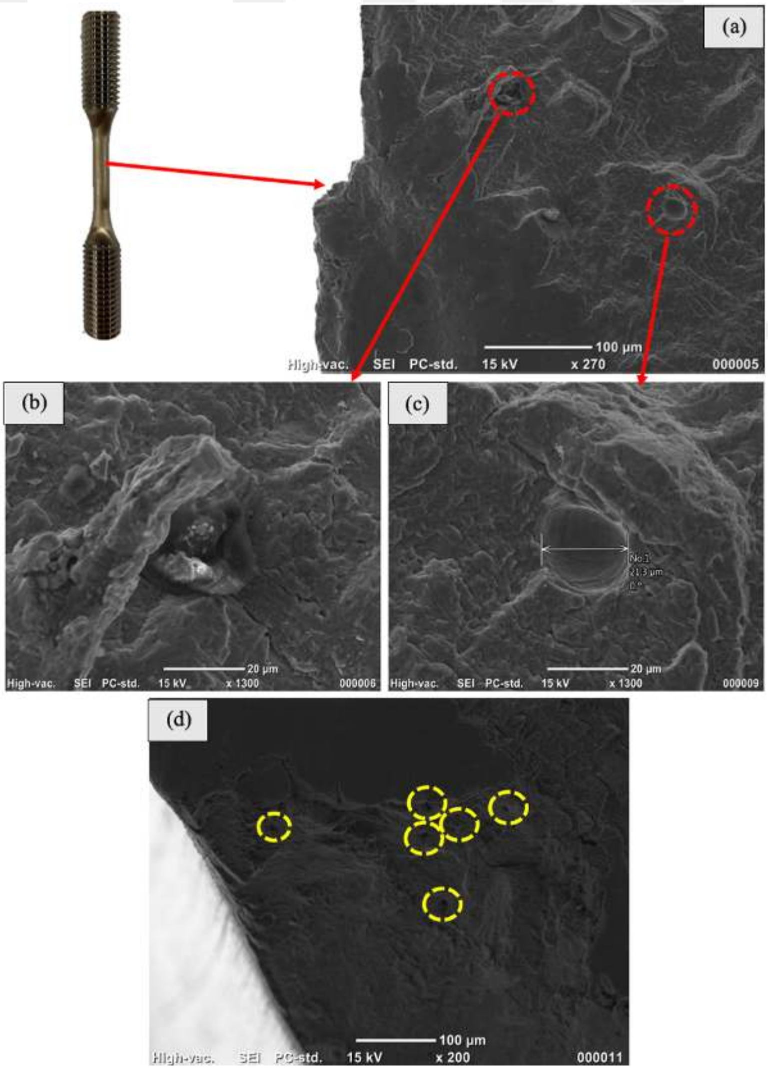

Figure 4.23. *Alpha case layered fatigue coupon fracture surface (a), lack of fusion defect example (b), unmelted powder defect example (c), microporosity examples (d)*

In order to test the fracture mechanism and mechanical properties in alpha layered materials, another examination was performed on the coupon where fracture was observed in the radius region of fatigue coupons. It reveals that, unlike the gage region examinations, the brittle fracture behavior of the alpha layer can be noticed in the radius region from the separation on the outer surface of the specimen. A detailed examination of the fracture surface microstructure shared in Figure 4.24. was carried out at higher magnifications. In the microstructure in Figure 4.24. (a), it can be seen that the crack initiation and propagation from a layer where an alpha case layer can be formed. Figure 4.24. (b), the microstructure of the crack initiation zone at higher magnification is given. Figure 4.24. (c), microstructure showing the presence of alpha layer causing crack initiation.

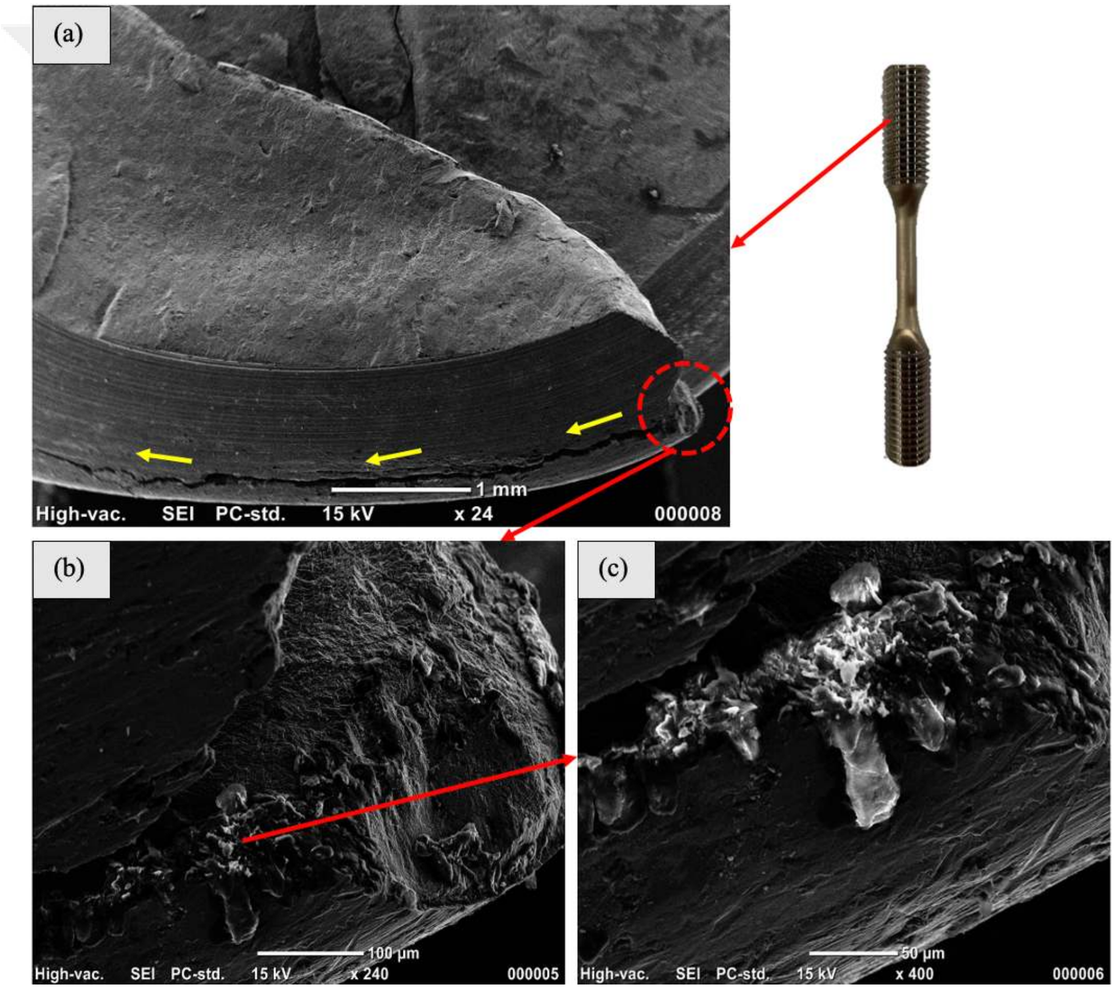

Figure 4.24. *Alpha case layered fatigue coupon fracture surface in radius region*

In order to clarify whether the alpha layer casued the crack initiation, areal elemental analysis result were taken from the regions indicated in the microstructure image given in Figure 4.24. (c). According to the elemental analysis results shared in Figure 4.25., a conclusion was obtained regarding the existence of an alpha layer rich in oxygen and titanium in the crack initiation region.

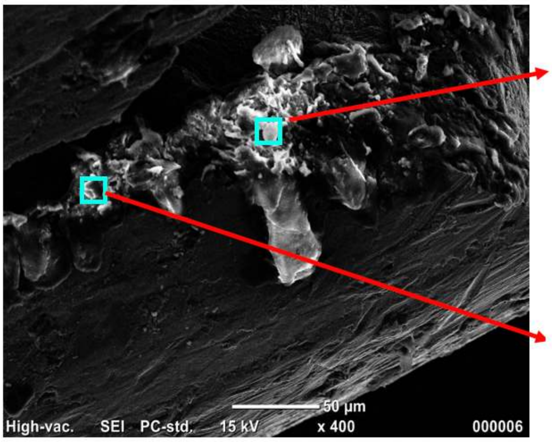

ZAF Method Standardless Quantitative Analysis

Fitting Coefficient : 1.0000

Element	(keV)	Mass%	Sigma	Atom%
O K*	0.525	100.00	32669.46	100.00
Al K*				
Ti K*				

ZAF Method Standardless Quantitative Analysis

Fitting Coefficient : 0.9999

Element	(keV)	Mass%	Sigma	Atom%
O K*	0.525	15.67	3914.96	36.58
Al K*				
Ti K*	4.508	33.98	523.71	26.50

Figure 4.25. *Elemental analysis result of crack initiation region*

In the microstructures shared in Figure 4.26., different crack initiation sites belonging to different fatigue coupons are shared. Unlike other cases, it was concluded from all fracture surface examinations that the alpha layer caused more than one crack initiation, and that the major reason was due to the additive production defects already present in the microstructure.

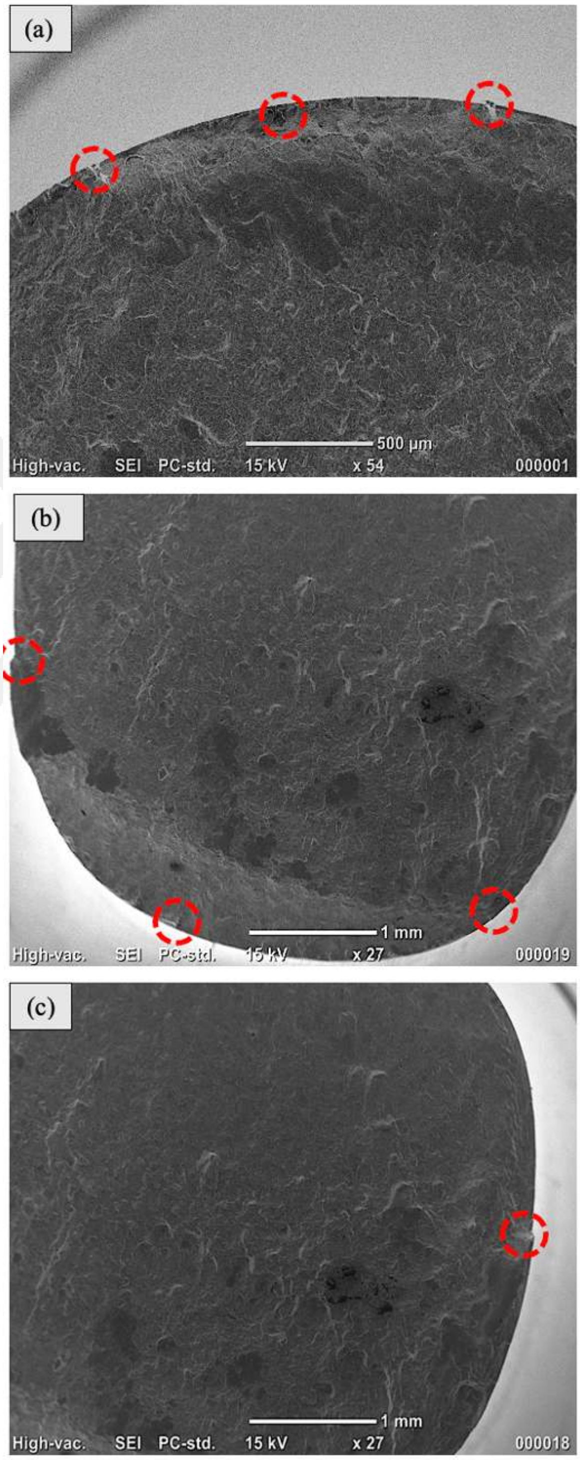

Figure 4.26. *Microstructures of various crack initiation points in alpha layered fatigue coupons*

4.4 Porosity Measurements

Porosity measurements were performed on the coupons with HIP and annealed appplied in order to figure out the type of change that was acquired in HIP parameter determined within the scope of thesis in comparison to the heat treated condition. It is essential to notice that a significant differences in the measurement results since this demonstrate the impact of the HIP parameter and the neccessity for the critical components.

The effect of HIP on microstructural porosity is indisputable and is a subject studied in the literature with quantitative measurements. Therefore, the porosity values from the coupons before and after HIP obtained within the scope of this research are given in Table 4.1.

Table 4.1. *Porosity values before and after HIP process*

Measurement	Before HIP	After HIP
1	0,296	0.138
2	0,2	0.173
3	0,169	0.09
4	0,518	0.106
5	0,317	0.114

The measured values for the heat treated condition are in agreement with the literature. The measurement results are reported at different inputs in (Mathe et al., 2021) confirm this. Representative of the measurements result shared in table, Figure 4.27.-4.30. provides microstructure examples of some of the pre- and post-process measurements.

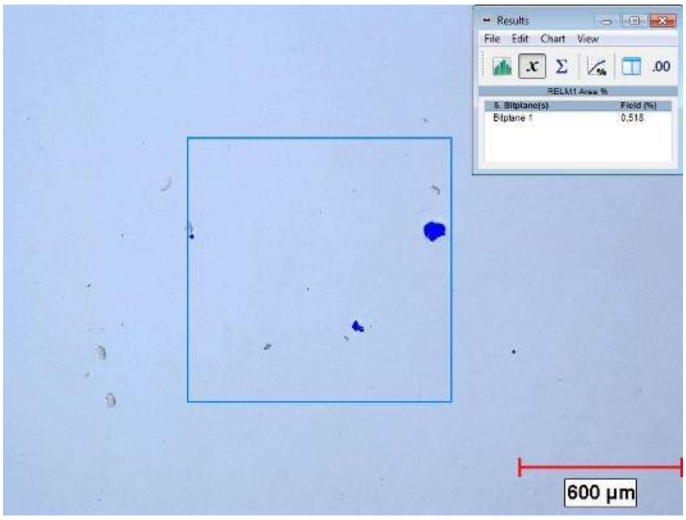

Figure 4.27. *Porosity result before HIP process coupon 1*

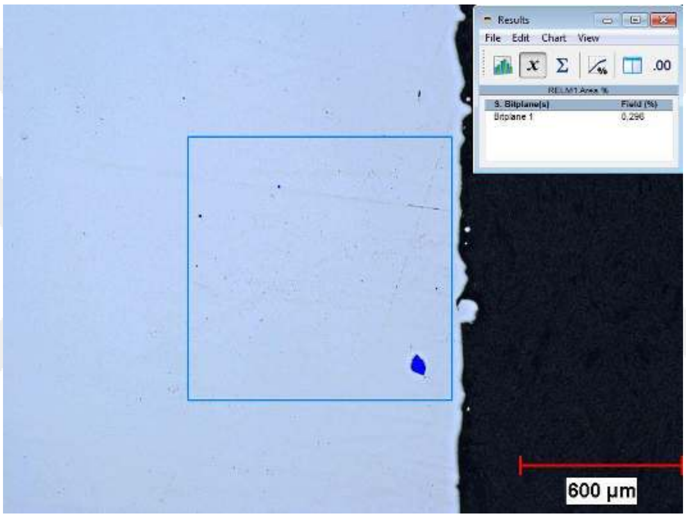

Figure 4.28. *Porosity result before HIP process coupon 2*

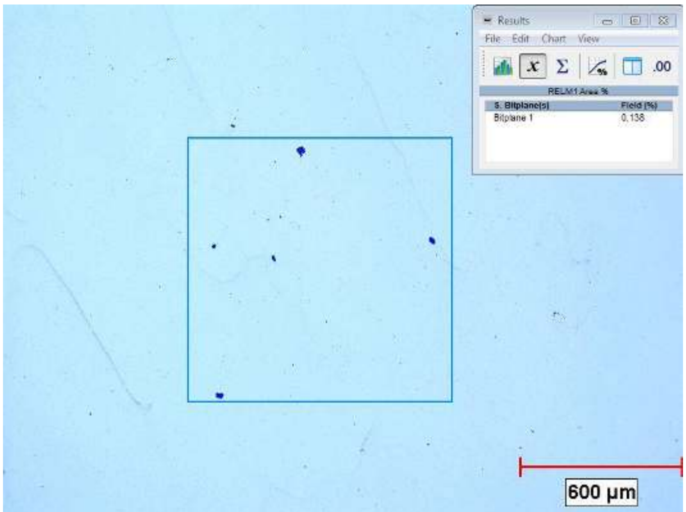

Figure 4.29. *Porosity result after HIP process coupon 1*

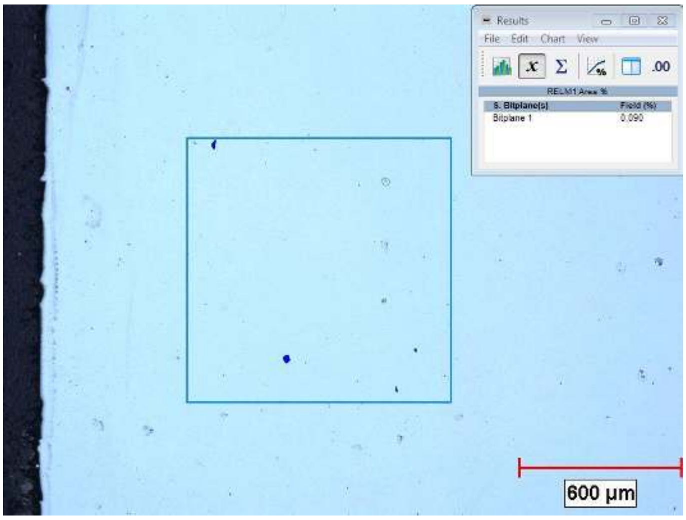

Figure 4.30.*Porosity result after HIP process coupon 3*

It was noticed that in the coupon findings, which were made in variety of numbers before and after HIP process, that both the porosity number an size dimished after the process compared to the before condition. It was determined that there was porosity with sharp edges in the microstructure of several coupons before the process, as given Figure 4.31.

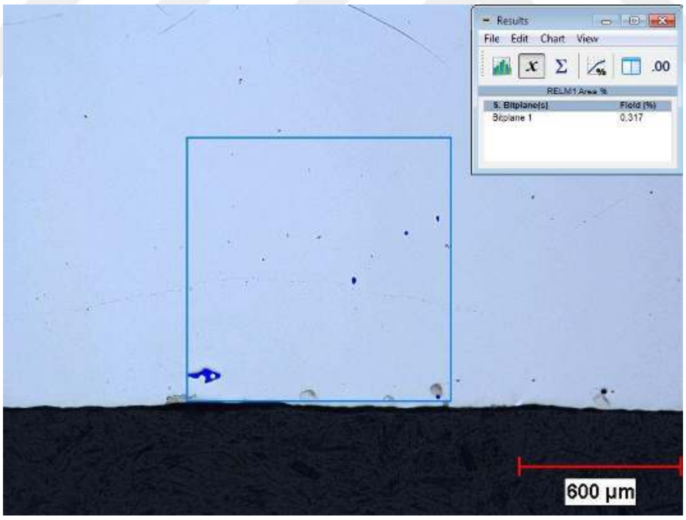

Figure 4.31. *Before HIP sharp porosity in coupon 5*

It proves that shape and irregularity of porosities formed in the SLM process help to become more homogenuous and round with HIP process. Since the sharp-cornered porosities are stress raising regions, they are considered as a factor that plays a major role in the negative direction for mechanical properties of the material. The effect of porosity result is also supported by the mechanical test data shared in the mechanical properties section within the scope of this research.

Another important finding obtained in line with examinations result was that although the porosity size decreased after the HIP process, the process was not very efffective in removing porosities closed to the surface. As an example of post-processing sub surface porosity that can be shown as an example of this finding is given in Figure 4.32.

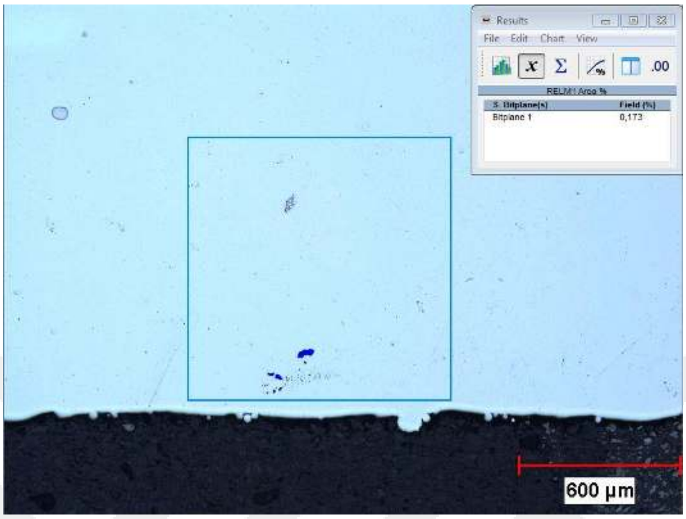

Figure 4.32 *After HIP process improper porosity*

An improvement of almost %60 was noticed when the average measurement result from the annealed coupons and the average of the HIPed coupons were compared. The graphic below shows the data and averages for the two processes.

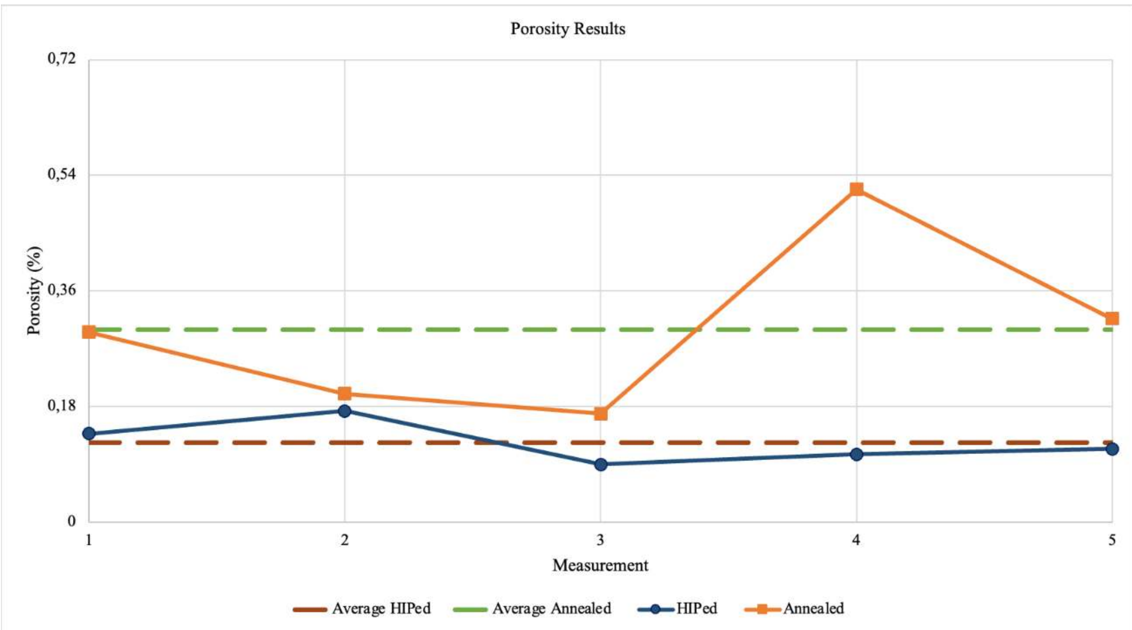

Figure 4.33. *Comparison of the porosity (%) results of annealed and HIPed specimens*

4.5 Hardness Results

The section where microstructure investigations are provided discusses into the great detail about the alterations in the microstructure brought about by the various processes identified within the thesis research. Vickers hardness measurement were made from the microstrucure coupons that were part of the post processes in order to ascertain how to change in microstructure affects the material's hardness. The averages of the repeated measurement results and literature data were compared. The results obtained with the study outputs applied with similar heat treatment and HIP parameters can be evaluated as compatible.

The hardness measurement of the microstructure with $\alpha+\beta$ phase distribution formed after the HIP process, which is the one of post-process evaluated within the scope of research, is shared in Figure 4.34.

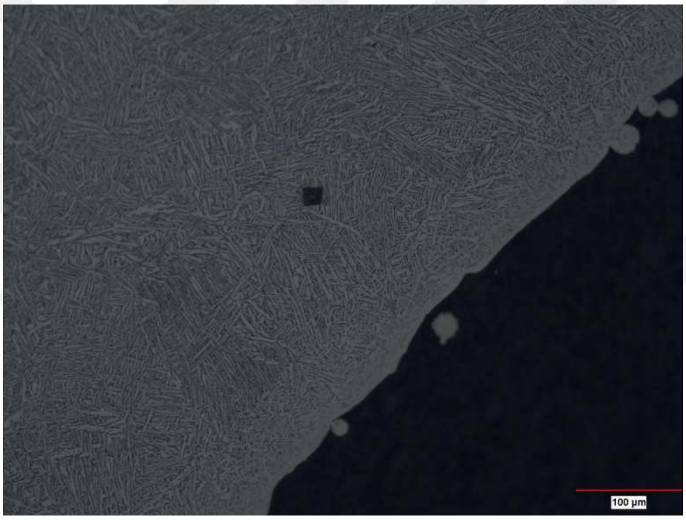

Figure 4.34. *Example of vickers indentation image of HIPed material*

The alpha layer that developed following the HIP process of the pre-machining condition in the round cylindirical test specimen was used to measurement hardness. It was preferable to utilize this coupon for measuring alpha case layer hardness since the final alpha layer thickness is excepted to be thicker.

The Figure 4.35. is given for the measurement where the hardness value of the HCP alfa phase formed by oxygen affinity of the titanium is expected to be high.

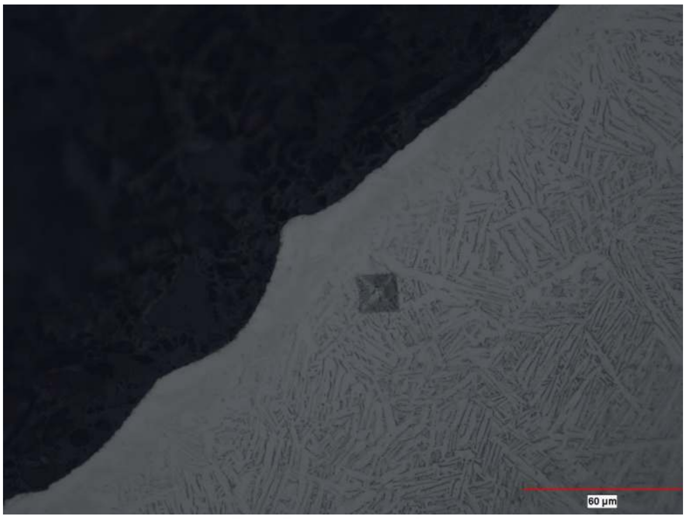

Figure 4.35. *Example of vickers indentation image of alpha case layer HIPed microstructure*

As shown in Figue 4.36., hardness measurement was taken from annealing heat treated microstructure coupon produced in the XY direction.

Figure 4.36. *Example of vickers indentation image of anneal heat treated material*

It is stated that microstructure section that in the as-built condition, the material has a martensitic internal structure and is not an ideal situation for additive manufacturing parts due to its lower ductility. The hardness measurement was performed as shown in Figure 4.37. to demonstrate that the material in this instance has a brittle characteristic.

Figure 4.37. *Example of vickers indentation image of as-built material*

Three measurement findings for various post-conditions in the investigation are shown in Table 4.2.

Table 4.2. *Vickers hardness results for various post-conditions*

Sample	Built orientation	Average of measurements (HV)
Annealing heat treated	XY	377,6
Annealing heat treated	Z	356
As-built	Z	395,16
HIPed	Z	332,7
Alpha case layer	Z	461,26

The measurement results show that as-built material with a martensitic microstructure has a greater hardness value and is more brittle than annealed condition, which is standard prosess flow for producing additive manufacturing parts. Based on the results, it can be explained that the use of material in the as-built case is not suitable especially for the aerospace parts. It was observed that the hardness value of the material decreased with the phase transformation obtained in the microstructure with the annealing heat treatment. According to the measurement results obtained after the HIP, it is seen that the material hardness decreases as a result of the equilibrium microstructure consisting of the α+β phase produced with the process temperature below the β transus of the material. Due to the lack of information on hardness value in the reference studies on alpha layer drawback, which is known to have a very high hardness caused thermal input in titanium additive parts, hardness measurement was taken from the alpha layer of the HIPed material. The alpha layer's hardness value was found to be relatively high based on the obtained data.

Hardness value obtained from the microstructure coupons are compared with the literature in the Figure 4.38.

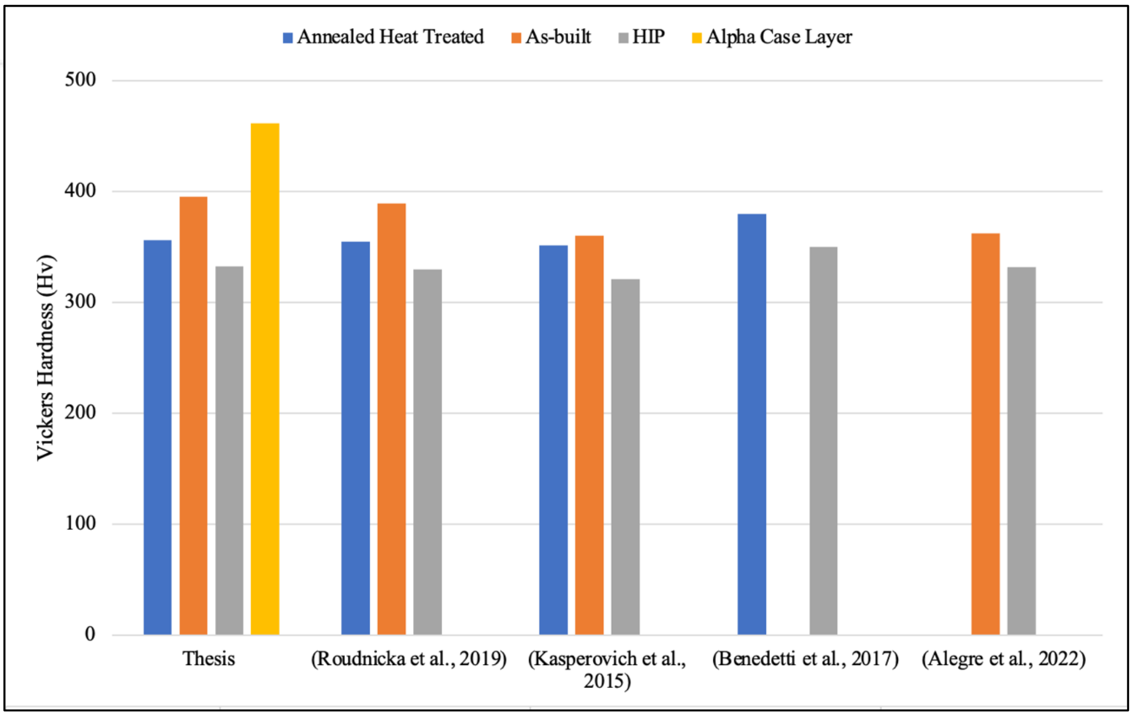

Figure 4.38. *Comparison of Vickers hardness results with literature findings*

4.6 XRD Characterizaton Results

The literature outputs and microstructure results section provides a detailed examinations of microstructures that were obtained using post-processing methods was performed within the parameters of the research. Additionally, to investigate the phase transformation that resulted in microstructure transformation, XRD characterization was performed. Figure 4.39. shows the XRD patterns for as-built, annealed and HIPed materials that were acquired within the research of the investigation.

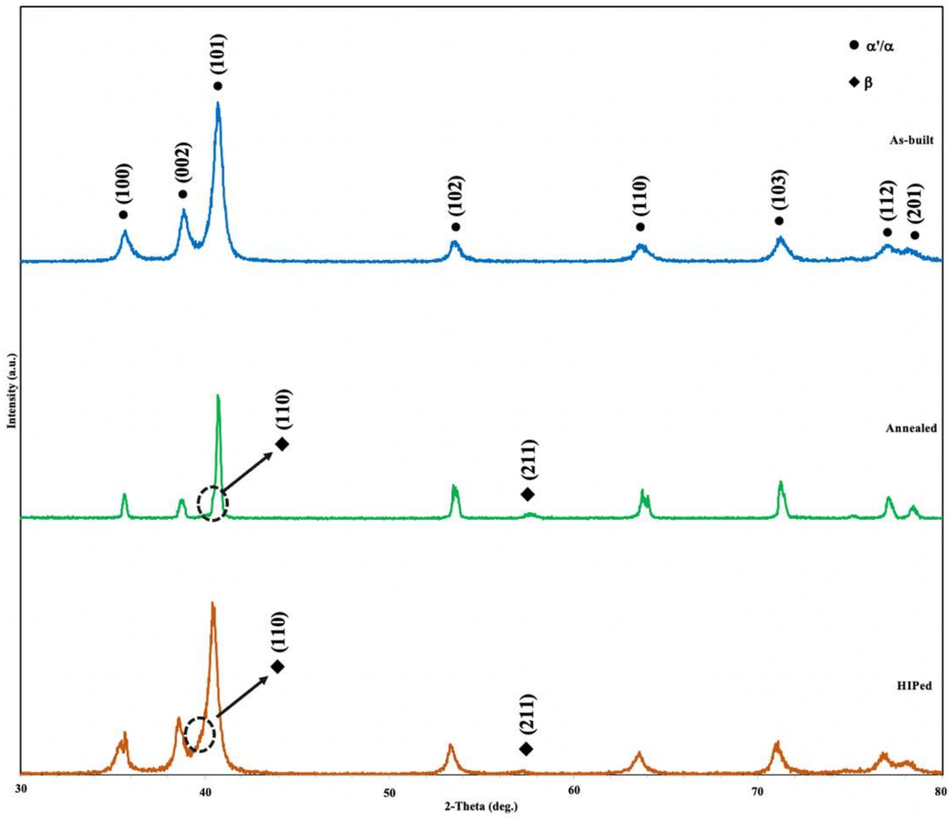

Figure 4.39. *XRD pattern of the as-built, annealed and HIPed SLM Ti64 materials*

According to the consequences obtained as a pattern of XRD analysis, it is seen that the peak intensity of peaks belonging to the as-built material is higher than the annealed heat treated material result. These results are consistent with the literature.(He et al., 2019) At the same time, the difference is explained by the presence of a finer α' phase in the microstructure. In the section where microstructure results are discussed, it is explained by the change in microstructure that the α' phase transformed into the α+β phase with the heat treatment. This situation can be proven by the β phase not observed in the as-built case being obtained as a result of annealed XRD analysis.

One of the topics covered in the literature is the investigation of martensitic transformation examples based on heat treatment temperature and the effect of heat treatment parameters on the phase transformation.(Cardon et al., 2020; Jimenez et al., 2022; D. Wang et al., 2022) When the XRD patterns of annealed heat treated material are interpreted, it is concluded that the β phase is obtained in microstructure with the procedure applied in the thesis, and the heat treatment temperature/time is effective on the martensitic transformation.

In annealed and HIPed material patterns that have β phase, the presence of phase at 2θ ≈ 38.5-39° β (110) was detected and it was observed that in results that was no peak in as-built condition since it did not contain β phase. The volume fraction of the phases that comprise the microstructure is shown by the relative intensities of the peaks in the XRD pattern. In contrast to other non-HIP conditions as an annealed case, a stronger β (110) peak was detected in the XRD pattern result of the HIPed material, which tended to intensify the β phase. The formation of the α+β equlibrium phase following the HIP process was verified by XRD characterization upon interpretation of the acquired pattern.

4.7 Mechanical Test Results

Tensile and fatigue tests of the materials included in the post-processing specified in the experimental procedure were conducted as a part of study's scope in order to ascertain how these processes affected the mechanical characteristics of aerospace parts. Tensile tests were also conducted for comparison with the literature and specification minimum data, even though fatigue behavior is the main limitation restricting the use of additive parts.

Coupons produced in two different built direction and two different test coupon geometries were used in tensile tests. While the test differences in built direction dependent tests and different test coupons data were extracted from the performed tests, it was aimed to extract the test results depending on the coupon geometry. The most important reason for this is parts with different wall thickness and height values on built platform are produced from the test coupon geometry in aerospace parts and is a relationship establish between the part and coupon. This subject which has been adressed with limited studies in literature research for different production method and built thicknesses, has also been examined within the scope of thesis.

Annealed ASTM E8 round specimen geometry and flat coupons were used to gather a significant amount of test data. By production coupons in various production cycle as a result of recurring manufacturing and on the same built platform, these tests were extented. Flat test samples are post-process group added because they have thiner thickness than round samples, since the nature of the additive manufacturing creates difference in the microstructural sense, which raises question about whether it will create a difference in mechanical test results. It was also added for the purpose of benchmarking with the results of ASTM E8, which is a standard test method. Since the coupon geometry belongs to flat test coupon geometry used in TEI's special material tests, detailed information about the coupon dimensions connot be shared. Studies have been conducted on various Ti64 SLM microflat geometries in the literature. It is possible that test data may differ according the different coupon dimensions. The reason for this that a number of factors can impact the material's mechanical performance including the variations in type of microstructure defects reported in literature, surface roughness following production, the residual stress level of the material and changes in the coupon's stress concentration regions brought about by alterations in the coupon geometry.(Munk et al., 2022; Zhang et al., 2019)

A small number of annealed flat test coupons were taken out of block that was manufactured and the test were subsequently added to test matrix in order to investigate how post-processing affected the height of the material on the built platform. In these specimens, it was aimed to determine the effect of build locations on tensile properties and compare them with other post-conditions.

The test results of the coupons machined from the round tensile coupon geometry with the HIP process parameters determined as a result of literature research were also included in the study. A discussed in the detail in introduction section outlining literature research on HIP process, tensile test of a sufficient number of coupons were performed in order to interpret and compare the test results.

Another post-condition studied within the scope of thesis, the alpha case layered sample group, was added to the test matrix. It has been noted that the literature is ineffective and lack of mechanical tensile test findings about the impact of the alpha layer on the tensile characteristics of materials produced with SLM Ti64. Hence, the tensile tests were performed on a small number of coupons compare to the other conditions. The purpose of adding these tests is to observe the primary effect of the alpha case layer on the fatigue characteristics of the material as well as its behavior on tensile properties.

As indicated in Figure 4.40., according to the referenced ASTM F3001 specification, the minimum test results to be obtained in Ti64 ELI materials produced with annealed heat treatment and the HIPed powder bed fusion method are 860 MPa. When the tensile test results performed in the all post-conditions used in the thesis study were evaluated, approximately the same level of test results were obtained in round machined specimens, flat sample geometry, flat coupon extract from block, and the test coupons with alpha case layers followed by annealed heat treatment. In HIPed specimens, lower data was obtained in the test result of the other conditions, and a decrease was observed in the UTS value. A general examination revealed the all post-conditions had test results achieved that the specification's minimum requirement.

The test results achieved in the Z direction is found to be lower than XY direction with a minor difference when the UTS and yield strength data of the test specimens builded in both directions in round and flat test geometries are assessed. The directional difference observed in the test results was explained by the fact that coupons produced in Z direction of molten metal have less layer bonding that coupons produced in the XY direction due to the cooling and solidification process of molten metal; this results in worse mechanical properties due to the nature of SLM.(L. Wang et al., 2017) Another important reason is explained as the presence of higher density α lath in columnar grains obtained in the Z direction in microstructure of materials with Z direction builted in the microstructure in the same direction. (Barba et al., 2020)In summary, the correlation depending on XY-Z direction obtained in round and flat coupon geometries can be evaluated as compatible.

A lower UTS and yield strength values were obtained in HIPed test coupons compared to the other annealed material conditions. Within the scope of literature research, it was explained that it was a result of the α+β equilibrium microstructure obtained in material processed above the β transition temperature with the HIP process.(Lv et al., 2023) In the test results, the decreases in the UTS and yield values due to the effect of the β phase formed in the martensitic microstructure specified in the literature studies are given in Figure 4.40 and Figure 4.41.

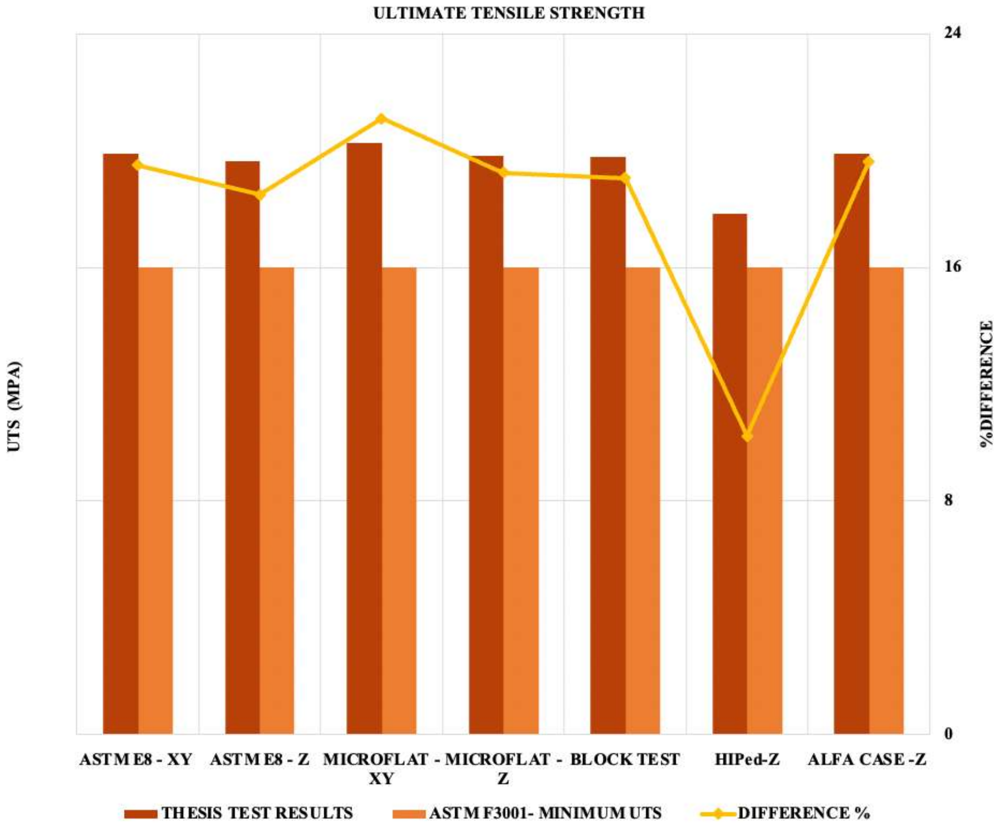

Figure 4.40. *UTS results of the post processes within the scope of thesis*

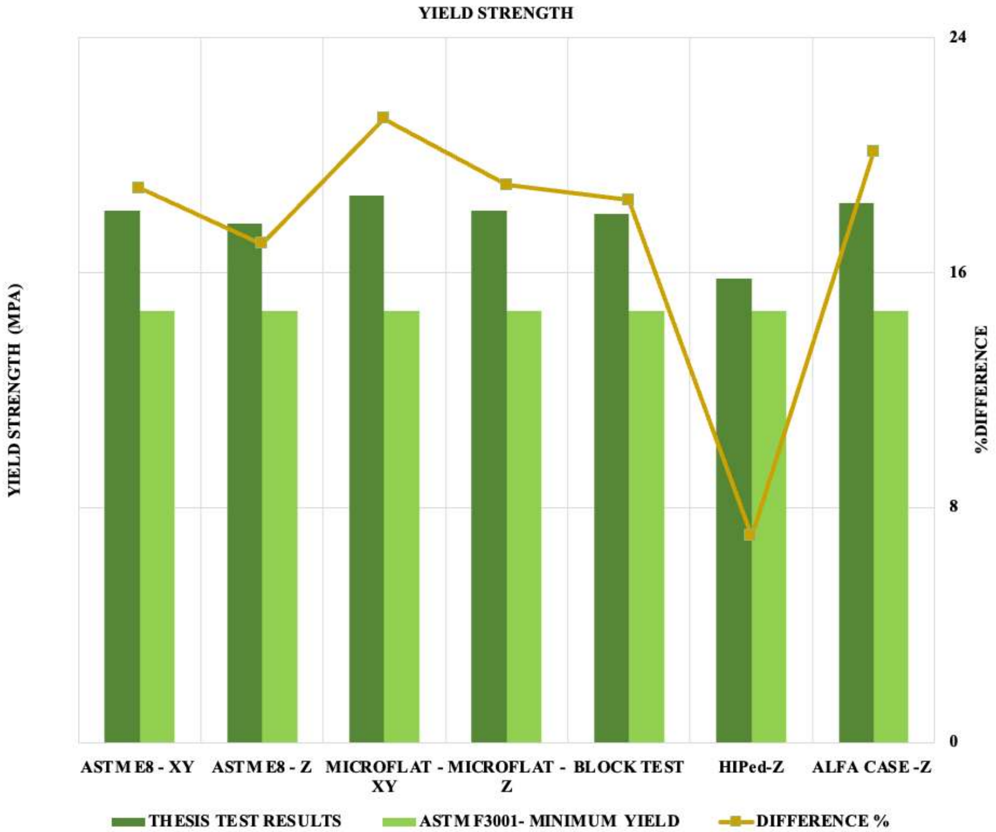

Figure 4.41. *Yield strength results of the post processes within the scope of thesis*

There were no significant differences between the round and flat sample geometries when they were compared within themselves in terms of UTS and yield strength. In both cases, a similar results were found in elongation values as shared Figure 4.42. It is noteworthy that the reduction area results are given in Figure 4.43. do not show compatible results in terms of UTS/yield strength due to the flat and round specimen geometry. In flat and and round test specimen, this may vary depending on various thickness and height values. However in general, this difference occurs due to the geometry is explained as the necking mechanism under stress during the test process and the change in the density area that undergoes deformation. The differences in the test results can be explained as decrease in cross section area due to localized strain and elongation result affected by the growth of neck during the test process. (June et al., 2023)

Since establishing the part-coupon correlation is important to the part design and analysis, flat tensile test coupons from different locations were tested in accordance with the dimensions of the block part produced to represent the aeorospace engine part. When the test results were evaluated, it observed that although there was no major difference in UTS and yield properties, elongation and reduction area results differed in addition to the different sample geometries produced in build substrate. The test results of elongation and reduction area showed differences. Therefore based on the results obtained scope of the thesis, it is concluded that tests should be carried out with samples having similar thickness and orientation to the critical positions in the part in order to obtain consistent properties. This situation has been emphasizes before by the literature. (Dzugan et al., 2018) It is clearly stated that changes in α/β phase distrubution in the microstructure and the resulting mechanical properties can be observed as a result of temperature value variance between the layers depending on the height of the build substrate. (Nahr et al., 2023)

The alpha layer has hard and brittle characteristics, therefore it is not allowed to be used in aerospace applications for the stress critical parts especially due to its negative effect on the fatigue properties of the material. Since there are only few studies in in the literature dealing with alpha case layered materials and there is not much data on effect of alpha case on mechanical properties, comparison with thesis data cannot be made. As explained detail in the section where the microstructure results of post-conditions are shared, it was concluded that the alpha case layer of the alpha layered specimens to which annealed heat treatment was applied varied between 15-20 microns. When the tensile test results performed with the test samples having alpha layer in this values range are analyzed, it is learned that it has UTS/yield results at approximately the same level as the round and flat test samples in the other annealed cases. According the tensile test results, the material's core properties are more critical and the surface layer's small amount of brittle alpha layer has not much impact on material's tensile characteristics in terms of UTS/yield strength. Since the alpha layer thickness will vary depending on the applied thermal process, these evaluations only measure the effect of the alpha layer formed as a result of the annealed heat treatment procedure within the scope of thesis.

When the ductility test results of shared post-conditions in Figure 4.42. are interpreted, it is seen that the ductility results in the coupons tested with the alpha case layer are lower than in other conditions. This test result also confirms that the alpha case layer reduced the ductility of the material. Based on these result, the difference in alpha layer is clearly revealed in tensile test result. When the elongation and reduction area results of alpha layered specimen in round specimen geometry and annealed round specimen are compared, the absence of major effect of alpha layer is explained by the following evaluations:

- The very thin thickness of the alpha layer formed on the surface may not have created major difference in the tensile test that have control over the bulk material properties and reveal its results.
- Annealing heat treatment may improve the base material properties so that little or no difference in strength is noticiable due to the alpha layer.
- Since a specimen test was performed on the machine surface profile in both evaluated cases, measuring the alpha layer effect on the as-built surface quality planned for future studies may give a more noticeable result.

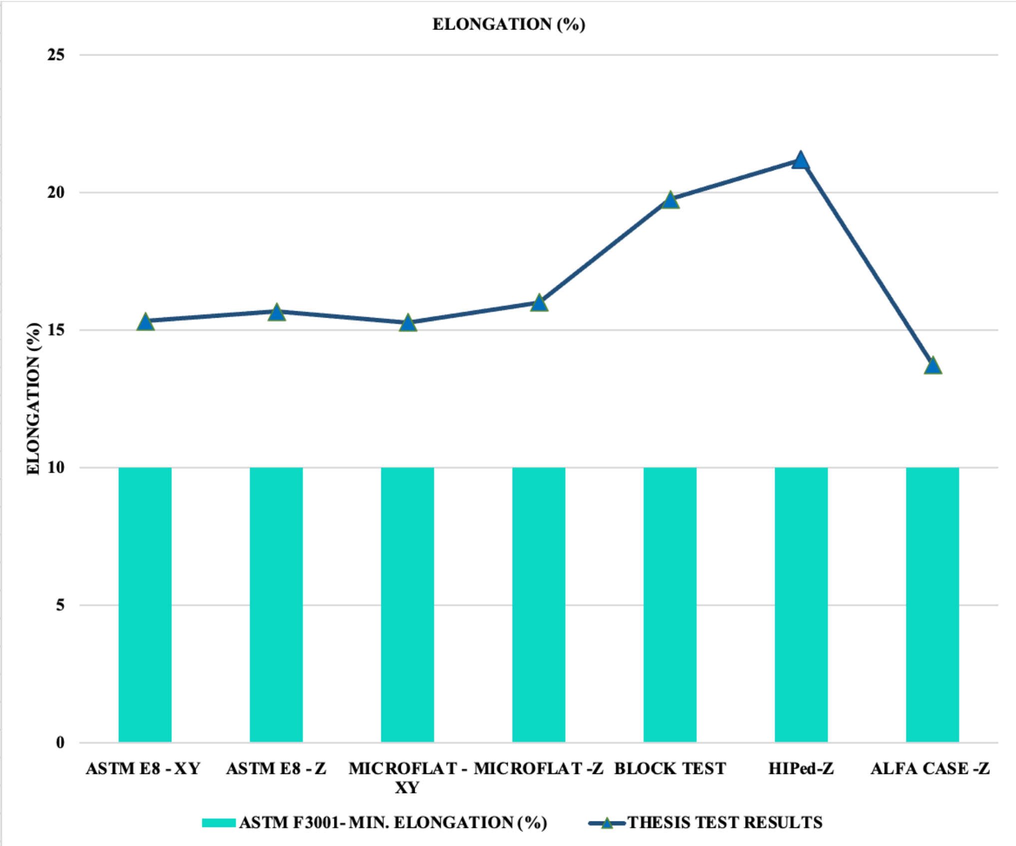

Figure 4.42. *Elongation test results of the post processes within the scope of thesis*

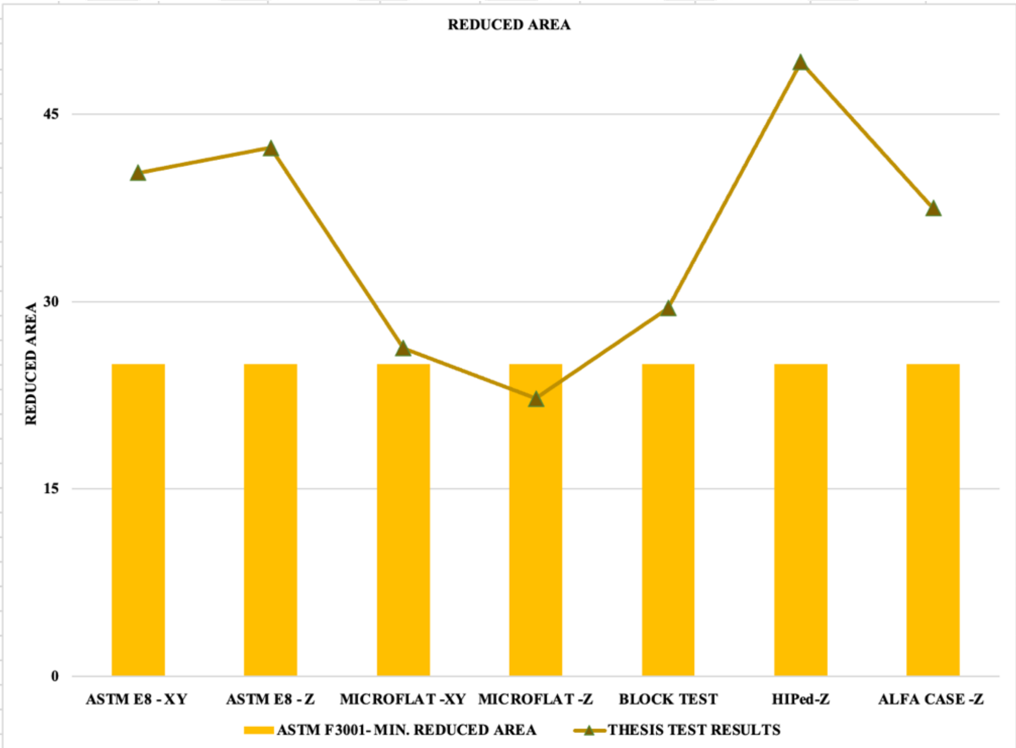

Figure 4.43. *Reduction area test results of the post processes within the scope of thesis*

The fatigue behavivor of the material, which is the primary characteristic that limits the application in aerospace parts, and its uncertainty in this regard led to fatigue tests being conducted for the post conditions established within the thesis for Ti64 parts produced with Ti64 SLM.

The SLM process, or in a more general sense, the additive manufacturing process, is stated in the interpretation of tensile test results together with the fact that the anisotropic materials produced exhibit lower mechanical behavior in the Z direction due to their nature. Therefore, since it would be more conservative for the evaluation of fatigue tests that take longer, test specimens in the Z direction were mostly used in the testing process. In the fatigue test, a lower fatigue life is expected since it is easier for the crack to propagate and continue along the grain boundaries in the Z direction. Especially considering that the results of the post processes studied within the scope of the thesis are intented to be used in aerospace applications and will be frequently subjected to cyclic loads under service conditions (case, blades, etc.), the fatigue performance of the parts is of great importance. The fact that the part is subjected to loading in the Z direction requires detailed examination of the anisotropic behavior in order to be able to make a reliable mechanical design evaluation.

Limited fatigue data for certain aerospace applications and the lack of reliable design allowences for SLM parts make a part-specific evaluation inadequate. The fatigue properties of the SLM Ti64 materials need to be identified in order to determine the proper manufacturing process during the part design phase and to perform a conformance assessment in accordance with that component life requirements. Therfore firstly, tests were carried out on the processed round coupon geometry of the annealing heat treated condition, which was also determined as the standard process flow within the scope of thesis for the SLM Ti64 materials.

Coupon groups belonging to two different directions, XY and Z were tested in the test matrix containing annealed heat treated round machined test specimens. Therefore, the surface roughness for these test specimens has the machined surface characteristic. Since the high surface roughness resulting from additive manufacturing is not present in the coupons, it is not expected to have an effect on the test results. In the literature, the negative effect of the high surface roughness value obtained as a result of SLM production on the fatigue life of the material is clearly stated. (Vayssette et al., 2019) For this reason, the as-built surface was not taken as a reference for the annealed condition in the additive parts to be produced as intented in the study. Additionally, the high surface rougness values are not preferred because they create different concerns in aero performance and non-destructive inspections processes.

The test results of the machined test coupons, which were only anneal heat treated, in XY and Z directions are given in the S/N curve shared in Figure 4.44. The elimination of residual stresses and microstructure modifiying are responsible for the surface quality enhancements influencing the HCF finding for Ti64 machined and annealed SLM coupons. While the annealing heat treatment lowers residual stresses by transforming the martensitic microstructure, the machining process contributes in the removal of the surface flaws. These effects work together to increase the material's fatigue resistance, proving the HCF performance with test results that are shared in two directions. The total fatigue performance is still influenced by elements like porosity, unmelted powder and SLM process optimization, as has been examined from the fracture surface characterization. For complete achievement of the fatigue resistance potential, these parameters must be adressed.

In the results shared in Figure 4.44, it is seen that lower HCF results are obtained in the Z annealed machined direction than in the XY annealed machined condition. The difference in these results can be explained by the columnar grain microstructure that creates low interfaces in the Z direction due to microstructure anisotropy. As in the tensile test results and low bonding between layers that can create delamination and crack inittiation. The Z direction test specimens show that, the fracture location of the coupons other than the run out coupons is the gage region. Fractures were observed in the gage, radius and thread regions of the coupons in the XY direction.

After SLM production, annealing heat treatment is applied to the part as specified in the experimental procedure. Then, it is seperated from the build substrate with EDM and is ready for post-processes. In the process, the alpha layer that will form after annealing heat treatment must be removed. Therefore, if the part geometry is suitable, the alpha layer that will reduce the fatigue life of the material from the part surface must be removed by machining. However, machining is not always suitable in terms of long process durations and machinability. Therefore, in the ideal process route, chemical abrasion method is used with the pickling process. Since only the alpha layer is not removed by the pickling process, sand blasting application must be done before the process. In other words, tests of the sand blasted + pickled coupons that represent the specified process flow of the part and can be a reference for the part surface quality were also carried out. The distrubution of test results on the S/N curve is shared in Figure 4.44.

One of the most significant aspects influencing fatigue performance when working with aerospace parts is any surface irregularity or micro crack that would increase stress, as these parts are typically subjected to high frequency loading. Consequently, surface roughness plays a significant role in characterizing the material's fatigue behavior. Although the machined surface quality is generally taken as a basis in the thesis, surface roughness measuraments were carried out in order to evaluate the test results related to other post-conditions that taken as reference for parts where machining cannot be effective. As a result of the surface roughness measurement on the as-built coupons, a value of approximately 9.15 Ra (±0.85 Ra) was obtained. It was observed that the surface roughness value changed to 5.15 Ra (± 0.85 Ra) after sand blasting. It was obtained that the surface roughness value decreaed to level 3 Ra (±0.75) with the pickling process applied after sand blasting. Sand blasting process creates small pits on the surface of the material, which increases the surfaces roughness. By applying sand blasting, semi-molten powder particles are removed after production and then a pickling process is applied, allowing for more effective chemical abrasion.

While the sandblasting is expected to have an adverse effect on the fatigue life of the material, it can be noted that it can improve fatigue resistance under certain conditions. It has been stated in studies that this improving effect may be due to the increased roughness creating compressive residual stresses on the surface which are beneficial for improving fatigue life by reducing crack initiation. The investigations have made it abundantly evident that the conditions can lead to the crack initiation in various chararacterization results are transmitted from the material surface to the interior after the sandblasting process and therfore have an effect on improving the fatigue behavior.(C. Yu et al., 2022) In addition, it can be said that the method has a positive effect on crack initiation and propagation by creating compressive stress by reducing the residual stresses that occur during the part production.(Avanzini et al., 2019) It is possible that this benefical effect may vary depending on the applied process parameters. Inappropriate process application may lead to a situation where crack initiation can be triggered on the surface. Therefore optimum process parameters that were previously verified for the process studied within the scope of the thesis were used.

As discussed in detail in the section where the fracture surface examination results of the fatigue specimens are shared, crack initiation regions were detected in the sand blasting process due to subsurface defects rather than the surface as stated in the literature. Therefore, the improvement in fatigue behavior can be explained through the microstructure-property relationship compared to the annealed condition. In sand blasted specimens, there are test specimens that are observed to crack from the gage region at a lower cycle compared to the others in the test group performed at same stress level. When it is associated with the fracture surfaces, it is concluded that the test failed due to subsurface porosities. While it was expected that the test would continue at average stress levels in the test matrix in the test coupons, the test was terminated earlier in the cycle because a crack was observed from the radius region. It is concluded that subsurface microstructure line are dominant in the sand blasted + pickling test group and these defects should be eliminated to improve fatigue life.

It is expected that the pickling process after the sand blasting process will not have an effect that will reduce internal stresses and create compressive stress due to the process. It is seen that this issue is not emphasized in the literature. Since it is a process aimed at removing material from the surface, there is a possibility that it can create a positive effect on fatigue by abrading material from the areas where there are surface and subsurface defects. In this test group tested within the scope of the thesis, the effects of the processes can be evaluated separately based on the literature, but the effects of both processes together are concluded with these test results.

The HCF test results shared in Figure 4.44. clearly show that a minor improvement was observed in the sandblasted + pickled coupons to the machined+ annealed condition. This improvement in the test results can also be explained by research findings in the literature. These findings demonstrate that the sand blasting + pickling alpha case removal procedures used following the annealing heat treatment will not result in decrease in the fatigue strength of the material in parts that cannot machined, and the part's design evaluation will not raise any concerns. It is possible to conclude that there has been improvement, particularly when examining the material's alternating stress results for the 10^7 cycles.

In the literature, the general practice is to study the fatigue test for the case where the process squence is applied HIP and then machining. In addition, the reducing effect the surface roughness from the production method on fatigue has been clearly revealed in case where HIP is applied to the additive manufacturing surface and no machining is done. (Dolev et al., 2022) However, since the HIP process used within the scope of this thesis is generally a costly process and is not applied, the effect of alpha layer formed due to the heat treatment in complex geometries and the termal imputs that the parts exposed after production has not been removed. Here, the general practices to compare two cases by removing the alpha layer effect formed after the machining on machined fatigue specimens that have been applied heat treatment and the observed the reduction in fatigue data.

In comparison to other post-conditions, there is a discernible increase in fatigue life when the results of HIPed coupons are examined in the S/N curve in Figure 4.44. It is evident that, in contrast to other conditions, all of specimens tested at various stress levels exhibit resistance over the extended cycle. With the exception of two test specimens, all of the specimens are run-out. The other two fractured specimen have a radius fracture zone. The part that examines the fracture surfaces of these specimen discusses the results of a detailed examinations.

It is stated that the main factor underlying the improvement of the fatigue strength of the HIP process is achieved by obtaining a microstructure with an $\alpha+\beta$ phase in the microstructure.(Roudnicka et al., 2019) At the same time, another important factor is shared with HIP as elimination of porosities and microvoids in the microstructure, which act as stress concentrators and create crack initiation zones with help of fatigue loading.(Cheng et al., 2022) The major difference compared to other situations can be explained in this way by literature. The effectiveness of fatigue behavior has been reported to vary based on various processes.

Fatigue life prediction for aerospace components operating under cyclic loads is critical to part design stage, as it has been concluded that the HIP process increases the endurance limit of the material by approximately two times compared to annealed material. Since the HIP process is a costly process, it is generally considered a neccessity in the process of parts with additive manufacturing potential. From the HIP fatigue test results within the scope of the thesis, it is revealed that if the part to be produced is a part that operating under cyclic loads a part whose fatigue life is importanti the addition of the HIP process at the design stage should be improve the fatigue life of the material.

Another important situation in SLM production Ti64 parts is the lack of information on how to evaluate the alpha layer formed on the surface of the part with any thermal input during the production phase of the part, repair or additional process application in terms of design. In the first setion where the literature is detailed, the effect of the alpha layer on fatigue life is discussed. However, no data has been reached on the mechanical effect of the alpha layer in all studies. Since removing the alpha layer is both mechanically and chemically difficult and not always effective processes, the effect of alpha layer on the fatigue properties of material has been determined with the fatigue test results shared in Figure 4.44.

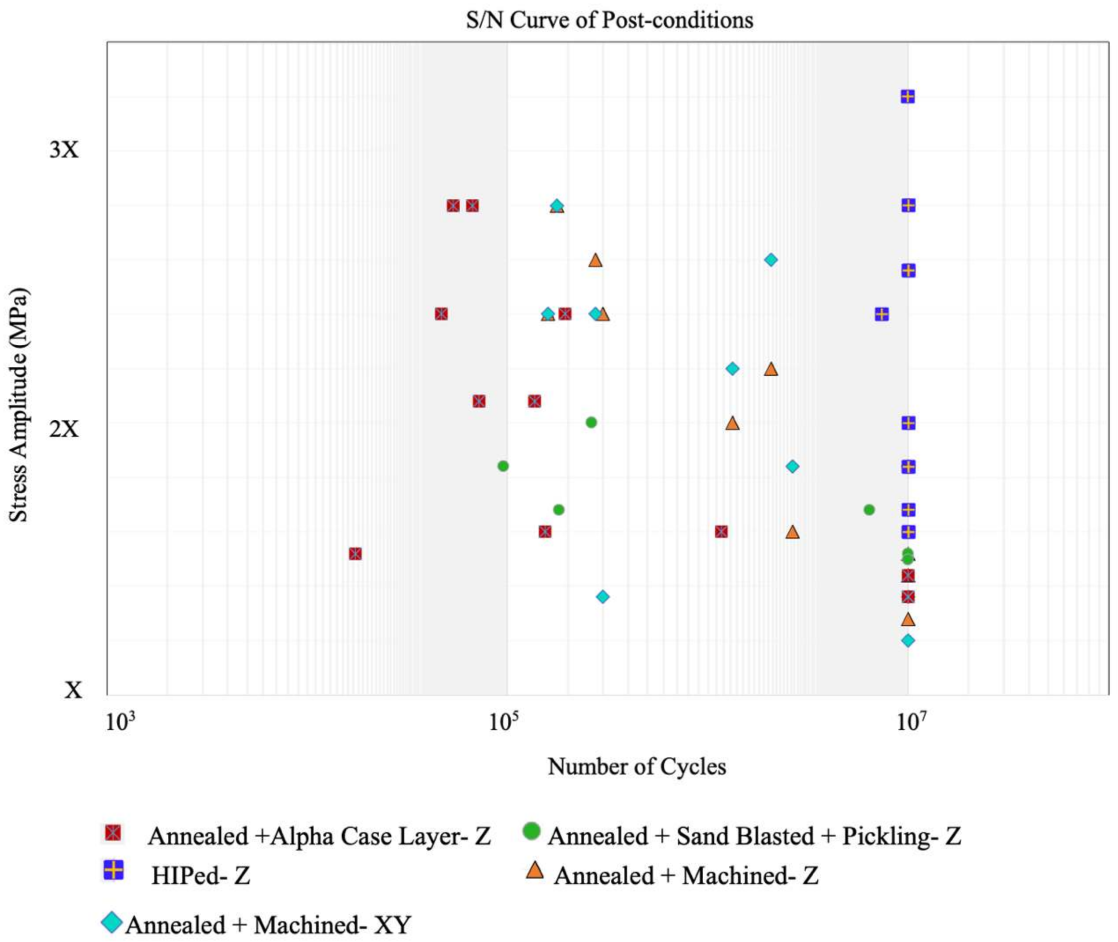

Figure 4.44. *S/N curve of thesis post-processes*

5. CONCLUSION AND FUTURE WORKS

As a result of the studies carried out to establish the relationship between the microstructure and mechanical properties of different post processes and to determine a process route that will be suitable for the requirements of aerospace parts according to the study outputs:

- The thesis examined both machined and non-machined process configurations in addition to SLM's ability to produce complex part since titanium material generates drawback from the thermal inputs, such as an alpha layer. For these two process route, fracture mechanic behavior was investigated in annealed + machined and sand blasted + pickling test groups. Although no negative effect of the sand blast pickling process was observed in HCF tests, a minor improvement in the endurance limit of the material was observed.
- The material's microstructure and literature findings indicate that it is unsuitable for utilization in aerospace parts in the as-built scenario. To produce the proper microstructure, a thermal process consequently becomes neccessary in the process flow. Due to the absence of mechanical data in the literature and the impact of the alpha layer created following the heat treatment process on the SLM fracture behavior, fatigue test were conducted using the alpha case. When compared to the standard annealed material, it was found that the alpha layer reduced the material's endurance limit by %15.
- When the flat and round coupon test results of different coupon geometries in which tensile tests were performed within the scope of study were compared, no major difference was observed in the UTS and yield strength results, while it was observed that there were differences in the results compared to the microstructure and stress concentration regions that changed depending on the geometry difference in the elongation and reduction area values. For component verification investigations including additive production, it subsequently became neccessary to select a coupon size that accurately represented the part geometry.
- According to the average of the porosity measurement results performed to understand the effectiveness of the HIP parameters used in the experiment, approximately 60% improvement was observed in the HIPed material conditions compared to the anneal heat treatment.

- As a result of this study, a database of different process flows that will be used for SLMed Ti64 aerospace parts and that are studied in order to advance design activities in this field has been created.
- Since the HIP process is not always applicable for cost-effective design, it was concluded that the fatigue test results of the materials to which the determined HIP parameter was applied showed an approximately 2 times improvement in the endurance limit of the material when compared with the standard annealed condition.
- The data outputs obtained at the end of the thesis will enable the selection of a material and process according to the mechanical requirements in the design, especially the fatigue requirements of the material. The process flow should be selected over HIP, and alpha layer removal should need s to remove after HIP, particularly for fatigue-critical parts.
- As a result of optical microscope microstructure and SEM fracture surface examinations, it was seen that the most effective situation in mechanical properties as well as post processes was the nonconformities resulting from the SLM process. Therefore, the situation that will strengthen the impacts of post processes will be the appropriate and low defect microstructure obtained as a result of ideal process parameters.
- For all post-conditions studied within the scope of the thesis, the minimum mechanical properties specified in the aerospace standards were provided.
- Although the improvement on the material surface after sand blasting process to helps to transfer the crack initiation areas from the surface to the sub-surface, it is seen that it has some limitation in the fatigue strength due to the large pores and irregularities on the sub-surface, which also effective in other conditions. When the results of different process outputs studied within the scope of thesis are compared; it is seen that the high hardness value can increase the resistance of the material against deformation and have a positive effect of fatigue strength. While on the other hand, a high hardness value creates a situation that triggers crack formation and therefore the material hardness can have a negative effect of the fatigue behavior of the material. Therefore, it is neccessary to examine the LCF behavior post-conditions in future studies.

- It has been observed that there is a need to plan studies on internal stresses that may affect the material mechanical test results of all post processes and to correlate the results.

REFERENCES

Alami, A. H., Ghani Olabi, A., Alashkar, A., Alasad, S., Aljaghoub, H., Rezk, H., & Abdelkareem, M. A. (2023). Additive manufacturing in the aerospace and automotive industries: Recent trends and role in achieving sustainable development goals. In *Ain Shams Engineering Journal* (Vol. 14, Issue 11). Ain Shams University. https://doi.org/10.1016/j.asej.2023.102516

Alegre, J. M., Díaz, A., García, R., Peral, L. B., & Cuesta, I. I. (2022). Effect of HIP post-processing at 850 °C/200 MPa in the fatigue behavior of Ti-6Al-4V alloy fabricated by Selective Laser Melting. International Journal of Fatigue, 163. https://doi.org/10.1016/j.ijfatigue.2022.107097

Al-Maharma, A. Y., Patil, S. P., & Markert, B. (2020). Effects of porosity on the mechanical properties of additively manufactured components: a critical review. In Materials Research Express (Vol. 7, Issue 12). IOP Publishing Ltd. https://doi.org/10.1088/2053-1591/abcc5d

AlMangour, B., Luqman, M., Grzesiak, D., Al-Harbi, H., & Ijaz, F. (2020). Effect of processing parameters on the microstructure and mechanical properties of Co–Cr–Mo alloy fabricated by selective laser melting. Materials Science and Engineering: A, 792. https://doi.org/10.1016/j.msea.2020.139456

Al-Rubaie, K. S., Melotti, S., Rabelo, A., Paiva, J. M., Elbestawi, M. A., & Veldhuis, S. C. (2020). Machinability of SLM-produced Ti6Al4V titanium alloy parts. Journal of Manufacturing Processes, 57, 768–786. https://doi.org/10.1016/j.jmapro.2020.07.035

Attaran, M. (2017). The rise of 3-D printing: The advantages of additive manufacturing over traditional manufacturing. Business Horizons, 60(5), 677–688. https://doi.org/10.1016/j.bushor.2017.05.011

Avanzini, A., Battini, D., Gelfi, M., Girelli, L., Petrogalli, C., Pola, A., & Tocci, M. (2019). Investigation on fatigue strength of sand-blasted DMLS-AlSi10Mg alloy. Procedia Structural Integrity, 18, 119–128. https://doi.org/10.1016/j.prostr.2019.08.146

Barba, D., Alabort, C., Tang, Y. T., Viscasillas, M. J., Reed, R. C., & Alabort, E. (2020). On the size and orientation effect in additive manufactured Ti-6Al-4V. Materials and Design, 186. https://doi.org/10.1016/j.matdes.2019.108235

Bartolomeu, F., Gasik, M., Silva, F. S., & Miranda, G. (2022). Mechanical Properties of Ti6Al4V Fabricated by Laser Powder Bed Fusion: A Review Focused on the Processing and Microstructural Parameters Influence on the Final Properties. In Metals (Vol. 12, Issue 6). MDPI. https://doi.org/10.3390/met12060986

Bernevig-Sava, M. A., Stamate, C., Lohan, N. M., Baciu, A. M., Postolache, I., Baciu, C., & Baciu, E. R. (2019). Considerations on the surface roughness of SLM processed metal parts and the effects of subsequent sandblasting. IOP Conference Series: Materials Science and Engineering, 572(1). https://doi.org/10.1088/1757-899X/572/1/012071

Bezuidenhout, M., Ter Haar, G., Becker, T., Rudolph, S., Damm, O., & Sacks, N. (2020). The effect of HF-HNO3 chemical polishing on the surface roughness and fatigue life of laser powder bed fusion produced Ti6Al4V. Materials Today Communications, 25. https://doi.org/10.1016/j.mtcomm.2020.101396

Blakey-Milner, B., Gradl, P., Snedden, G., Brooks, M., Pitot, J., Lopez, E., Leary, M., Berto, F., & du Plessis, A. (2021). Metal additive manufacturing in aerospace: A review. Materials and Design, 209. https://doi.org/10.1016/j.matdes.2021.110008

Cardon, A., Mareau, C., Ayed, Y., van der Veen, S., Giraud, E., Dal Santo, P., & Van Der Veen, S. (2020). Additive Manufacturing. 39. https://doi.org/10.1016/j.addma.2020.101766ï

Cegan, T., Pagac, M., Jurica, J., Skotnicova, K., Hajnys, J., Horsak, L., Soucek, K., & Krpec, P. (2020). Effect of hot isostatic pressing on porosity and mechanical properties of 316 l stainless steel prepared by the selective laser melting method. Materials, 13(19), 1–26. https://doi.org/10.3390/ma13194377

Cerri, E., Ghio, E., & Bolelli, G. (2022). Ti6Al4V-ELI Alloy Manufactured via Laser Powder-Bed Fusion and Heat-Treated below and above the β-Transus: Effects of Sample Thickness and Sandblasting Post-Process. Applied Sciences (Switzerland), 12(11). https://doi.org/10.3390/app12115359

Chen, S. guang, Zhang, Y. du, Wu, Q., Gao, H. jun, Gao, Z. han, & Li, X. (2021). Effect of solid-state phase transformation on residual stress of selective laser melting Ti6Al4V. Materials Science and Engineering: A, 819. https://doi.org/10.1016/j.msea.2021.141299

Cheng, M., Lu, Z., Wu, J., Guo, R., Qiao, J., Xu, L., & Yang, R. (2022). Effect of thermal induced porosity on high-cycle fatigue and very high-cycle fatigue behaviors of hot-isostatic-pressed Ti-6Al-4V powder components. Journal of Materials Science and Technology, 98, 177–185. https://doi.org/10.1016/j.jmst.2021.04.066

Cordeiro, J. M., & Barão, V. A. R. (2017). Is there scientific evidence favoring the substitution of commercially pure titanium with titanium alloys for the manufacture of dental implants? In Materials Science and Engineering C (Vol. 71, pp. 1201–1215). Elsevier Ltd. https://doi.org/10.1016/j.msec.2016.10.025

Cutolo, A., Elangeswaran, C., de Formanoir, C., Muralidharan, G. K., & Van Hooreweder, B. (2019). Effect of Heat Treatments on Fatigue Properties of Ti–6Al–4V and 316L Produced by Laser Powder Bed Fusion in As-Built Surface Condition. Minerals, Metals and Materials Series, 395–405. https://doi.org/10.1007/978-3-030-05861-6_36

Dangal, B., & Jung, S. (2023). The Impact of Additive Manufacturing Constraints and Design Objectives on Structural Topology Optimization. Applied Sciences (Switzerland), 13(18). https://doi.org/10.3390/app131810161

Deshmukh, V., Kadam, R., & Joshi, S. S. (2017). Removal of alpha case on titanium alloy surfaces using chemical milling. Machining Science and Technology, 21(2), 257–278. https://doi.org/10.1080/10910344.2017.1284558

Designation: F3001 − 14 Standard Specification for Additive Manufacturing Titanium-6 Aluminum-4 Vanadium ELI (Extra Low Interstitial) with Powder Bed Fusion 1. (n.d.). https://doi.org/10.1520/F3001-14

Dolev, O., Ron, T., Aghion, E., & Shirizly, A. (2022). Effect of HIP Defects on the Mechanical Properties of Additive Manufactured Ti6Al4V Alloy. Metals, 12(7). https://doi.org/10.3390/met12071210

Du Plessis, A., Le Roux, S. G., Els, J., Booysen, G., & Blaine, D. C. (2015). Application of microCT to the non-destructive testing of an additive manufactured titanium component. Case Studies in Nondestructive Testing and Evaluation, 4, 1–7. https://doi.org/10.1016/j.csndt.2015.09.001

du Plessis, A., & Macdonald, E. (2020). Hot isostatic pressing in metal additive manufacturing: X-ray tomography reveals details of pore closure. Additive Manufacturing, 34. https://doi.org/10.1016/j.addma.2020.101191

Dzugan, J., Seifi, M., Prochazka, R., Rund, M., Podany, P., Konopik, P., & Lewandowski, J. J. (2018). Effects of thickness and orientation on the small scale fracture behaviour of additively manufactured Ti-6Al-4V. Materials Characterization, 143, 94–109. https://doi.org/10.1016/j.matchar.2018.04.003

Eshawish, N., Malinov, S., Sha, W., & Walls, P. (2021). Microstructure and Mechanical Properties of Ti-6Al-4V Manufactured by Selective Laser Melting after Stress Relieving, Hot Isostatic Pressing Treatment, and Post-Heat Treatment. Journal of Materials Engineering and Performance, 30(7), 5290–5296. https://doi.org/10.1007/s11665-021-05753-w

Fraczek-Szczypta, A., Wedel-Grzenda, A., Benko, A., Grzonka, J., & Mizera, J. (2017). Interaction of carbon nanotubes coatings with titanium substrate. Applied Physics A: Materials Science and Processing, 123(2). https://doi.org/10.1007/s00339-016-0740-1

Frazier, W. E. (2014). Metal additive manufacturing: A review. In Journal of Materials Engineering and Performance (Vol. 23, Issue 6, pp. 1917–1928). Springer New York LLC. https://doi.org/10.1007/s11665-014-0958-z

Funch, C. V., Somlo, K., Poulios, K., Mohanty, S., Somers, M. A. J., & Christiansen, T. L. (2020). The influence of microstructure on mechanical properties of SLM 3D printed Ti-6Al-4V. MATEC Web of Conferences, 321, 03005. https://doi.org/10.1051/matecconf/202032103005

Gaddam, R., Sefer, B., Pederson, R., & Antti, M. L. (2013). Study of alpha-case depth in Ti-6Al-2Sn-4Zr-2Mo and Ti-6Al-4V. IOP Conference Series: Materials Science and Engineering, 48(1). https://doi.org/10.1088/1757-899X/48/1/012002

Gaiani, S., Ferrari, E., Gozzi, M., Di Giovanni, M. T., Lassinantti Gualtieri, M., Colombini, E., & Veronesi, P. (2023). Impact of Post-Process Heat Treatments Performed on Ti6Al4V Titanium Alloy Specimens Obtained Using LPBF Technology. Technologies, 11(4). https://doi.org/10.3390/technologies11040100

Gao, B., Zhao, H., Peng, L., & Sun, Z. (2023). A Review of Research Progress in Selective Laser Melting (SLM). In Micromachines (Vol. 14, Issue 1). MDPI. https://doi.org/10.3390/mi14010057

Gong, H., Rafi, K., Gu, H., Janaki Ram, G. D., Starr, T., & Stucker, B. (2015). Influence of defects on mechanical properties of Ti-6Al-4V components produced by selective laser melting and electron beam melting. Materials and Design, 86, 545–554. https://doi.org/10.1016/j.matdes.2015.07.147

Gonzalez, D. (2020). Process Specification for Pickling, Etching, and Descaling of Metals.

He, J., Li, D., Jiang, W., Ke, L., Qin, G., Ye, Y., Qin, Q., & Qiu, D. (2019). The Martensitic Transformation and Mechanical Properties of Ti6Al4V Prepared via Selective Laser Melting. Materials, 12(2). https://doi.org/10.3390/ma12020321

Hirata, T., Kimura, T., & Nakamoto, T. (2020). Effects of hot isostatic pressing and internal porosity on the performance of selective laser melted AlSi10Mg alloys. Materials Science and Engineering: A, 772. https://doi.org/10.1016/j.msea.2019.138713

Huang, R., Riddle, M., Graziano, D., Warren, J., Das, S., Nimbalkar, S., Cresko, J., & Masanet, E. (2016). Energy and emissions saving potential of additive manufacturing: the case of lightweight aircraft components. Journal of Cleaner Production, 135, 1559–1570. https://doi.org/10.1016/j.jclepro.2015.04.109

Isa, M. R., Zaroog, O. S., Yunus, M. A., Sanny Bavu, V. R., & Rosmi, N. (2018). Effect of sandblasting process on mechanical properties of ASTM A516 grade 70 steel. Key Engineering Materials, 765 KEM, 222–226. https://doi.org/10.4028/www.scientific.net/KEM.765.222

Jaber, H., Kónya, J., Kulcsár, K., & Kovács, T. (2022). Effects of Annealing and Solution Treatments on the Microstructure and Mechanical Properties of Ti6Al4V Manufactured by Selective Laser Melting. Materials, 15(5). https://doi.org/10.3390/ma15051978

Jamshidi, P., Aristizabal, M., Kong, W., Villapun, V., Cox, S. C., Grover, L. M., & Attallah, M. M. (2020). Selective laser melting of ti-6al-4v: The impact of post-processing on the tensile, fatigue and biological properties for medical implant applications. Materials, 13(12), 1–16. https://doi.org/10.3390/ma13122813

Jimenez, E. H., Kreitcberg, A., Moquin, E., & Brailovski, V. (2022). Influence of Post-Processing Conditions on the Microstructure, Static, and Fatigue Resistance of Laser Powder Bed Fused Ti-6Al-4V Components. Journal of Manufacturing and Materials Processing, 6(4). https://doi.org/10.3390/jmmp6040085

Joshi, S. C., & Sheikh, A. A. (2015). 3D printing in aerospace and its long-term sustainability. Virtual and Physical Prototyping, 10(4), 175–185. https://doi.org/10.1080/17452759.2015.1111519

June, D., Mayeur, J. R., Gradl, P., Wessman, A., & Hazeli, K. (2023). Effects of Size, Geometry, and Temperature on Additively Manufactured Ti-6al-4v Titanium Alloy. https://doi.org/10.2139/ssrn.4577754

Karami, K., Blok, A., Weber, L., Ahmadi, S. M., Petrov, R., Nikolic, K., Borisov, E. V., Leeflang, S., Ayas, C., Zadpoor, A. A., Mehdipour, M., Reinton, E., & Popovich, V. A. (2020). Continuous and pulsed selective laser melting of Ti6Al4V lattice structures: Effect of post-processing on microstructural anisotropy and fatigue behaviour. Additive Manufacturing, 36. https://doi.org/10.1016/j.addma.2020.101433

Kasperovich, G., & Hausmann, J. (2015). Improvement of fatigue resistance and ductility of TiAl6V4 processed by selective laser melting. Journal of Materials Processing Technology, 220, 202–214. https://doi.org/10.1016/j.jmatprotec.2015.01.025

Kónya, J., Jaber, H., Kovács, T. A., & Hargitai, H. (2024). Effects of selective laser melting building directions and surface modifications on surface roughness of Ti6Al4V alloy. Discover Applied Sciences, 6(1). https://doi.org/10.1007/s42452-024-05656-0

Kouprianoff, D., & du Preez, W. (2023). Reducing time and cost of the heat treatment post-processing of additively manufactured Ti6Al4V. Materials Today Communications, 35. https://doi.org/10.1016/j.mtcomm.2023.106186

Krakhmalev, P., Fredriksson, G., Yadroitsava, I., Kazantseva, N., Du Plessis, A., & Yadroitsev, I. (2016). Deformation behavior and microstructure of Ti6Al4V manufactured by SLM. Physics Procedia, 83, 778–788. https://doi.org/10.1016/j.phpro.2016.08.080

Kuntoğlu, M., Salur, E., Canli, E., Aslan, A., Gupta, M. K., Waqar, S., Krolczyk, G. M., & Xu, J. (2023). A state of the art on surface morphology of selective laser-melted metallic alloys. In International Journal of Advanced Manufacturing Technology (Vol. 127, Issues 3–4, pp. 1103–1142). Springer Science and Business Media Deutschland GmbH. https://doi.org/10.1007/s00170-023-11534-7

Leuders, S., Thöne, M., Riemer, A., Niendorf, T., Tröster, T., Richard, H. A., & Maier, H. J. (2013). On the mechanical behaviour of titanium alloy TiAl6V4 manufactured by selective laser melting: Fatigue resistance and crack growth performance. International Journal of Fatigue, 48, 300–307. https://doi.org/10.1016/j.ijfatigue.2012.11.011

Leyens, C. (Christoph), & Peters, M. (Manfred). (2003). Titanium and titanium alloys : fundamentals and applications. Wiley-VCH.

Lim, S., Ko, Y., Hong, D., Kim, M., & Song, S. J. (2024). Impact of Additive Manufacturing Surface Roughness on the Aerodynamic Performance of Axial Compressor Blades. International Journal of Aeronautical and Space Sciences. https://doi.org/10.1007/s42405-024-00769-7

Liu, S., & Shin, Y. C. (2019). Additive manufacturing of Ti6Al4V alloy: A review. Materials and Design, 164. https://doi.org/10.1016/j.matdes.2018.107552

Longhitanoa, G. A., Larosaa, M. A., Munhoza, A. L. J., De Carvalho Zavagliaa, C. A., & Ierardia, M. C. F. (2015). Surface finishes for Ti-6Al-4V alloy produced by direct metal laser sintering. Materials Research, 18(4), 838–842. https://doi.org/10.1590/1516-1439.014415

Louvis, E., Fox, P., & Sutcliffe, C. J. (2011). Selective laser melting of aluminium components. Journal of Materials Processing Technology, 211(2), 275–284. https://doi.org/10.1016/j.jmatprotec.2010.09.019

Lu, D., Liu, Z., Wei, X., Chen, C., & Wang, D. (2023). Effect of post-processing methods on the surface quality of Ti6Al4V fabricated by laser powder bed fusion. Frontiers in Materials, 10. https://doi.org/10.3389/fmats.2023.1126749

Lv, Z., Li, H., Che, L., Chen, S., Zhang, P., He, J., Wu, Z., Niu, S., & Li, X. (2023). Effects of HIP Process Parameters on Microstructure and Mechanical Properties of Ti-6Al-4V Fabricated by SLM. Metals, 13(5). https://doi.org/10.3390/met13050991

Magerramova, L., Vasilyev, B., & Kinzburskiy, V. (2016). NOVEL DESIGNS OF TURBINE BLADES FOR ADDITIVE MANUFACTURING. http://proceedings.asmedigitalcollection.asme.org/pdfaccess.ashx?url=/data/conferences/asmep/89507/

Mashigo, L., Möller, H., & Gassmann, C. (2021). Comparison of the mechanical properties of Grade 5 and Grade 23 Ti6Al4V for wire-arc additive manufacturing. The Journal of the Southern African Institute of Mining and Metallurgy, 121. https://doi.org/10.17159/2411

Mathe, N. R., Tshabalala, L. C., Hoosain, S., Motibane, L., & du Plessis, A. (2021). The effect of porosity on the mechanical properties of Ti-6Al-4V components manufactured by high-power selective laser melting. International Journal of Advanced Manufacturing Technology, 115(11–12), 3589–3597. https://doi.org/10.1007/s00170-021-07326-6

Meier, M. A., Gooding, W. J., Fabian, J., & Key, N. (2020). Considerations for using additive manufacturing technology in centrifugal compressor research. Journal of Engineering for Gas Turbines and Power, 142(3). https://doi.org/10.1115/1.4044937

Mishra, R. R., Kumar, R., Sahoo, A. K., & Panda, A. (2020). Machinability behaviour of biocompatible Ti-6Al-4V ELI titanium alloy under flood cooling environment. Materials Today: Proceedings, 23, 536–540. https://doi.org/10.1016/j.matpr.2019.05.402

Mohite, N., Biradar, S., & Shankar Jha, J. (2017). Development and removal of alpha-case layer from heat treated Titanium alloys. http://www.asme.org/about-asme/terms-of-use

Moridi, A., Demir, A. G., Caprio, L., Hart, A. J., Previtali, B., & Colosimo, B. M. (2019). Deformation and failure mechanisms of Ti–6Al–4V as built by selective laser melting. Materials Science and Engineering: A, 768. https://doi.org/10.1016/j.msea.2019.138456

Moussaoui, K., Rubio, W., Mousseigne, M., Sultan, T., & Rezai, F. (2018). Effects of Selective Laser Melting additive manufacturing parameters of Inconel 718 on porosity, microstructure and mechanical properties. Materials Science and Engineering: A, 735, 182–190. https://doi.org/10.1016/j.msea.2018.08.037

Munk, J., Breitbarth, E., Siemer, T., Pirch, N., & Häfner, C. (2022). Geometry Effect on Microstructure and Mechanical Properties in Laser Powder Bed Fusion of Ti-6Al-4V. Metals, 12(3). https://doi.org/10.3390/met12030482

Nagesha, B. K., Anand Kumar, S., Vinodh, K., Pathania, A., & Barad, S. (2020). A thermo-Mechanical modelling approach on the residual stress prediction of SLM processed HPNGV aeroengine part. Materials Today: Proceedings, 44, 4990–4996. https://doi.org/10.1016/j.matpr.2020.12.940

Nahr, F., Rasch, M., Burkhardt, C., Renner, J., Baumgärtner, B., Hausotte, T., Körner, C., Steinmann, P., Mergheim, J., Schmidt, M., & Markl, M. (2023). Geometrical Influence on Material Properties for Ti6Al4V Parts in Powder Bed Fusion. Journal of Manufacturing and Materials Processing, 7(3). https://doi.org/10.3390/jmmp7030082

Nicoletto, G., Maisano, S., Antolotti, M., & Dall'aglio, F. (2017). Influence of post fabrication heat treatments on the fatigue behavior of Ti-6Al-4V produced by selective laser melting. Procedia Structural Integrity, 7, 133–140. https://doi.org/10.1016/j.prostr.2017.11.070

Özsoy, K., Duman, B., & İçkale Gültekin, D. (n.d.). Metal Part Production with Additive Manufacturing for Aerospace and Defense Industry.

Pereira, T., Kennedy, J. V., & Potgieter, J. (2019). A comparison of traditional manufacturing vs additive manufacturing, the best method for the job. Procedia Manufacturing, 30, 11–18. https://doi.org/10.1016/j.promfg.2019.02.003

Petrousek, P., Bidulska, J., Bidulsky, R., Kocisko, R., Fedorikova, A., Hudak, R., Rajtukova, V., & Zivcak, J. (2017). Mechanical properties and porosity of Ti-6Al-4V alloy prepared by AM technology. MM Science Journal, 2017(FEBRUARY), 1752–1755. https://doi.org/10.17973/MMSJ.2017_02_2016190

Popovich, A., Sufiiarov, V., Polozov, I., Borisov, E., & Masaylo, D. (2016). Producing hip implants of titanium alloys by additive manufacturing. International Journal of Bioprinting, 2(2), 78–84. https://doi.org/10.18063/IJB.2016.02.004

Qian, M., Xu, W., Brandt, M., & Tang, H. P. (2016). Additive manufacturing and postprocessing of Ti-6Al-4V for superior mechanical properties. In MRS Bulletin (Vol. 41, Issue 10, pp. 775–783). Materials Research Society. https://doi.org/10.1557/mrs.2016.215

Rafi, H. K., Karthik, N. V., Gong, H., Starr, T. L., & Stucker, B. E. (2013). Microstructures and mechanical properties of Ti6Al4V parts fabricated by selective laser melting and electron beam melting. Journal of Materials Engineering and Performance, 22(12), 3872–3883. https://doi.org/10.1007/s11665-013-0658-0

Roudnicka, M., Mertova, K., & Vojtech, D. (2019). Influence of hot isostatic pressing on mechanical response of as-built SLM titanium alloy. IOP Conference Series: Materials Science and Engineering, 629(1). https://doi.org/10.1088/1757-899X/629/1/012034

Sahoo, S., Jha, B. B., & Mandal, A. (2021). Powder metallurgy processed TiB2-reinforced steel matrix composites: a review. In Materials Science and Technology (United Kingdom) (Vol. 37, Issue 14, pp. 1153–1173). Taylor and Francis Ltd. https://doi.org/10.1080/02670836.2021.1987705

Say, W. C., & Tsai, Y. Y. (2004). Surface characterization of cast Ti-6Al-4V in hydrofluoric-nitric pickling solutions. Surface and Coatings Technology, 176, 337–343. https://doi.org/10.1016/S0257-8972Ž03.00747-3

Schenk, R. (n.d.). 6 The Corrosion Properties of Titanium and Titanium Alloys.

Schmidt, F. F., & Wood, R. A. (n.d.). HEAT TREATMENT O F TITANIUM AND TITANIUM ALLOYS.

Seth, P., Jha, J. S., Alankar, A., & Mishra, S. K. (2022). Alpha-case Formation in Ti–6Al–4V in a Different Oxidizing Environment and Its Effect on Tensile and Fatigue Crack Growth Behavior. Oxidation of Metals, 97(1–2), 77–95. https://doi.org/10.1007/s11085-021-10079-y

Shunmugavel, M., Polishetty, A., & Littlefair, G. (2015). Microstructure and Mechanical Properties of Wrought and Additive Manufactured Ti-6Al-4V Cylindrical Bars. Procedia Technology, 20, 231–236. https://doi.org/10.1016/j.protcy.2015.07.037

Song, B., Zhao, X., Li, S., Han, C., Wei, Q., Wen, S., Liu, J., & Shi, Y. (2015). Differences in microstructure and properties between selective laser melting and traditional manufacturing for fabrication of metal parts: A review. In Frontiers of Mechanical Engineering (Vol. 10, Issue 2, pp. 111–125). Higher Education Press. https://doi.org/10.1007/s11465-015-0341-2

Spear, A. D., & Ingraffea, A. R. (2013). Effect of chemical milling on low-cycle fatigue behavior of an Al-Mg-Si alloy. Corrosion Science, 68, 144–153. https://doi.org/10.1016/j.corsci.2012.11.006

Specification for Additive Manufacturing Titanium-6 Aluminum-4 Vanadium ELI (Extra Low Interstitial) with Powder Bed Fusion. (2014). ASTM International. https://doi.org/10.1520/F3001-14

Specification for Additive Manufacturing Titanium-6 Aluminum-4 Vanadium with Powder Bed Fusion. (2014). ASTM International. https://doi.org/10.1520/F2924-14

Sun, Y. Y., Lu, S. L., Gulizia, S., Oh, C. H., Fraser, D., Leary, M., & Qian, M. (2020). Fatigue Performance of Additively Manufactured Ti-6Al-4V: Surface Condition vs. Internal Defects. JOM, 72(3), 1022–1030. https://doi.org/10.1007/s11837-020-04025-7

Superseding NASA-HDBK-6025 GUIDELINES FOR THE SPECIFICATION AND CERTIFICATION OF TITANIUM ALLOYS FOR NASA FLIGHT APPLICATIONS. (2014).

Tao, P., Li, H. xue, Huang, B. ying, Hu, Q. dong, Gong, S. li, & Xu, Q. yan. (2018). Tensile behavior of Ti-6Al-4V alloy fabricated by selective laser melting: effects of microstructures and as-built surface quality. China Foundry, 15(4), 243–252. https://doi.org/10.1007/s41230-018-8064-8

Tepylo, N., Huang, X., & Patnaik, P. C. (2019). Laser-Based Additive Manufacturing Technologies for Aerospace Applications. In Advanced Engineering Materials (Vol. 21, Issue 11). Wiley-VCH Verlag. https://doi.org/10.1002/adem.201900617

Ter Haar, G. M., & Becker, T. H. (2018). Selective laser melting produced Ti-6Al-4V: Post-process heat treatments to achieve superior tensile properties. Materials, 11(1). https://doi.org/10.3390/ma11010146

Ter Haar, G. M., & Becker, T. H. (2021). Low temperature stress relief and martensitic decomposition in selective laser melting produced Ti6Al4V. Material Design and Processing Communications, 3(1). https://doi.org/10.1002/mdp2.138

Townsend, A., Senin, N., Blunt, L., Leach, R. K., & Taylor, J. S. (2016). Surface texture metrology for metal additive manufacturing: a review. In Precision Engineering (Vol. 46, pp. 34–47). Elsevier Inc. https://doi.org/10.1016/j.precisioneng.2016.06.001

Vayssette, B., Saintier, N., Brugger, C., El May, M., & Pessard, E. (2019). Numerical modelling of surface roughness effect on the fatigue behavior of Ti-6Al-4V obtained by additive manufacturing. International Journal of Fatigue, 123, 180–195. https://doi.org/10.1016/j.ijfatigue.2019.02.014

Veiga, C., Davim, J. P., & Loureiro, A. J. R. (2012). PROPERTIES AND APPLICATIONS OF TITANIUM ALLOYS: A BRIEF REVIEW. In Rev. Adv. Mater. Sci (Vol. 32).

Vermesse, E., Mabru, C., & Arurault, L. (2013). Surface integrity after pickling and anodization of Ti-6Al-4V titanium alloy. Applied Surface Science, 285(PARTB), 629–637. https://doi.org/10.1016/j.apsusc.2013.08.103

Wang, D., Wang, H., Chen, X., Liu, Y., Lu, D., Liu, X., & Han, C. (2022). Densification, Tailored Microstructure, and Mechanical Properties of Selective Laser Melted Ti–6Al–4V Alloy via Annealing Heat Treatment. Micromachines, 13(2). https://doi.org/10.3390/mi13020331

Wang, L., Ma, C., Huang, J., Ding, H. Y., & Chu, M. Q. (2017). Microstructure and tensile properties of Ti-6Al-4V alloys manufactured by selective laser melting with optimized processing parameters. IOP Conference Series: Materials Science and Engineering, 265(1). https://doi.org/10.1088/1757-899X/265/1/012015

Wang, M., Yan, H., Lu, Q., Zhang, P., & Liu, K. (2024). Selective Laser Melted Ti-6Al-4V Alloy after Post-Heat Treatments: Microstructure, Mechanical Properties and

Fatigue Behavior. Journal of Materials Engineering and Performance. https://doi.org/10.1007/s11665-024-09504-5

Wang, P., Chen, F. hua, Eckert, J., Pilz, S., Scudino, S., & Prashanth, K. G. (2021). Microstructural evolution and mechanical properties of selective laser melted Ti-6Al-4V induced by annealing treatment. Journal of Central South University, 28(4), 1068–1077. https://doi.org/10.1007/s11771-021-4680-3

Williams, J. C., & Boyer, R. R. (2020). Opportunities and issues in the application of titanium alloys for aerospace components. Metals, 10(6). https://doi.org/10.3390/met10060705

Xu, J., Gruber, H., Deng, D., Peng, R. L., & Moverare, J. J. (2019). Short-term creep behavior of an additive manufactured non-weldable Nickel-base superalloy evaluated by slow strain rate testing. Acta Materialia, 179, 142–157. https://doi.org/10.1016/j.actamat.2019.08.034

Yang, J., Yu, H., Yin, J., Gao, M., Wang, Z., & Zeng, X. (2016). Formation and control of martensite in Ti-6Al-4V alloy produced by selective laser melting. Materials and Design, 108, 308–318. https://doi.org/10.1016/j.matdes.2016.06.117

Yihong, K., Tor, S. B., & Loh, N. H. (2014). Comparison of two metallic additive manufacturing technologies: Selective laser melting and electron beam melting. Proceedings of the International Conference on Progress in Additive Manufacturing, 0, 231–239. https://doi.org/10.3850/978-981-09-0446-3_033

Yu, C., Huang, Z., Zhang, Z., Wang, J., Shen, J., & Xu, Z. (2022). Effects of sandblasting and HIP on very high cycle fatigue performance of SLM-fabricated IN718 superalloy. Journal of Materials Research and Technology, 18, 29–43. https://doi.org/10.1016/j.jmrt.2022.02.077

Yu, H., Li, F., Wang, Z., & Zeng, X. (2019). Fatigue performances of selective laser melted Ti-6Al-4V alloy: Influence of surface finishing, hot isostatic pressing and heat treatments. International Journal of Fatigue, 120, 175–183. https://doi.org/10.1016/j.ijfatigue.2018.11.019

ZHANG, H., DONG, D., SU, S., & CHEN, A. (2019). Experimental study of effect of post processing on fracture toughness and fatigue crack growth performance of selective laser melting Ti-6Al-4V. Chinese Journal of Aeronautics, 32(10), 2383–2393. https://doi.org/10.1016/j.cja.2018.12.007

Zhang, S., Rauniyar, S., Shrestha, S., Ward, A., & Chou, K. (2019). An experimental study of tensile property variability in selective laser melting. Journal of Manufacturing Processes, 43, 26–35. https://doi.org/10.1016/j.jmapro.2019.03.045

CURRICULUM VITAE

ORCID ID : 0009-0001-6839-6318

Name Surname : Aslınur ATAKLI

Foreign Language : English

Education and Professional Background:

- **Master's degree** **(Feb 2022 - Jan 2025)**
  Eskişehir Technical University
  Institute of Graduate Programs
  Materials Science and Engineering

- **Bachelor's degree** **(Aug 2016 – Aug 2021)**
  Eskişehir Technical University
  Faculty of Engineering
  Material Science and Engineering

Professional Union/Association/Organization Memberships:

- **Material and Process Development Engineer**
  Eskişehir -Tusas Engine Industries Inc.
  March 2021- cont.

Type, Name and Information, Location of Publication/Activity

- B. Parlak, A. Ataklı, O. Acar, and E. Özeren, (2022). Surface treatment effects on chemical milling performance of L-PBF produced Ti6Al4V ELI. Journal of Additive Manufacturing Technologies.